

Quasi-Static and Dynamic Testing of Composite Materials

A Major Qualifying Project Report

Submitted to the Faculty

of the

WORCESTER POLYTECHNIC INSTITUTE

In Partial Fulfillment of the Requirements for the

Degree of Bachelor of Science

in Aerospace Engineering

Submitted by:

Harrison Hertlein

Nathan Thomas Siegel

Jacob Wilson

Marysol Zamaniego Cuahonte

Date: March 22, 2019

APPROVED BY:

Professor Nikhil Karanjgaokar

Aerospace Engineering Program

Department of Mechanical Engineering

Certain Materials are included under the fair use exemption of the U.S. Copyright Law and have been prepared according to the fair use guidelines and are restricted from further use.

Abstract

Mechanical testing is a standard and essential part of any design and manufacturing process and absolutely critical in the field of Aerospace engineering. Whether it is characterizing the properties of materials or providing validation for final products, ensuring safety is the principal mission of mechanical testing. Testing also plays a key role in ensuring a cost-effective design as well as technological evolution and superiority. The goal of this project was to develop experimental technique and protocols for evaluating the mechanical properties of a wide variety of materials under different loading conditions. The aforementioned project objective was achieved through two separate but mutually complementary efforts: 1) development of a testing apparatus for quasi-static testing and 2) modification and improvement of the current Split Hopkinson Pressure bar setup for dynamic testing.

Tensile Testing is accredited to AC7101 through PRI Nadcap for aerospace testing and is approved directly by many Aerospace entities including GEAE, Boeing, Messier-Dowty, Cessna etc. The first sub-team focused on analyzing the existing design and make suitable revisions to the Tensile Tester Setup. The first team also drastically improved the user experience and safety of the tensile testing setup for untrained undergraduate students. A functional strain measurement system complementary to the existing device and automated test procedures to perform various quasi-static tests were successfully implemented. The strain fields on the specimen gage section were measured using Digital Image Correlation (DIC) and specimen force was measured using load cell sensor. The team also developed user-friendly LabView VI based routines to provide both manual and closed-loop feedback control for displacement actuation. These LabView routines provide the user with the ability for obtain a constant actuation rate for the monotonic tensile tests or achieve a constant force condition for the tensile creep tests. The final version of experimental apparatus can provide a engineering stress-strain relationships for a wide range of aerospace materials.

The SHPB apparatus is widely used by the Aerospace Community to analyze the mechanical properties of various materials under dynamic loading conditions such as the impact loading

experienced by landing gear or other flight impact events. The second team was responsible of performing a critical performance analysis of the previous version of Split Hopkinson Pressure Bar, SHPB to identify any limitations. The team also devised effective solutions to overcome the limitations of previous version of the SHPB and implemented these revisions to structural, electrical and control components of the SHPB setup. Thus the overall goal is to ensure that the SHPB apparatus would measure accurate and consistent readings to study mechanical response of ceramics, polymer composites, and metals under dynamic loading. This SHPB setup relies on the assumption of one-dimensional wave propagation, which allows it to measure stress and strain of a tested material using merely the test sample dimensions and strain signals in the incident and transmitted bars. Since the previous SHPB setup only allowed the testing of metals and metallic alloys, it was modified to further facilitate the testing of polymers and composite samples.

Acknowledgements

The authors would like to thank Professor Nikhil Karanjgaokar, as well as graduate students Sharada Bhavanam, Hrachya Kockaryan, and Prajwal Bharadwaj, for advising the project and providing technical support. They would also like to thank the Washburn Machine Shops and Higgins Laboratory Work Shop at Worcester Polytechnic Institute for assistance with the fabrication of parts for the apparatus. Finally, the authors sincerely appreciate the financial support for their work from the Department of Aerospace and Mechanical Engineering at Worcester Polytechnic Institute.

Table of Authorship

Quasi-Static and Dynamic Testing of Composite Materials	1
Abstract	2
Acknowledgements	4
Table of Authorship	5
1. Introduction	7
1.1 Quasi-Static Testing - Tensile Tester	7
1.2 Dynamic Testing - Split Hopkinson Pressure Bar	8
2. Literature Review	10
2.1 Tensile Tester Literature Review	10
2.1.1 Digital Image Correlation Software	12
2.1.2 Potentiometer Theory	13
2.1.3 PID Control Theory	14
2.1.4 Theory Equations	16
2.2 Split Hopkinson Pressure Bar Literature Review	17
2.2.1 Assumptions in order to have a valid SHPB Experiment	17
2.2.2 Current Setup of the Split Hopkinson Pressure Bar	19
2.2.3 Nomenclature	26
2.2.4 Theory Equations	27
3. MQP Purpose and Methods	32
3.1 Project Goals	32
3.2 Project Design Requirements, Constraints, and Other Considerations	34
3.3 Project Management	36
3.4 MQP Objectives, Methods, and Standards	38
3.4.1 Tensile Tester	38
3.4.2 Split Hopkinson Pressure Bar	38
3.5 MQP Tasks and Timetables - Gantt Charts	40
4. Tensile Tester Modifications	41
4.1 Physical Modifications and Additions to the Tensile Tester	41
4.2 Direct Strain Measurement	43
4.3 DIC	46
4.4 Program Modifications and Additions to the Tensile Tester	52

4.5 Tensile Tester Data	57
5. Split Hopkinson Pressure Bar Modifications	66
5.1 Summary of Modifications to the SHPB	66
5.2 Circuit Improvements:	67
5.3 Trigger Improvements:	71
5.4 Pulse Shapers:	71
5.5 Strain Gauge Location:	73
5.6 Blast Box:	74
5.7 Matlab Code Improvements:	75
5.8 Alignment	78
5.9 Calibration	81
5.10 Accurate and Consistent Data Acquisition	82
6 Summary	93
7 Conclusion	94
8. Recommendations for Future Work	95
9. Project Broader Impacts	96
References	98
Appendix A	102
How to Use the Split Hopkinson Pressure Bar	102
Appendix B	104
How to Use the Oscilloscope for the SHPB	104
Appendix C	106
Trouble shooting the SHPB	106
Appendix D	109
How to Use the Tensile Tester	109
How to Use the LabView Programs	110
Appendix E	112
How to Use the VIC 2D 2009 Software	112
Appendix F	113
SHPB Matlab Code:	113
Appendix G	121
Tensile Tester MATLAB Code:	121

1. Introduction

Mechanical testing of materials is important in engineering in order to understand the properties of a material in order to determine how best to use it. However, the mechanical properties of aerospace materials such as metal alloys, composites etc can change significantly with variety of factors such as loading condition, loading rate, and temperature. In order to determine the best candidate material for a particular application, the mechanical properties of the material must be evaluated in similar test conditions. In aerospace applications in particular, the structural materials can be subjected to both static and dynamic loading conditions. This is why there must be the consideration of using both a static tester, such as a tensile tester, and a dynamic tester, such as a split-Hopkinson pressure bar, to determine if the material chosen can handle the potential loading conditions set by the desired application.

1.1 Quasi-Static Testing - Tensile Tester

Tensile tests are used to determine how materials will behave under tension load. In a simple tensile test, a sample is typically pulled to its breaking point to determine the ultimate tensile strength of the material. A tensile tester setup usually consists of the loadframe, the controller, and often DIC, or digital image correlation software. There is currently a tensile tester setup with some of these components built in an unfinished condition in WPI's Multipurpose Lab. This tester currently runs using LabView code, but it is not setup to handle constant strain or force rate upon the samples. An issue with setting up control for the tester for these conditions is that there is also no way to measure the strain on a sample currently. This project will oversee the addition of the constant strain and force rate controller in the LabView controller, as well as all the necessary equipment in order to have it run with some level of accuracy. In addition, the setup will also gain a system of post-test strain analysis with the addition of digital image correlation software. This addition does require the design and setup of a camera system to

record the samples and provide the data necessary for the DIC software provided by the Aerospace and Mechanical Engineering Departments.

1.2 Dynamic Testing - Split Hopkinson Pressure Bar

Aerospace engineers, when designing an airplane or a spacecraft, must take into account circumstances such as environmental challenges, weight specifications, flight launch issues, and impacts caused by heavy structural loads. As a result, engineers need to produce aerospace components that ensured the safety of the passengers and those impacted by the flight, as well as ensuring that the material used for the vehicle is economical, tenacious, but most importantly it must be strong and enduring to successfully complete tasks without material failure. In the aerospace industry in particular, dynamic testing is used to analyze material used for situations such as dynamic loading conditions occurring in airplane landing gear or in-flight impact events such as bird strikes or debris. It's vital to know the material's properties under these conditions in order to determine how a specific material will respond at high strain rate testing. The stress-strain curve of any material under dynamic loading can be determined using the Split Hopkinson Pressure Bar Apparatus.

The SHPB works by firing a projectile at a series of metal bars with a material sample between two of these bars. Strain gages on the metal bars then measure the resultant strain wave from the projectile's impact which are analyzed to obtain the stress-strain curve for the sample material. The typical SHPB setup consists of two main bars on each side of the material sample, often made of solid steel. This setup works well for testing of metal samples, however problems arise when testing composite or softer material samples. As the strain wave passes through the interface between the metal bars and sample, some of the wave is reflected. The amount reflected is dependent on the speed at which the wave can travel through a material, with a larger mismatch of this property between materials resulting in a greater reflection. This in turn results in a lower signal for the strain gages to read reducing the accuracy of the measurements, making the accuracy of the setup of primary importance.

There is currently a constructed SHPB setup constructed, however it is currently only made to handle metal samples, and with these traditional samples does not obtain consistent

results, and is prone to error. Changes were made to the circuit itself, the settings of the oscilloscope, the methods in which the setup was aligned, among other improvements to greatly increase both the reliability and accuracy of the setup when testing materials of all types. These improvements allow the SHPB to measure traditional metal samples with ease, and will also allow students to use the setup to test the dynamic stress-strain relationship even in homemade composite materials with accuracy.

2. Literature Review

2.1 Tensile Tester Literature Review

In engineering, one of the most important measurable aspects of a material is the stress-strain curve. Tensile testers are able to measure the components of stress-strain curves for a material, using a system of an actuator and grips with a load cell for the stress, and often one of several methods for strain measurement. This combination allows for the use of the theory equations and find the attributes of a material to be tested. This enables the determination of the properties of a known or an unknown material, and measure what it can handle.

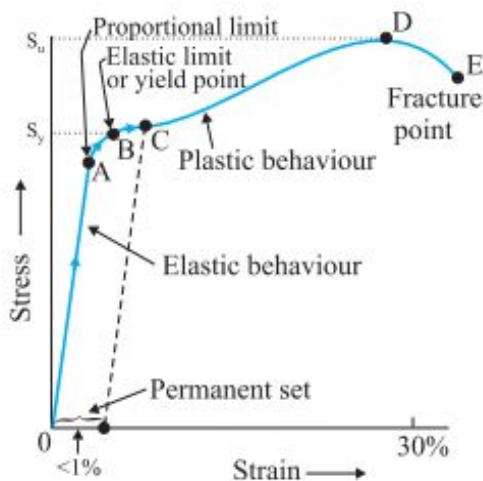


Figure (1): Stress-strain Graph (Hooke's Law and Stress-strain Curve, 2018)

On a stress-strain graph, there are many locations of interest that can be analyzed to learn about the properties of the material (Hooke's Law and Stress-strain Curve, 2018). In a typical stress-strain curve, the initial section is the elastic region of the curve (seen on Figure 1 as the section from the origin to point labeled A), in this area, the material stretches in an elastic or a reversible manner. The point where the linear elastic region starts to curve is known as the yield strength (point B on Figure 1). The yield strength corresponds to the point at which the material starts to permanently change shape, or plastically deform. This is important to note as many applications may depend upon the material not deforming, or minimally deforming. At the peak

of the curve (point D on Figure 1) is the maximum tensile strength of the material. This is the point where the material can handle the highest force load. The maximum tensile strength can be useful, but it is often within the plastic deformation section of the material. Plastic deformation of the material, can be seen on the sample by “necking” or reduction in the diameter or cross-section of the sample. The end of the stress-strain graph is the point at which the sample breaks (point E on Figure 1).

Due to the inertia and controls of the tensile tester, the actuator requires some time to reach the desired actuation velocity to properly load the sample. This deviation in the actuation rate can result in inaccuracy in the measured stress-strain response. The aforementioned issue can be approached in several ways. The first such approach involves the preloading of the sample. The problem with preloading the sample is that it will be put under some stress before the test begins. Another way to solve this issue, which was considered, is the addition of a slack adapter apparatus. This system would add slack to the actuator and allow it to start to pull upon the system without preloading the sample. The issue with the slack adapter, is that it will still be preloaded by the weight of the adapter.

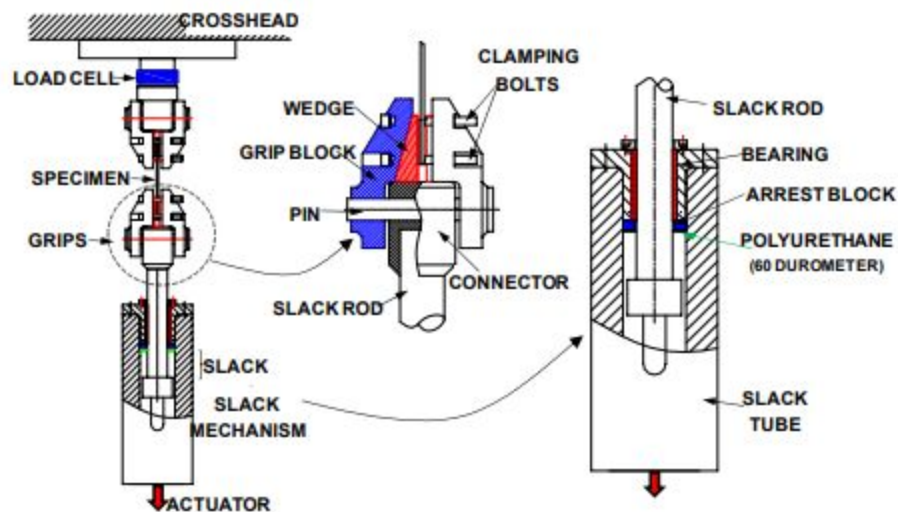


Figure (2): Slack Adapter Model from *Stroke rates and Strain rates: A parametric Study*

As seen in the image above, the slack adapter is made with a capped tube with a rod that can hook onto the edge of the end cap to allow it to pull on the sample. This allows the rod to move freely until it reaches the end and once the tester is pulling with full speed, and the control system is fully working, then the actuator can apply the force onto the sample. This system does require measurement and consideration of the conditions of the actuator being used. The slack adapter will have to be properly sized so that upon reaching the end of the tube, the rod must be moving at its required actuation velocity.

2.1.1 Digital Image Correlation Software

With tensile testing, there is the need of strain measurement to be used for creating the stress-strain curves. To measure the strain of a sample, there are a few methods to accomplish it. Two such methods are using a linear variable differential transformer (or LVDT), and strain gauges. Strain gauges must be attached onto the sample by gluing it on and must be attached to a system to read the voltages that come from the movement of the sample. Linear variable differential transformers work in a similar manner where they must be attached to the sample, and will output a voltage based off of the movement of the sample. The difference between the strain gauge and LVDT however, is their method of attaching to the sample. The issue with both of these methods is that they require the attachment to a sample which can be invasive and even damage the sample itself. Digital image correlation is a different method which captures a series of images during a test and analyzes it afterwards. A setup of this variety requires no invasive procedure that would attach or damage a sample in anyway as it is purely optical in nature. DIC also provides a full field analysis of the materials where the strain gauges and LVDT both provide localized data only.

DIC software uses correlation of an image to track the displacement of points on a sample. From this correlation, a strain map can be created, tracking the displacement of a point on the sample with reference to the original image which is under no loading. To improve the efficiency of this software, a speckle pattern on the sample should be applied for the software to properly track small points and reference the pattern as it deforms. A speckle pattern on the whole of the sample will allow the software to create a more accurate full field strain

distribution. The main disadvantage of this software is that the addition of a speckle pattern is required to be applied and if it is not dense enough, it would be less accurate.

2.1.2 Potentiometer Theory

A potentiometer is a type of resistor that can change its resistance based on an input. It may have two or three electrical terminals and will have one mechanical input. Two-terminal potentiometers are less frequently used and are not usually used as high-precision sensors. Three-terminal potentiometers are generally of higher quality, see more use in modern electronics, and are more useful for the Tensile Tester.

A three-terminal potentiometer is essentially a voltage divider where the total resistance of the two resistors is constant, but the resistance of each potentiometer can change. Structurally, this means that a solid conductive element is connected to an electrical terminal at either end and a “wiper” can move along the element in one axis (Potentiometers, 2013).

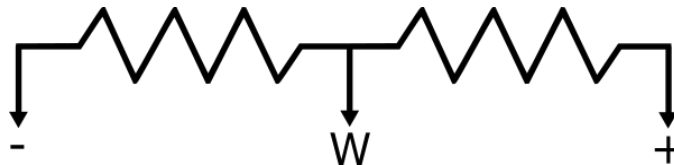


Figure (3): Wiring Diagram of a Potentiometer

In typical use, the conductive element is connected to a voltage source at one end and a reference ground at the other end. By moving the wiper across the element, a voltage response can be produced. The function of voltage vs position can be adjusted by changing the size of the conductive element at different locations. For the tensile tester a linear function is used to simplify calculation and operation.

Many measured properties go into selecting a proper potentiometer (i.e. power rating, contact resistance, seals, terminal types, etc.), but for the purposes of this MQP the most important property is called the independent linearity. The linearity of a potentiometer is defined as the maximum deviation from the defined voltage vs position function, as a percentage of the

excitation voltage (Potentiometers, 2013). A potentiometer with a low linearity follows the theoretical voltage function closely, while a high linearity will not. To accurately sense small changes in position, the linearity of the sensor must be very low.

Two types of potentiometers are candidates for use in the Tensile Tester. A rotary potentiometer has a rotating shaft that holds the wiper, allowing it to sense rotary motion, while a linear potentiometer has a probe that moves along one axis, allowing it to sense position.

2.1.3 PID Control Theory

A PID controller is a very commonly used closed-loop feedback controller that is composed of three components: a Proportional controller, an Integral controller, and a Derivative controller (Tehrani, 2012). By summing the response of the three different controllers to an input signal, a control output can be generated to eliminate the error. The primary advantage to a PID controller is that it can provide accurate control for a wide range of disturbing forces, while remaining simple to implement. The two main disadvantages to a PID controller is that it's difficult to implement on complicated systems, and that tuning can be difficult.

The first component, the Proportional controller, is simple to describe. The output, P, is the current error multiplied by a gain value, K_p . For low values of K_p , the steady-state error is high, but the change in output for a given change in error is low, keeping the system more stable. In contrast, a high value for K_p will reduce the steady-state error, but will generate a larger change in output for a given change in error, reducing stability (Tehrani, 2012). The equation below is used in discrete-time applications, like the Tensile Tester.

$$P(t) = K_p * error(t) \quad (\text{Eq. 1})$$

The second component, the Integral controller, is less simple. The output, I, is the integral of all the past error in the system, multiplied by a gain value K_i . This controller has the primary goal of eliminating steady-state error in the system. For low values of K_i , the steady-state error will slowly decrease, but only small amounts of overshoot will be experienced. For high values of K_i , the steady-state error will be corrected quickly, but may result in excessive overshoot and instability. Integral controllers are also susceptible to wind-up, where a transient force may cause a large buildup which will take time to decrease, causing additional error (Tehrani, 2012). The

equation below is used in discrete-time applications. A proper integral would be used for study of PID systems, but this method is less computationally complex, making more applicable to high-speed loops.

$$I(t) = K_I * error(t) * \Delta t + I(t - \Delta t) \quad (\text{Eq. 2})$$

The third component, the Derivative controller, computes the slope of the error function and multiplies it by a gain value K_D . This controller prevents overshoot and increases the stability of the system overall. Low K_D values may not reduce the response enough, while high K_D values may reduce the system response too much, increasing the settling time of the system (Tehrani, 2012). The equation below is used in the same situations as the above Integral controller, and is subject to the same assumptions.

$$D(t) = K_D * \frac{error(t) - error(t - \Delta t)}{\Delta t} \quad (\text{Eq. 3})$$

The tensile tester only uses one sensor at a time (either the force sensor or the position sensor), and only has one output (the linear actuator), the PID controller can be dropped in easily, as the system isn't complicated from a controls perspective. Tuning the system is still difficult, but that just requires additional tests. However, despite the apparent simplicity of the system, choosing the correct gain values may either involve trial and error or advanced and expensive tools (Tehrani, 2012).

The classical tuning method is the manual method, where each value is selected based off of the tuner's experience from other PID systems in the past. This method is commonly used in systems where performing multiple tests is easy, and there's little need for aggressive control responses. If aggressive tuning is acceptable, then the Ziegler-Nichols method is better. A small amount of math is necessary, but this method does reduce the amount of time spent tuning. Other methods exist as well, but most require significant investments of time or money, or result in imprecise tuning (Tehrani, 2012).

2.1.4 Theory Equations

With the tensile tester, a few equations were used for the basics of the calculation of the values.

$$\sigma = \frac{F}{A} \quad (\text{Eq. 4})$$

Where F is force on the sample, A is the area of the sample, and σ is the stress.

Using Hooke's law, the Modulus of Elasticity or the Young's Modulus (E) is calculated to determine the stiffness of the material. This relationship is defined as:

$$E = \frac{\sigma}{\varepsilon} \quad (\text{Eq. 5})$$

Where σ is the stress and ε is the strain on the material.

Yield Strength of a material, or the point at which the material stops linearly deforming, and starts to plastically deform, can also be determined.

With the equations, the strain of the material is determined.

There are two types of strain that can be calculated, True Strain or Engineering Strain. These are determined by the equations:

$$e = \frac{L - L_0}{L_0} = \frac{\Delta L}{L_0} \quad (\text{Eq. 6})$$

$$\varepsilon = \ln\left(\frac{L_i}{L_0}\right) \quad (\text{Eq. 7})$$

Where ε is the True Strain on the material, e is the Engineering Strain on the material, L is the end length, L_0 is the original length, ΔL is the change in the length and L_i is the instantaneous length.

2.2 Split Hopkinson Pressure Bar Literature Review

2.2.1 Assumptions in order to have a valid SHPB Experiment

Five key assumptions must be fulfilled in order to accurately calculate the stress and strain of a test specimen using SHPB experimental setup. The five assumptions are as follows:

- 1.The stress wave propagation in the bars is one dimensional
- 2.The specimen-bar interfaces remain plane at all times
- 3.The specimen is in stress equilibrium after the initial ringing period
- 4.The specimen is not compressible
- 5.Friction and inertia effects in the specimen are minimum, where they can be negligible

Failure to follow through with the assumptions during a SHPB experiment will lead to incorrect unsatisfactory results. Going further in depth in the assumptions. The consequences of invalid assumptions and methods to ensure proper experimental setup are discussed below. The stress wave traveling through the incident bar, transmission bar, and specimen must be a one-dimensional wave. To achieve this outcome, all aspects of the experiment, from the gas gun to the transmission bar, must be aligned to a very high degree of accuracy along a single axis. In addition to this, properties of the incident and transmission bars can be optimized in order to help ensure this effect. In general, the greater the length to diameter ratio, the more one-dimensional the stress wave propagation can be assumed to be. Increasing the length to diameter ratio reduces the influence of Poisson's effects, thereby reducing the radial deformation of the bar. Additionally, close to the ends of the bars, stress is not uniformly distributed radially. This becomes an issue in determining the locations in which to place strain gages, as strain gages are mounted only to the surface of the bars. Mounting strain gages farther from the ends of the bar mitigates this effect as the stress values become evenly distributed. Literature suggests placing strain gages at least ten bar diameters away from the specimen, or at the midspan of a bar, which is at least twenty bar diameters in length.

Assumption number two, a planar interface between the bars and specimen, follows the trend of the previous assumption of proper experimental alignment. There are two main ways non-planer contact between bars and specimen can occur. The first is simply if the ends of any component are poorly designed or machined such that the end surfaces are not circular and perpendicular to the length of the bar. The second way in which this assumption can be invalidated could occur even if the bar-specimen interfaces begin the experiment in a planar fashion. If the stiffness of the specimen is much greater than the bars, the specimen may create an impression in the bars subsequently ending the initial planar condition.

The typical reading from a strain gage attached to either the incident or transmitted bar shows a roughly trapezoidal pulse. However, following the initial rise, the strain reverberates slightly before settling to an equilibrium state. This reverberation is often referred to as the 'ringing up' period. Only after this period is the specimen assumed to be in stress equilibrium. It is difficult to determine a specific instance when this assumption is met but some literature suggests after five or so 'rings' the specimen has roughly equal stress on both ends. Apart from analyzing the data following the experiment, this ringing period can be accounted for in part using a pulse shaper, typically a soft metal that deforms between the striker bar and incident bar. Pulse shapers can alter rise time, pulse shape, reverberation, and dispersion. Using a thinner specimen can also reduce the ringing up period simply since the wave must travel a shorter distance each reverberation.

The assumption of incompressibility can't be ensured through experimental setup as it is a property of the specimen's material. Compressibility can only be controlled through selection of specimen materials. The assumption of incompressibility ensures constant material properties such as density in the experiment. The last assumption requires that frictional and inertial effects in the specimen are minimized. Incompressible specimens have the tendency to deform radially if strained axially due to Poisson's effects. Friction at the ends of the specimen can restrict this deformation and create a barreling effect. To avoid frictional effects, ends of bars and specimen must be precisely machined and properly lubricated. Frictional effects also become more significant as the thickness of the specimen decreases. Inertial effects can influence results in these types of tests, especially at very high strain rates. Additionally, intrinsic and extrinsic

properties of the specimen affect inertial effects. Generally, smaller specimens, as well as low density and high stiffness materials, reduce error introduced from these inertial effects. Clearly, a significant amount of optimization in the length, diameter, and material used in the experiments bars and samples must take place.

2.2.2 Current Setup of the Split Hopkinson Pressure Bar

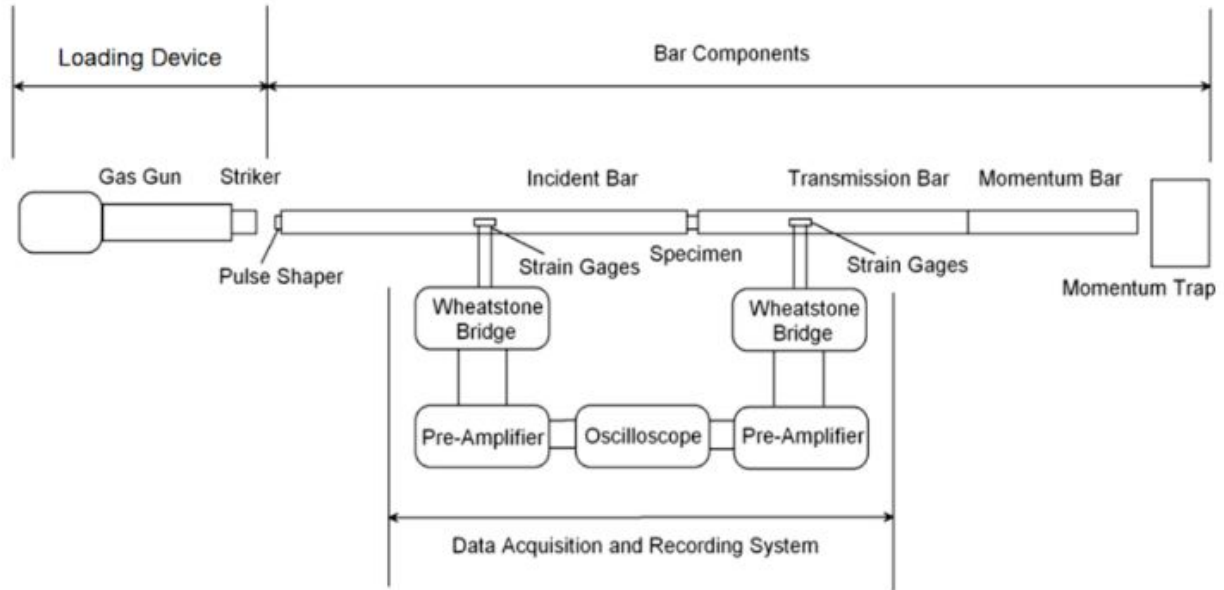


Figure [4]:Schematic of Split Hopkinson Pressure Bar [Split Hopkinson (Kolsky) Bar, 2011]

The Split Hopkinson Pressure Bar is composed of three main parts, a loading device, made of the gas gun and the striker projectile bar, the bar components which is made up of the pulse shaper, incident bar, the test sample, transmission bar, strain gages, and a momentum trap, and finally the data acquisition and recording components which is made of amplifiers, and oscilloscope and DC Power Supplies. SHPB uses a gas gun to accelerate the striker bar at a determined pressure. The striker bar then collides with the pulse shaper that is placed in front of the incident bar in order to reduce dispersion and excess noise. The stiker bar impact with the incident bar sends a compressive strain wave that propagates along the incident bar until it reaches the sample being tested. Once the strain wave reaches the sample, it will react in one of three ways, the strain wave is absorbed by the sample, it continues to flow and leads through the

transmission bar, or the remainder of the wave is reflected back through the incident bar. The momentum trap at the end was set in place in order to absorb the excess linear momentum coming from the transmission bar, this prevents additional, reflected strain waves to propagate back and cause misreadings in the experiment measurements. Strain gages are attached to the incident and transmission bars at either side of the test sample in order to get an accurate reading of the incident, transmitted, and reflected strain waves. Attached to the strain gauges there are is a power supply on either side that transmits and excitation voltage which is then increased with the use of amplifiers in order to increase the resolution of the minute voltage changes of the strain gage signal. Lastly, the oscilloscope would be used to records this new signal as well as the original voltage from the power supply.

In the engineering industry, a variety of different methods have been used to measure dynamic loading on material. Some of which include the Charpy/ Izod Impact Test, the Gardner Impact Test, and of course the Miniature Kolsky Bar. The Charpy/Izod Impact Test is a system comprised of a weighted pendulum equipped with a striker is released downward from a known height towards the test specimen in a motion that will break off a piece of the specimen. The impact tests are relatively the same except for the alignment of the test specimen with respect to the pendulum. The test specimen is aligned vertically with it fastened facing the pendulum during the Izod Impact Test whereas in the Charpy Impact Test the test specimen is aligned horizontally with it fastened facing away from the pendulum. The energy absorbed by the impact can be calculated using the initial height of the pendulum. In comparison, the Gardner Impact Test is comprised of a variable mass impactor as its striker that is vertically released downward towards the test specimen, which is similar to the SHPB setup however it is vertical. Using the relationship between the mass and initial height of the striker the energy of the impact can be determined for the test specimen. Likewise, the impact force can also be determined using an accelerometer. Because of the system's configuration, it can be applied to various materials of different shapes, sizes, and orientations. The data collected is both precise and accurate for normal and oblique impacts, and the test specimen itself can be dropped in place of using a striker. Even though the Gardner Impact Test can accommodate a wide variety of materials it has

been primarily useful amongst various rubbers and plastics. Finally, as the name implies, the Miniature Kolsky Bar is a miniaturized version of the Kolsky / Split Hopkinson Pressure Bar setup. The main difference is the reduced geometry of the system, it allows for the measurement of the strain pulse using interferometric measurements deduced from the interference patterns generated by the combination of two waves of equivalent length across the gratings at the midpoint of the bar. The smaller geometry is beneficial in preventing dispersion effects as the pulse's rise time is shortened and a state of equilibrium can be reached quicker the miniaturized Kolsky bar method runs into altercations when a transmitter bar is used as well as it struggles to accurately measure transverse displacement oscillations, which is why the regular sized Kolsky/Split Hopkinson Bar is preferred for this experiment and preferred by most other universities conducting dynamic testing.

The original Hopkinson Pressure Bar modification done by Kolsky utilized explosives as a means of propulsion for the projectile, the current setup involving the gas gun is a safer and more controllable replacement in order to achieve consistent repeatable results. The custom WPI gas gun is capable of launching the projectile striker bar at a consistent and measurable velocity making the experiment repeatable. The gun is made of seven parts the chamber, a barrel, a charging valve, a discharging valve, attached pressure gages, a rapid discharge plunger mechanism, and a muffler. The gas gun is attached to an external air compressor which pressurizes the gas gun when the charging valve is opened. Once the gas gun is pressured to the desired amount, the charging valve must be closed. If the charging valve isn't shut off before the gas gun is fired severe damage to the equipment, a misfire of the gas gun, and incorrect measurement. As a means of further precaution the external compressor should also be disconnected and shut off when not in use. Once the gas gun is loaded laboratory personnel must be cleared from the area near the Split Hopkinson Pressure Bar prior to firing the projectile. In order to fire the gas gun, the lever attached to the discharging valve must be opened rapidly, if it is opened too slowly the pressure will not be released adequately which will also create discrepancies in the measurement. The opening of the valve will create a pressure differential across the plunger mechanism. This occurs when the plunger retracts and uncovers the barrel,

which would release the collected pressurized air through the barrel of the gas gun causing the projectile to be fired. The projectile is then fired out of the gun up to a velocity of 100 meters per second. The first thing the projectile impacts would be a pulse shaper placed ahead of the incident bar, which is capable of reducing noise and dispersion effects from altering the final results. The purpose of a pulse shaper is to “shape the strain impulse” which results in a smoother wave recorded along the incident bar. Depending on the type of material being tested and the amount of pressure being stored in the gas gun the pulse shapers can come in a variety of materials. The pulse shapers need to be thin and preferably with a smaller diameter of that the incident bar. The pulse shapers can be punched out from thin copper sheets of 14 gauge or thinner for testing on tougher metals, paper or cardboard for softer testing materials and lower pressure powered into the gas gun, or any other thin material that is able to mitigate the effects during experimentation.

There are specific criteria that the SHPB must meet in the design of the bars to obtain correct measurements. The SHPB is required to meet the following guidelines:

1. Minimum length of the transmission bar must be twenty times the diameter of the bar.
2. Transmission bar must be at least twice the length of the projectile striker bar.
3. Incident bar must be twice the length of the transmission bar.

At its origin, these requirements were applied to the MQP’s Split Hopkinson Pressure Bar. In order to find the minimum length of the transmission bar, its diameter must be determined. In this specific project setup, all the bars have a diameter of 0.75 inches. Taking the first and third requirements into account, the minimum length of the transmission bar must be twenty times the bar’s diameter and the incident bar must be twice the length of the transmission bar. Therefore the minimum length of the incident bar is required to be 30 inches and the transmission bar needs to be at least 15 inches. Now taking the projectile striker bar of the requirements into consideration, the striker bar length is a crucial part of the apparatus since it affects the amplitude and length of the stress wave directly. For this project, the SHPB needs to be able to accommodate striker bars ranging from 6 to 18 inches. The reason for having an 18

inch long projectile is to give the SHPB the capability to test not just on hard metals such as Steel which is where the shorter projectile bars are used, but also be used on softer materials such as composite materials. With stiffer material, the stress-strain response is overwhelmed by the linear elastic region over smaller strain region, therefore this test requires a smaller bar. Softer materials have elastic and plastic responses which occur non-uniformly over much greater strain magnitudes, therefore this test requires a longer wave and in turn requires a longer bar. The dimension transmission bar must be at least twice the length of the longest projectile, which is 18 inches. Therefore the transmission bar must be increased in length to be was adjusted to be 36 inches. This will also affect the incident bar's length in accordance to the third rule. The incident bar now is adjusted to be a length of 72 inches.

No matter the material that is being tested, the specimen sample must be cylindrical and smaller in diameter than the diameter of the bars. The test samples currently in use have a diameter of half an inch, in comparison, the dimensions of the adjacent bars have a diameter of three fourths of an inch. It is crucial for the specimen to also be thin in thickness in order to fulfill the the assumptions required of the Split Hopkinson Pressure Bar. The thinness of the bar is essential in order to neglect both axial and radial inertia effects as well as to ensure there is compression on the test sample, instead of bending or buckling which could be caused if the test sample is too long. However, the test sample must also keep equilibrium and be long enough to ensure that the strain rate is not too high. A convenient way to ensure that the thickness is an adequate measurement in conjunction with the sample's diameter, is by using the length to diameter ratio of $\sqrt{3}/4$. Another necessary requirement for the test sample as well as any bars that make contact or impact on another it that the surfaces must be extremely lubricated . The bars and test sample should also have a smooth, sanded parallel surface on the flat side of the test samples in order to fit tightly and flush between the incident and transmission bars. The lubrication and flat surfaces are necessary for this experiment because as the length of the specimen is compressed, according to Poisson's effect, the diameter also in turn expand, therefore, excess friction would result in barreling of the sample. Having a well lubricated smooth surface will allow the experiment to comply with one of the five SHPB assumption.

Another essential component of the MQP SHPB is the momentum trap. The momentum trap is comprised of a clay block, reinforced with a rubber backing, followed by a wood, then a steel backing. Each component of the momentum is necessary for the setup and each contributes different things. The clay is used to absorb the momentum from the transmission bar by deforming. The rubber is used to absorb most of the remaining momentum flowing past the clay. The wood is used to absorb the unabsorbed momentum from the previous two backings and finally, the steel backing is used to brace all the components of the momentum trap to the larger SHPB structure.

This portion of the apparatus is necessary to avoid unwanted reflection waves flowing back through the transmission bar which can cause interferences and will alter the strain wave data being collected. Another benefit to the momentum trap is that it prevents additional stress being placed on the SHPB components that are already being placed under a large load. Apart from preventing wave interferences, the momentum trap is vital for the safety of the user since the component prevents the transmission bar at the end to propel outward or ricochet upon impact from the projectile.

Strain gauges are a fundamental part in recording different waves that the Split Hopkinson Pressure Bar creates. The strain gauges are placed on either side of the desired test sample in order to record the incident, transmission, and reflected wave after impact. One pair of strain gauges was placed on a specific area on the incident bar and a second pair of strain gauges was placed on a specific area on the transmission bar. This specific location is determined by the pulse length which is found experimentally as well as the wave speed throughout the bar, the location needs to be specific and consistent to avoid reflected pulses from overlapping. The strain gauges used are of the brand Omega with $120\Omega \pm 0.3\%$ resistance and a gage factor of 2.14. These specific strain gauges were chosen for their ability to work under a broad temperature range without much variation in resistance, and their durable design enabling them to be used in dynamic testing without breaking. The strain gauges will measure a one-dimensional compressive strain wave by configuring the strain gauges in a half bridge and placing them at equidistant around the circumference of the transmission and incident bar. To

balance this bridge, the gauges will be connected at opposite branches of the wheatstone bridge and as well as other gauges of the same resistance, however, these will be located on the breadboard and soldered on. Having the strain gauges at opposite sides of the bar is useful to cancel out minor bending and torsional effects of the strain wave. Using the data acquired using the strain gauges, the expected maximum reflected strain signal can be calculated by using the strain rate, wave speed, sample length, gage factor, and excitation voltage.

In order to be able to analyze the measurements provided by the SHPB experiment, amplifiers were used to improve the resolution and further analyze the range that is being provided by the multiple attached strain gauges. The original output coming from the strain gauges is on the order of millivolts, meaning if this signal was not amplified poor resolution would be read, which could lead to errors in the data results. As the gain increases, measurement noise also increases because the aggregated signal is further amplified. The precise gain must be determined experimentally for each material, this gain is used to balance low noise with a high resolution. For the steel sample measured in this experiment, a gain of 51 was used. Since the oscilloscope is setup to a maximum input voltage of ten volts, the newly amplified strain signal is easily measurable by the oscilloscope. The resulting data will then have a minimized amount of noise and the data set is smaller allowing it to fit within the range limitations of the amplifier.

In this setup a rapid data acquisition system device must be set in order to read the fast wave speed which is on the order of thousands of meters per second. The oscilloscope is capable of accomplishing this task, it is able to record the high-speed wave. For this project the Tektronix MDO3024 oscilloscope is being used. It was chosen for its wide capabilities, to be able to take measurements at a rate of up to 200 MHz and has a 16-bit resolution. This setup also provides four analog channels, which is the exact amount needed for the series of dynamic tests. One of the channels is for the strain gages on the incident bar, one for the strain gages on the transmission bar, one for the excitation voltage at the incident bar, and one for the excitation voltage at the transmission bar. This oscilloscope is capable of saving data externally, which can be done using a flash drive to export the measurements from the experiments and export them to a computer for further processing and analysis using computer software such as Matlab.

2.2.3 Nomenclature

σ = Amplitude of stress pulse

$\dot{\varepsilon}$ = strain rate

ε = amplitude of strain

v = velocity

L_s = length of striker bar

C = elastic wave speed of material

t = time

F = force

H_s = Original length of test specimen

A = cross-sectional area

E = Young's modulus

u = Displacement of bar

\dot{u} = Velocity or Strain Pulse

I = Incident

T = Transmitted

R = Reflected

2.2.4 Theory Equations

Using the following equations as well as consistently implementing the necessary assumptions in order to validate the SHPB data, will result in the desired stress and strain values of the specimen.

Beginning with the one-dimensional wave equation:

$$\frac{\partial^2 u}{\partial x^2} = \left(\frac{1}{c_{0B}^2} \right) \frac{\partial^2 u}{\partial t^2} \quad \text{Eq. 8)}$$

In this system, it ensured that the striker bar and the incident bar were created from the same material and it's surfaces had the same diameter. The stress amplitude of the incident pulse can then be calculated using:

$$\sigma_I = \frac{1}{2} \rho_B C_B v_{st} \quad \text{(Eq. 9)}$$

The strain amplitude of the incident pulse can also be calculated using:

$$\varepsilon_I = \frac{1}{2} \cdot \frac{v_{st}}{C_B} \quad \text{(Eq. 10)}$$

Utilizing the one dimensional stress wave theory, the particle velocity can be calculated at both ends of the test specimen, assuming that the stress waves propagate through the incident bar and the transmission bar with no accountable dispersion. The following equations are used to calculate the velocity at the incident and transmission bars, respectively:

$$v_1 = C_B(\varepsilon_I - \varepsilon_R) \quad \text{(Eq. 11)}$$

$$v_2 = C_B \varepsilon_T \quad \text{(Eq. 12)}$$

Using the incident and transmission velocities, the average engineering strain rate can be calculated:

$$\dot{\epsilon} = \frac{v_1 - v_2}{L_s} \quad (\text{Eq. 13})$$

$$\dot{\epsilon} = \frac{C_B}{L_s} (\epsilon_I - \epsilon_R - \epsilon_T) \quad (\text{Eq. 14})$$

As well as the specimen strain:

$$\epsilon = \int_0^t \dot{\epsilon} dt \quad (\text{Eq. 15})$$

$$\epsilon = \frac{C_B}{L_s} \int_0^t (\epsilon_I - \epsilon_R - \epsilon_T) dt \quad (\text{Eq. 16})$$

Furthermore, the stress at either end of the test specimen are calculated as lowercase sigma using elastic relation equations:

$$\sigma_1 = \frac{A_B}{A_s} \cdot E_B (\epsilon_I + \epsilon_R) \quad (\text{Eq. 17})$$

$$\sigma_2 = \frac{A_B}{A_s} \cdot E_B \cdot \epsilon_T \quad (\text{Eq. 18})$$

As one of the five SHPB assumptions, it is assumed that the stress is at equilibrium which can be expressed with the equation:

$$\sigma_1 = \sigma_2 \quad (\text{Eq. 19})$$

Equate the equations above in order to solve for the transmitted strain pulses in the specimen:

$$\epsilon_I + \epsilon_R = \epsilon_T \quad (\text{Eq. 20})$$

Which can be utilized to further simplify the original equation for the average strain:

$$\dot{\epsilon} = -2 \frac{C_B}{L_s} \epsilon_R \quad (\text{Eq. 21})$$

As well as the strain in the specimen:

$$\varepsilon = -2 \frac{C_B}{L_s} \int_0^t \varepsilon_R dt \quad (\text{Eq. 22})$$

The stress of the specimen is also able to be simplified, assuming sigma 1 and sigma 2 are the same:

$$\sigma = \frac{A_B}{A_S} E_B \varepsilon_T \quad (\text{Eq. 23})$$

In the case of the SHPB, the stress wave will propagate through a long rod, 72 inches, the stress wave will then take form of the strain energy. As the stress wave propagates through the incident bar, its elastic strain energy can be calculated with the following equation:

$$E_1 = V_1 \int_0^{\varepsilon_1} \sigma d\varepsilon \quad (\text{Eq. 24})$$

The deformed volume of the incident bar is found using the equation:

$$V_1 = A_0 C_0 T \quad (\text{Eq. 25})$$

Similarly, the elastic strain energy can be found for the reflected wave:

$$E_R = \frac{1}{2} A_B C_B E_B T \varepsilon_R^2 \quad (\text{Eq. 26})$$

As well as the transmitted wave:

$$E_T = \frac{1}{2} A_B C_B E_B T \varepsilon_T^2 \quad (\text{Eq. 27})$$

Contribution of the bars' elastic strain energy to the specimen deformation can be calculated as:

$$\delta_E = E_I - E_R - E_T \quad (\text{Eq. 28})$$

$$\delta_E = \frac{1}{2} A_B C_B E_B T (\varepsilon_I^2 - \varepsilon_R^2 - \varepsilon_T^2) \quad (\text{Eq. 29})$$

Further simplified as:

$$\delta_E = -A_B C_B E_B T \varepsilon_R \varepsilon_T \quad (\text{Eq. 30})$$

The kinetic energy contribution in the incident bar after the incident wave flows through is expressed with the equation:

$$K_I = \frac{1}{2}mv_I^2 \quad (\text{Eq. 31})$$

With the mass of the deformed portion of the incident bar being:

$$m = \rho_B A_B C_B T \quad (\text{Eq. 32})$$

And the particle velocity of the deformed portion of the incident bar being:

$$v_I = C_B \varepsilon_I \quad (\text{Eq. 33})$$

The kinetic equation can now be rewritten using the new values for mass and velocity:

$$K_I = \frac{1}{2}\rho_B A_B C_B^3 T \varepsilon_I^2 \quad (\text{Eq. 34})$$

The equation above can be applied to the reflected and transmitted pulses as well.

The equation below demonstrated the contribution kinetic energy has on the test specimen deformation:

$$\delta_K = K_I - K_R - K_T \quad (\text{Eq. 35})$$

$$\delta_K = \frac{1}{2}\rho_B A_B C_B^3 T \left(\varepsilon_I^2 - \varepsilon_R^2 - \varepsilon_T^2 \right) \quad (\text{Eq. 36})$$

Further simplified to:

$$\delta_K = -\rho_B A_B C_B^3 T \varepsilon_R \varepsilon_T \quad (\text{Eq. 37})$$

In the SHPB experiment it can be assumed that the test specimen has a perfectly plastic response, therefore its deformation energy can be simplified as:

$$E_s = A_s L_s \sigma_y \varepsilon_p \quad (\text{Eq. 38})$$

The yield strength of the test specimen will then equate to:

$$\sigma_y = \frac{A_B}{A_s} E_B \varepsilon_T \quad (\text{Eq. 39})$$

And the plastic strain of the specimen equates to:

$$\varepsilon_p = \dot{\varepsilon} T \quad (\text{Eq. 40})$$

$$\varepsilon_p = -2 \frac{C_B}{L_s} \varepsilon_R T \quad (\text{Eq. 41})$$

The final test specimen deformation energy can be expressed as:

$$E_s = -A_B E_B C_B T \varepsilon_R \varepsilon_T \quad (\text{Eq. 42})$$

$$E_s = 2\delta_E \quad (\text{Eq. 43})$$

$$E_s = 2\delta_K \quad (\text{Eq. 44})$$

Meaning the energy coming from the elastic strain energy will provide half of the required energy for the specimen to plastically deform. Indicating that the incident kinetic energy will contribute the other portion of the energy.

3. MQP Purpose and Methods

3.1 Project Goals

The overall goal of the project is to make two working testing systems for materials testing. These testers would be used for the Aerospace Department, for testing as a part of laboratory work for engineering courses being offered at WPI.

For Quasi-Static experiments, the tensile tester would be ideal to measure stress-strain curves of a desired material in order to determine properties of known or unknown material. Goals set out specifically for the Quasi-Static Tensile Tester System are to build a working testing system capable of analyzing the strain on a sample using digital image correlation. This would include:

1. The repair and familiarization of the current tensile tester
2. The development of new code to control the tester in strain and force constant tests
 - a. Testing of the code for each updated version
 - b. Improve user friendliness of the program
3. The addition of a linear potentiometer for strain rate control
 - a. The tuning of the linear potentiometer
4. The setup and acquisition of digital image correlation hardware such as:
 - a. Monochrome camera
 - b. Camera cable
 - c. Image capture software for use with the camera
 - d. Tripod
5. Familiarization of the DIC software VIC 2D
6. Running several successful tests with similar data

7. Create a guide to use the tensile tester

For experiments pertaining Dynamic testing, the Split Hopkinson Pressure Bar (SHPB) apparatus would be utilized for this task. The SHPB is capable of testing the dynamic stress-strain reaction of materials a typical test can be done at a high strain rates in the range of 10^2 to 10^4 s^{-1} . Data at such high strain rates is applied to the assessment of structures that are subject to dynamic loads in order to ensure the safety and structural integrity of structures being analyzed. The Dynamics Testing utilizing the Split Hopkinson Pressure Bar require the following goals to be met:

1. Improve the reliability of the SHPB.
 - a. Replace the unreliable solderless breadboards.
 - b. Replace the unstable shunt resistors.
 - c. Redesign the trigger to prevent the oscilloscope from triggering early.
 - d. Redesign setup on transmission bars to prevent reflected wave overlap.
2. Improve the accuracy of the SHPB.
 - a. Develop a way to completely balance the wheatstone bridges located in the circuits.
 - b. Improve the Matlab code to provide more accurate stress-strain curves.
 - c. Develop a clear procedure to align and calibrate the SHPB.
3. Increase the user friendliness of the SHPB.
 - a. Create a blast box to prevent projectiles from ricocheting.
 - b. Improve the Matlab code to enable users to more easily and accurately obtain stress-strain curves.
 - c. Develop more detailed guides on using the SHPB.
 - i. Guides for conducting tests.
 - ii. Guides for using equipment such as the oscilloscope.
 - d. Develop a guide to troubleshooting the SHPB.
4. Conduct tests on various materials with the SHPB.

- a. Conduct tests on harder metals such as steel.
- b. Conduct tests on softer metals such as aluminum and copper.
- c. Conduct tests on nonmetal materials.
- d. For the above materials obtain consistent results for each material.
- e. Compare test results with results obtained by outside sources.

3.2 Project Design Requirements, Constraints, and Other Considerations

For the project, there were a few constraints for the whole project, as well as the individual parts. This was due to the major requirement of the given budget of the MQP itself, and the requirements for finishing the MQP. The major budget constraint was that it was an overall budget of \$1,000 (\$250 per person as given to by WPI to use). A large portion of the budget would have to be allocated to the purchase of a camera for digital image correlation for the tensile tester. The purchase of the camera was heavily considered in order to reduce the drain of the budget. This required careful research into a camera with the highest possible quality image capture, and frame rate to be able to capture video or images that would provide the digital image correlation software with the best images for strain measurement. In researching the camera, it was also desired that the price of the camera do not exceed three-quarters of the budget to allow for the purchase of other needed equipment and materials.

The secondary constraint for the project was the desire for the testers to be used by undergraduate students as a part of their labs to fulfill engineering course requirements and to learn more about materials testing. This desired end result required that the equipment must be in a functional state that would allow accurate results.

For the Split Hopkinson Pressure Bar setup includes the following individual requirements. All the bars in the setup must be aligned perfectly straight in order to create a one dimensional test and gain accurate results by ensuring proper stress wave propagation in the bars. The surfaces of the test specimen bar must be insured to be continuously planar at all times. This can be done by adjusting the surface where the apparatus is placed on, ensuring it is horizontally planar. It is also required for the specimen being tested to not be a compressible material, in order to obtain adequate and accurate results. Another essential requirement is for there to be

minimum friction and inertia effect in the test specimen and between any and all impacted bars. This can be done by ensuring proper lubrication on all surfaces being impacted and extensive sanding and polishing of surfaces to make certain that they are all planar and flush to each adjacent bar. A time constraint was also set on this project with only three terms, each with 7 weeks to complete the project, time was limited and had to be managed efficiently. One of the drawbacks and issues run into during the project is all the wait time spent. Items had to be purchased in anticipation or else a week would be spent realistically without much productivity without the required item. Also getting the components machined at WPI's Washburn Laboratory Shops proved to be a long process by not being an advanced user of the shop. The delays began from getting appointments set up with the lab managers for consultations, assistance with the software, advice on the proper tools to use, and finally assistance in the manufacturing of parts and necessary components. During the final term it was discovered that Higgins Laboratory in the Aerospace Department had the same setup as provided by Washburn but with a much quicker turnover time.

3.3 Project Management

Due to the nature of the project, with having to develop two testing apparatuses, the team had no team leader, but rather split into two groups with one member in charge of a specific task for that group. The members would switch as to who is in charge depending upon the knowledge and ability of each team member relative to the task. This means that while it may list each member as being responsible for each task, often the member was the head of that task and portions may have been delegated to the other group member as needed.

Harrison Hertlein	Nathan Siegel	Jacob Wilson	Marysol Zamaniego
Tensile Tester Team	Tensile Tester Team	SHPB Team	SHPB Team
DIC camera and adapter research and acquisition	Acrylic samples were cut using the Laser Cutter.	Created acrylic sample via sanding.	Copper pulse shapers were created using an Arbor Press
DIC software usage and acquisition	Linear potentiometer selection and installation.	Modified Matlab program to be more accurate and user friendly.	Created Steel test samples utilizing CNC Lathe and the required software to create ESP files.
DIC data analysis	Electronics box design and emergency power cut-out system.	Aligned and realigned SHPB whenever necessary.	Breadboards and external components (broken strain gauges and wires) were replaced and soldered.

Harrison Hertlein	Nathan Siegel	Jacob Wilson	Marysol Zamaniego
Tensile Tester Team	Tensile Tester Team	SHPB Team	SHPB Team
Sample preparation for tests (surface painting and speckling)	LabView PID control systems (Force-hold and strain-rate).	Made circuit improvements: installing variable resistors, replacing shunt resistors, characterizing gain.	Blast box was created for safety purposes during tests.
LabView UI Improvement	MATLAB data analysis.	Conducted SHPB tests on steel, copper, acrylic, and aluminum samples.	Solidworks and ANSYS were used to create and simulated a bars together test of the SHPB.
		Processed SHPB test data in Matlab to obtain plots and stress-strain curves.	Meetings were coordinated. Rooms and projector for weekly meetings were reserved for each term.
		Fixed the SHPB whenever issues arose i.e. broken strain gauges, wires, etc.	
		Wrote SHPB user guides.	

3.4 MQP Objectives, Methods, and Standards

3.4.1 Tensile Tester

- The analytical software tools used for the Tensile Testing apparatus include:
 - Simulink was used to model the PID controller to obtain initial gain values to tune, reducing tuning time on the tensile tester.
 - LabView was used to collect force and displacement data, actuate the linear actuator, and to execute the PID control loops for the force-hold and constant strain-rate testing programs.
 - VIC-2D 2009 was used to calculate principal strains from a video of the sample as it undergoes a test.
 - MATLAB was used to generate force, strain, and stress-strain graphs utilizing data obtained from both LabView and VIC-2D 2009.
- The tensile tester has to control a linear actuator, which exerts a load on a sample that is held in place with two testing grips. A load cell and linear potentiometer will provide force and displacement data, which can be turned into stress and strain data, following the assumptions made in the theory equations section for this apparatus.
- ASTM D3039 for composite materials

3.4.2 Split Hopkinson Pressure Bar

- The Split Hopkinson Pressure Bar has no specific standards to oblige to, but the software and testing setup requirements are discussed below.
- The analytical software tools used for the SHPB apparatus include:
 - SolidWorks was used to model the SHPB test system's physical characteristics such as specific material used and the actual dimensions of the apparatus' bars.
 - ANSYS was used to replicate the actual experiment in perfect conditions as well as create a consistent and accurate stress-strain curve for the experiment at a

“Bars Together Test” in order to compare to the stress-strain curve created using MATLAB and the data provided from the experiments.

- MATLAB was used to calculate curves and create stress-strain graphs utilizing SHPB test data acquired from the oscilloscope. The bulk of the MATLAB code was taken from previous year’s project however, significant improvements were made to its accuracy and the code was made to be easier to understand for users.
- In order to conduct experiments on the SHPB, the system had to be developed utilizing a gas gun in order to propulse a projectile onto a specified area in order to collide with a series of adjacent bars and a sample test specimen. These bars will then be analyzed using strain gauges, and an oscilloscope to obtain test data from the experiment. The SHPB must follow a series of assumptions that are discussed in detail in sections above, however, these assumptions are utilized to ensure accurate results are being collected.

4. Tensile Tester Modifications

4.1 Physical Modifications and Additions to the Tensile Tester

One MQP team had previously worked on the tensile tester in the past. This team performed the initial feasibility study, defined standards that the tester needed to adhere to, and started work on the machine. They designed and machined the structural components so that only small deflections would be observed in the frame, as well as selecting a load cell, linear actuator, and grips to be used in the tester. They also developed a basic LabVIEW program to control the tester and record data. At the end of their MQP, their tester was fully assembled and could accurately measure the force being exerted on a sample by the linear actuator. However, their chosen method of displacement measurement wasn't accurate enough to provide usable data over the range of the tests performed. Improvements to the strain measurement system would be needed both to produce useful data and to be used in the control system of the tester. For the capabilities of the tester at the end of their MQP, their LabVIEW program was sufficient, however in order for reliable and fast tests to be performed a control loop needed to be added, as well as improvements to the user interface.

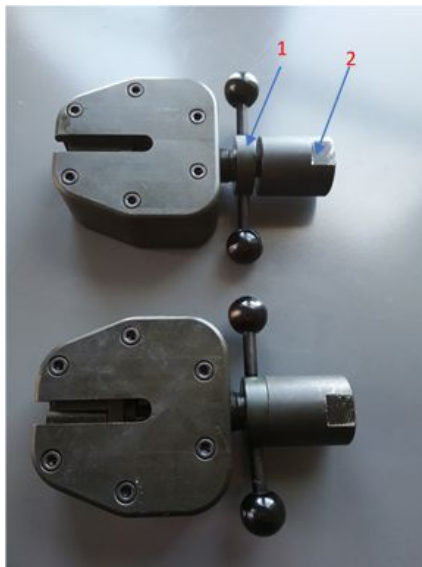


Figure (5): Tensile Tester Grips Disassembly Diagram

In addition to controls and sensor upgrades, maintenance was required for the tester. In observing the tester, it was apparent that maintenance such as tightening bolts, and fixing the grip was required to bring it up to a more usable state. Fixing the grip involved needing to separate the sections of the grips as labeled below as 1 and 2 in Figure 5, due to the two parts being stuck together. With help of Washburn Labs, the grips were able to be taken apart, regrease, and reassemble the grips so that they both work similarly.

Two other physical additions to the tester were made. First, a mounting adapter for the LCP12S sensor described in the next section had to be machined. This had to be designed so that it wouldn't interfere with the grips or the linear bearings attached to the moving base of the tester. Second, an electrical limit switch had to be added to keep the moving base from striking the LCP12S sensor or its mounting adapter. This switch was designed using Autodesk EAGLE, and all of the traces are appropriately sized to withstand the PA-17 actuator running under full load. The relay used is a TE Connectivity 1432866-1 automotive relay, chosen for its high continuous current throughput, standard form factor, and low cost.



Figure (6): LCP12S Mounting Adapter



Figure (7): Electrical Limit Switch

4.2 Direct Strain Measurement

DIC (Digital Image Correlation) is the primary method of strain detection in the Tensile Tester. However, DIC requires post-processing to calculate the principal strains of each sample, so it cannot be used during the test itself, and cannot provide a preliminary indicator of the success of the test. In order to provide both of those capabilities, a potentiometer of some kind is the logical choice for position. Potentiometers provide capabilities that other sensors do not, at vastly reduced costs.

Last year, the tensile tester used a rotary potentiometer that came with the PA-17 Linear Actuator. This potentiometer was selected for coarse position control, but was unreliable for displacements under 1 cm. In order to accurately detect strain in a sample, a much higher precision sensor is required.

Although the specifications of the rotary potentiometer aren't listed, the linearity can be determined by moving the actuator at a constant rate and measuring the voltage response. The closer the response is to the theoretical line, the lower the linearity.

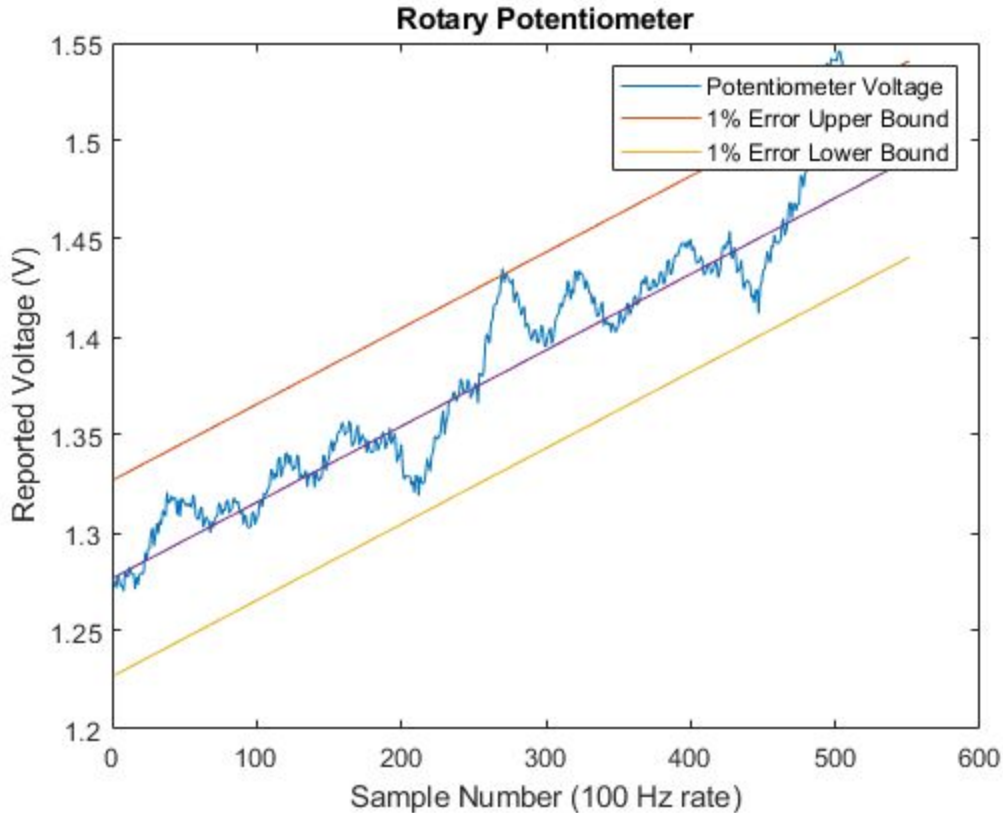


Figure (8): PA-17 Potentiometer Linearity Test

The above graph shows a constant-motion test, with an upper and lower bound listed, showing that this potentiometer has a linearity of roughly 1%. This linearity would be acceptable for sensing purposes, but the potentiometer sweeps over the entire range of the actuator’s movement. The model of PA-17 that was purchased in the previous year has a travel distance of 24 inches (61 cm), therefore the maximum precision that can be reliably measured is approximately .61 cm (1% of the total range). Because manufacturing long samples is impractical, most materials cannot be measured by this sensor.

Improving the fidelity of the displacement measurement is essential to obtain a strain estimate accurate enough to use as preliminary data and as a control input for the LabView automated testing methods developed. In order to do so, a new potentiometer is needed. After consideration of several different sensors, the ETI Systems’ LCP12S-25-10K sensor was determined to be sufficient for use on the tensile tester. It is a linear potentiometer with a total resistance of 10K Ohms, a linearity of 1%, and a total travel distance of 1 inch (2.54 cm).

Although the linearity of the LCP is the same as the PA-17's potentiometer, the LCP only operates over a 2.54 cm range, as opposed to the PA-17's 61 cm range. The addition of this sensor increases the measurement precision by more than 24 times, which is sufficient for strain rate control and some preliminary data analysis. Additional reasons for the selection of this sensor over others was its small form factor, low price, and the inclusion of a spring return, which simplified integration with the rest of the system.

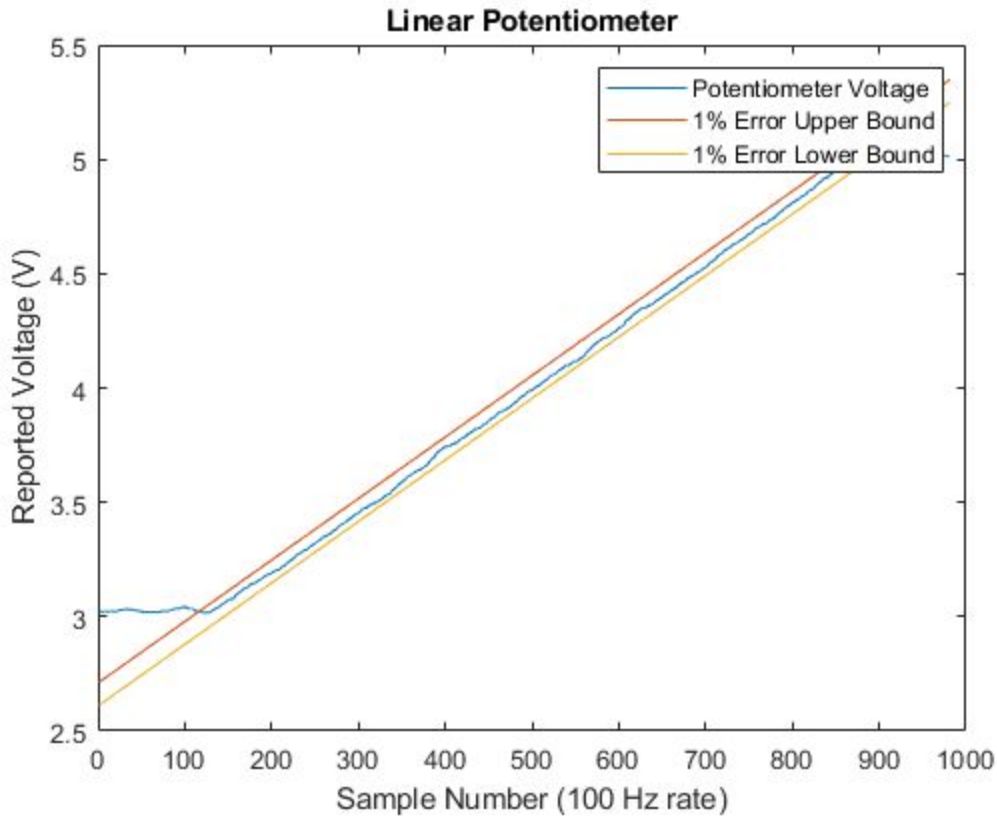


Figure (9): LCP12S Potentiometer Linearity Test

The graph above shows a similar test to the one performed on the PA-17 actuator's potentiometer. The error is well within the 1% upper and lower bounds, as prescribed by the LCP's datasheet. Upon further analysis, the actual linearity is closer to 0.5% for this particular sensor, allowing more accurate measurements to be made. To better show how much more accurate the new sensor is, the error bars from the LCP are superimposed on the PA-17's potentiometer test below:

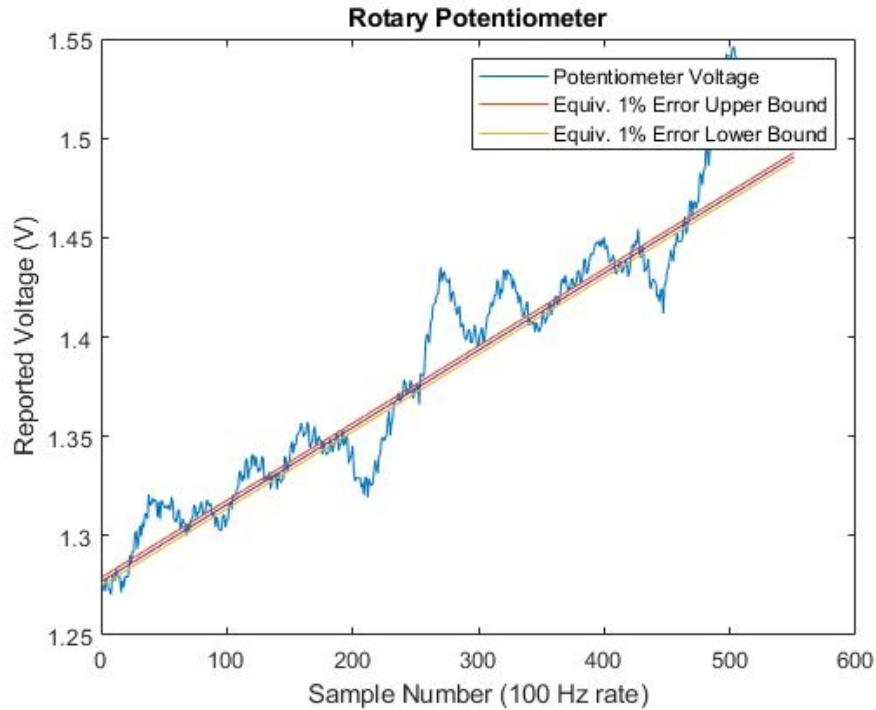


Figure (10): PA-17 Potentiometer Linearity Comparison

4.3 DIC

The use of a digital image correlation software with the tester was planned from previous years. To use the software, access was provided by the Aerospace Department, and it opened up the requirements of what camera would be needed. DIC works as a correlation software for images with a variation on the pattern present. It compares the different frames that are used compared to a reference frame, so that the software can track the movement or distortion of the material that is being tested. This means a camera with a decent frame rate and higher resolution would be required. The patterning that would need to be created for its use also determined the requirements of how to pattern the sample that will be tested.

One of the assumptions/requirements for the use of the digital correlation software, is that the camera must be planar to the sample, Figure (11). This is to eliminate any 3-dimensional strain calculations from needing to be used and allows for the use of only one camera to measure

the strain in the sample as a 3-dimensional strain analysis would require two cameras and different software.

The chosen camera ended up being from Edmund Optics, a monochrome camera for use in strain measurement, model CM3-U3-13Y3M ½" Chameleon®3 from FLIR. A monochrome camera was used as monochrome cameras record values of an image in shades of grey, or as a color value between white and black. This helps in the DIC as there is a higher resolution due to a simpler sensor with higher imaging capabilities, and the DIC can use those values in its calculation. The camera also required two adapters in order to use the lens provided by the grad program. This was an adapter from a CS- to C-mount lens, and a C- to F-mount lens. This is due to the lens being a Nikon F-mount lens.



Figure (11): DIC Camera Setup with Lens and Lens Adapters

Other minor but still necessary requirements for the DIC was the purchase of a tripod and cable for use in the communication with the camera. The tripod is necessary for a stable setup of the camera and to help ensure that as little vibration passing through to the camera as possible. The tripod also allows to easily frame the sample in the image to be captured. As for the cable, it was required for communication with the camera and control of it from the FlyCap 2 software. With the cable and the software, it makes it capable of being controlled and saving the images captured.

One of the issues that appeared with the software is the flicker of the lights in the running of the DIC. It provided a visual flicker in the images of the brightness on the background of the image while recording and may have contributed to some error in the software's analysis of the strain. In researching this, it was found that the outlets provide AC power at 60Hz (Country Household Voltages) and fluorescent lights typically run at about 120Hz (Veitch, 1995). The camera was then set to 30 fps, which means that there exists the overlap of the flash of the lights and the capture of the images, while there is no visual difference in the images captured, there may be a source of error in the images themselves, and there is still the flicker in the images when observing.

Another issue that became apparent was the density of the pattern of the sample. In the first set of results, there wasn't proper full field strain distributions apparent in the sample as shown in other typical samples. This full field strain distribution, is typical of uniform strain in the sample which is what was being attempted in the samples created (Technical Spotlight, 2014). In consulting with the advisor for the project, a much denser pattern on the samples was suggested. The differences in the patterning and the differences in the analysis from other sources' tests are shown below.

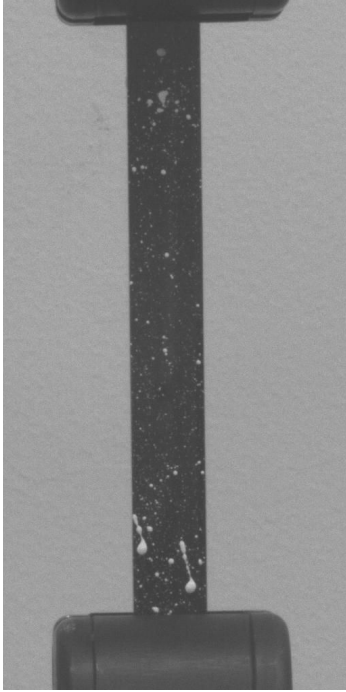


Figure (12): Acrylic Test Sample 1

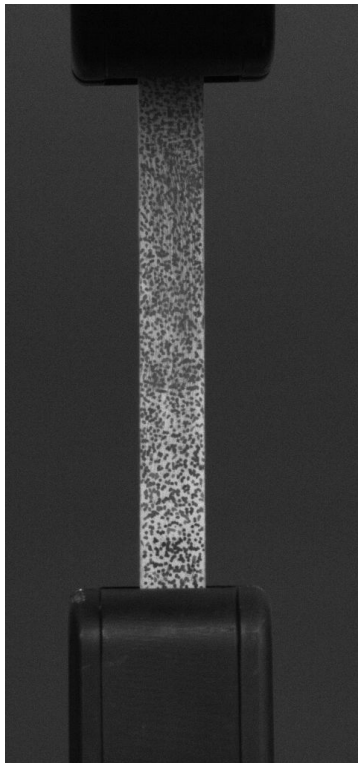


Figure (13): Acrylic Test Sample 3

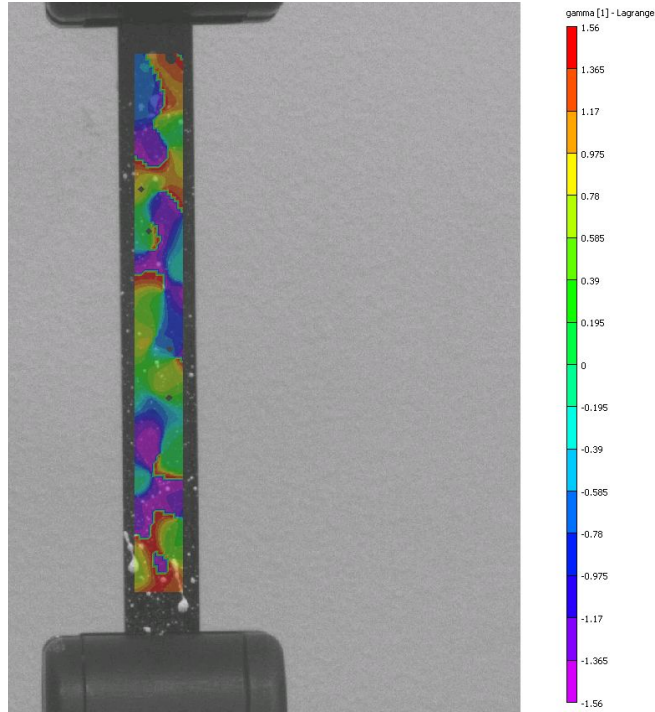


Figure (14): Acrylic Test Sample 1 Example Full Field Strain Distribution

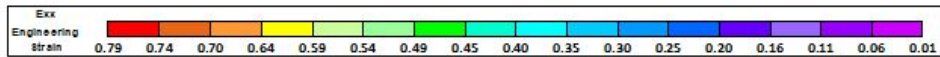
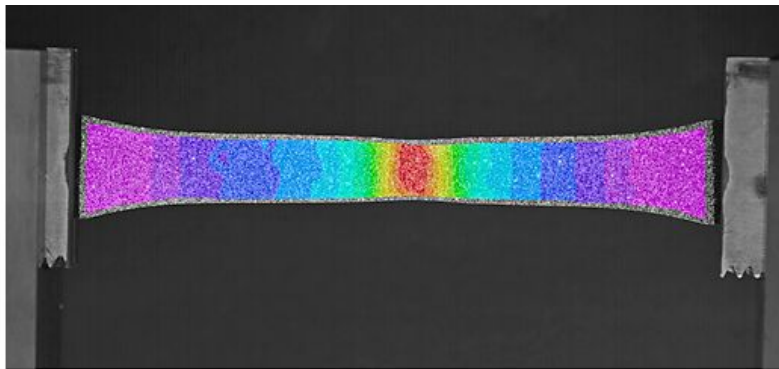


Figure (15): Full Field Strain Distribution of a Test Sample from *Veryst Engineering*

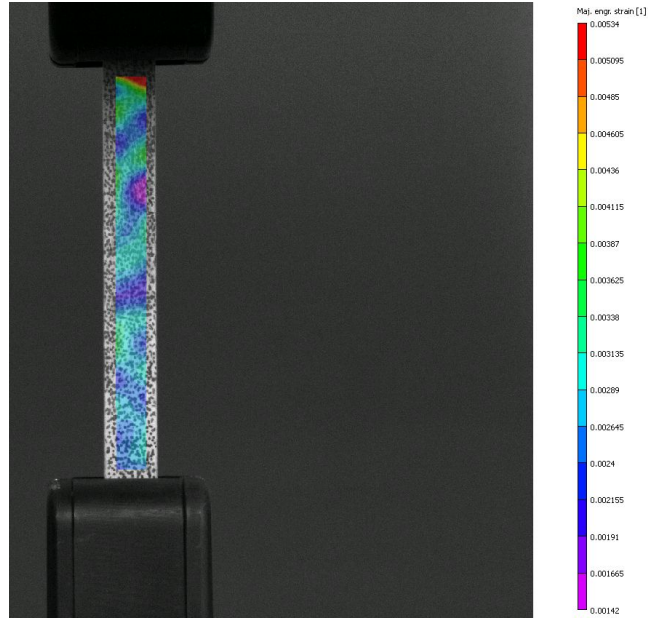


Figure (16): Acrylic Test Sample 3 - Example Improved Full Field Strain Distribution

As one can see from the full field strain distributions in the above figures, the improved patterning was able to show better strain distributions across the samples that made it clearer that the sample is under a uniform load, and that the variation of the full field strain distribution was from the inadequate patterning of the sample being able to be picked up by the digital image correlation software.

4.4 Program Modifications and Additions to the Tensile Tester

The LabView program that existed at the beginning of this year's MQP had little organization and was difficult to use. There was a dialogue box that showed where the data was recorded, two graphs that displayed force and position, and a slider that controlled the movement of the linear actuator.



Figure (17): Original LabView Program

This program was difficult to use, because it required accurate clicking on a small area (the slider), and was always recording, making the test setup more difficult. The first changes made were to simplify the manual control, adding in buttons to move at set speeds, and to enable or disable data recording, allowing setup to be performed without restarting the program. The emergency stop button was also connected to the PWM control loop, which immediately stops the actuator.

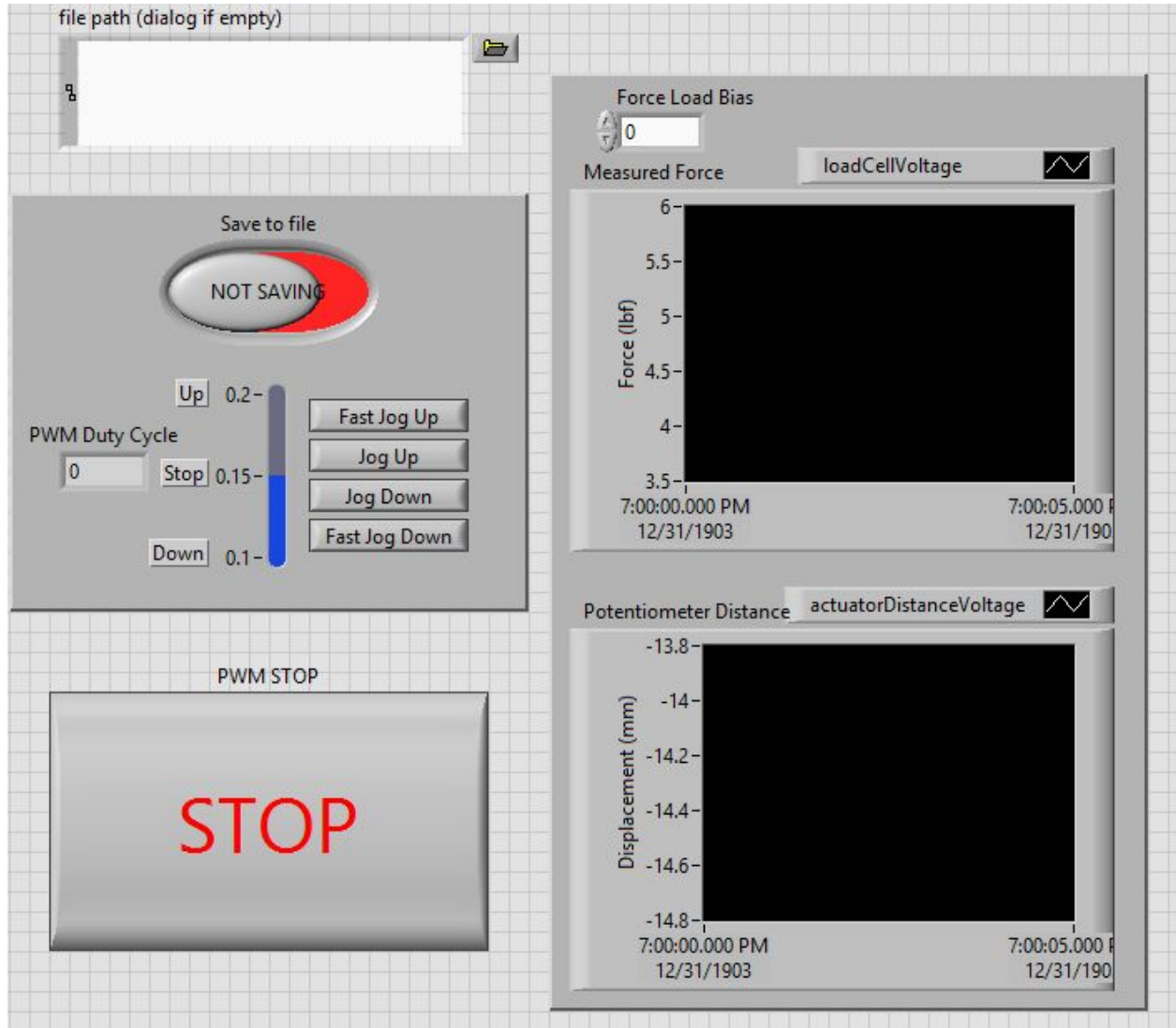


Figure (18): Manual Control Panel

The PID controller was implemented in the PWM loop of the LabView program for simplicity. Since the PID controller would feed into the PWM loop. The equations used to develop this controller are listed in the literature review section, along with several code blocks and smoothing terms to eliminate actuator jitter due to sensor noise.

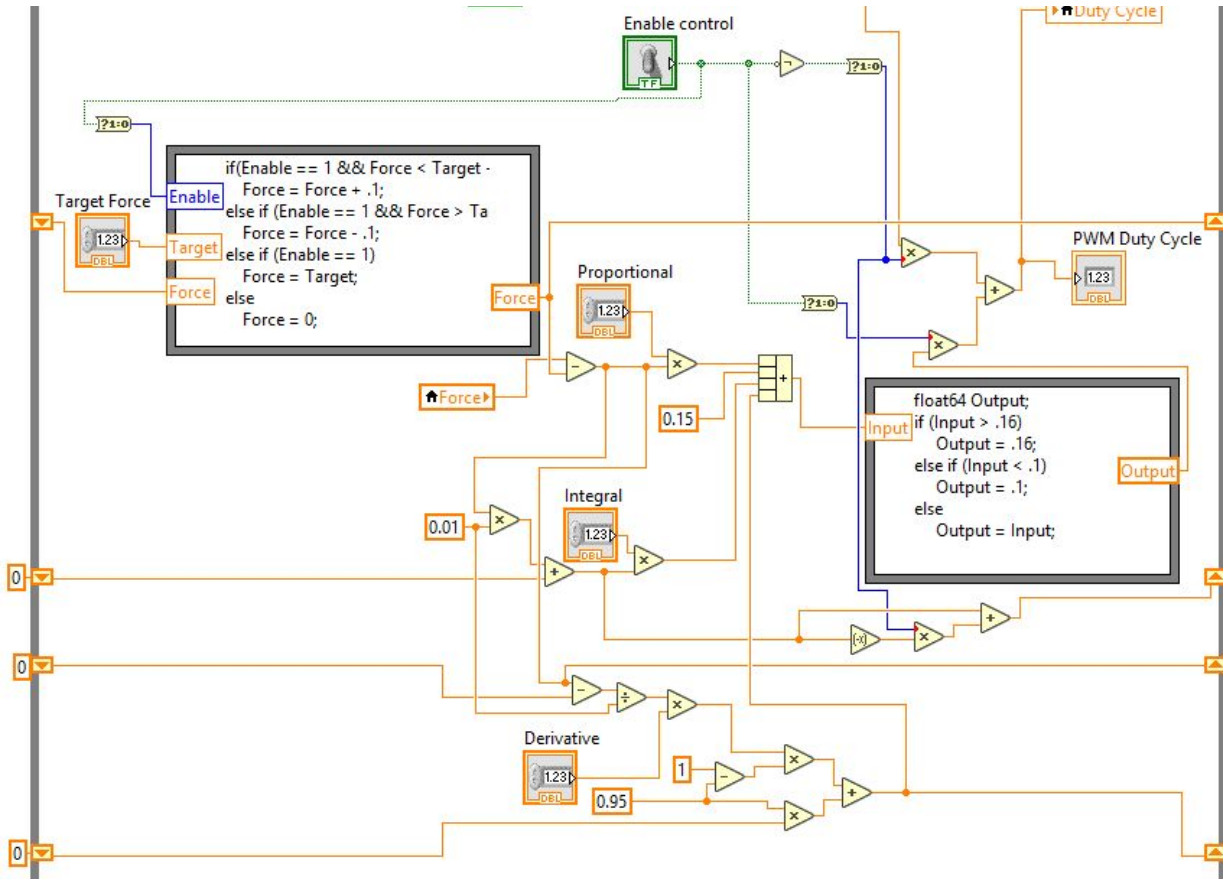


Figure (19): PID Loop Block Diagram

After PID had been implemented in LabView, the first program that was written was a force-hold test, where the tensile tester would ramp up the force that the sample experiences until it reaches a set value, where it continues to hold indefinitely. This type of test is called a creep test and is useful for determining the strain response of materials to constant loads (Long Term Performance of Polymers). The panel on the right contains all the indicators and adjustable variables required to operate the force-hold program.

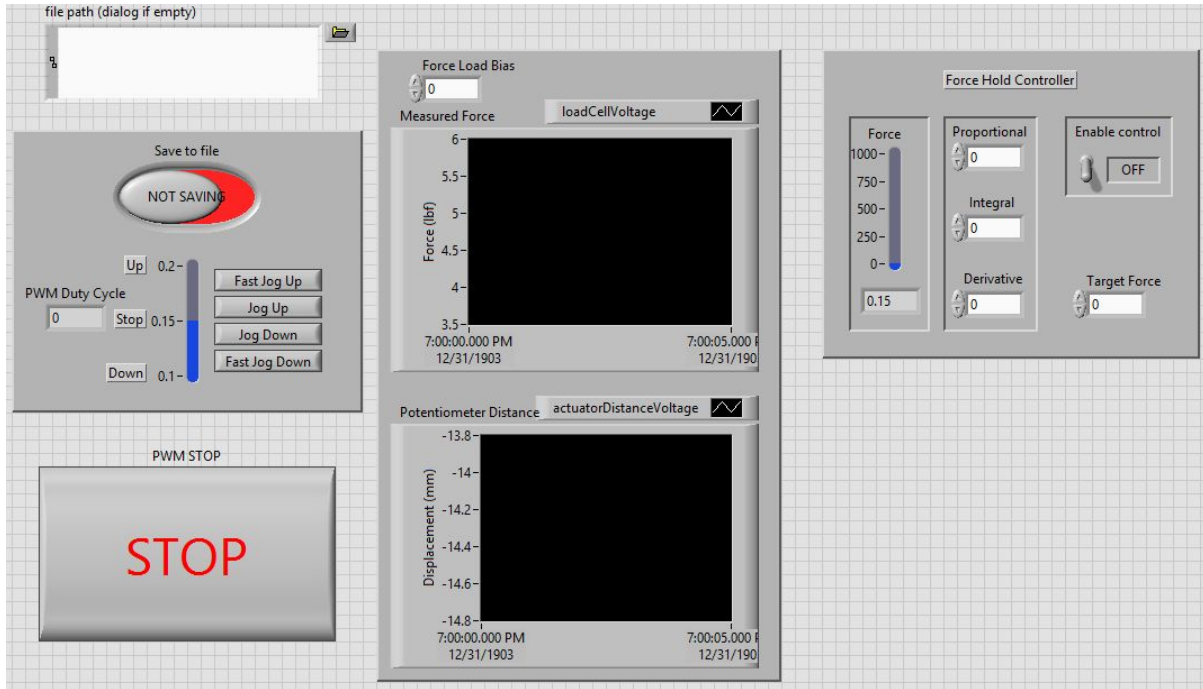


Figure (20): Force Hold Program

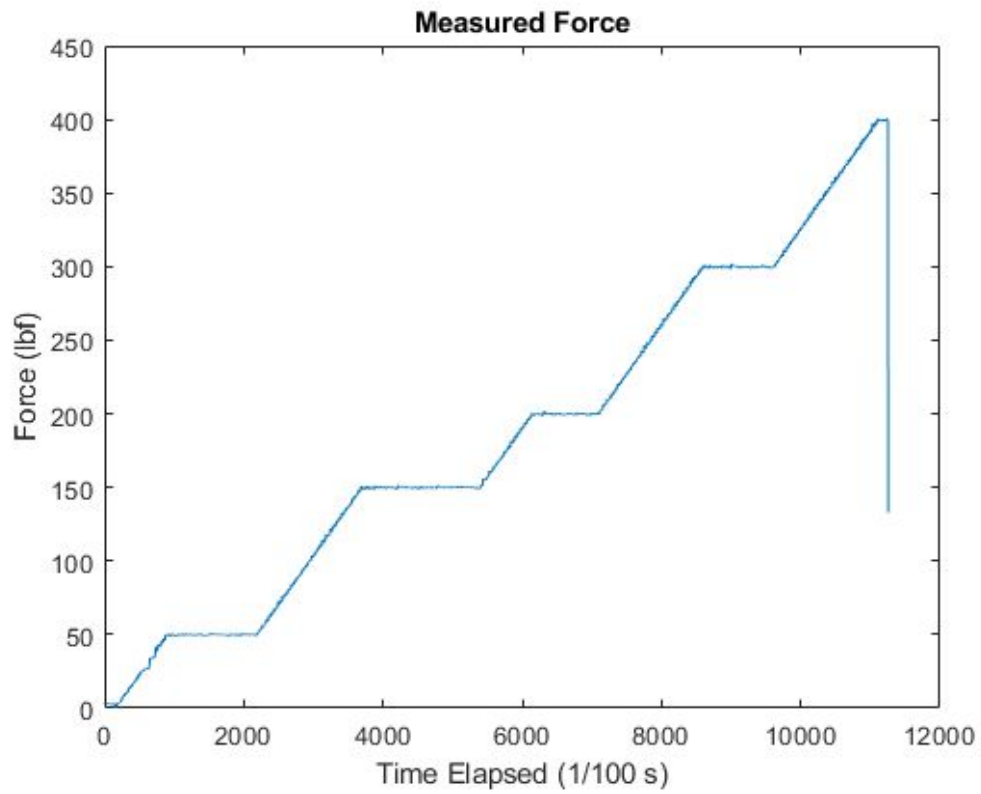


Figure (21): Enabled Force Hold Controller

After the force-hold program had been implemented, the program was adapted to use the linear potentiometer's position, to move the base of the tester at a constant rate. This type of test is standard for determining stress-strain curves (Khlystov, 2013). Like the above program, the panel on the right contains all the indicators and adjustable variables required to operate the strain-rate program.

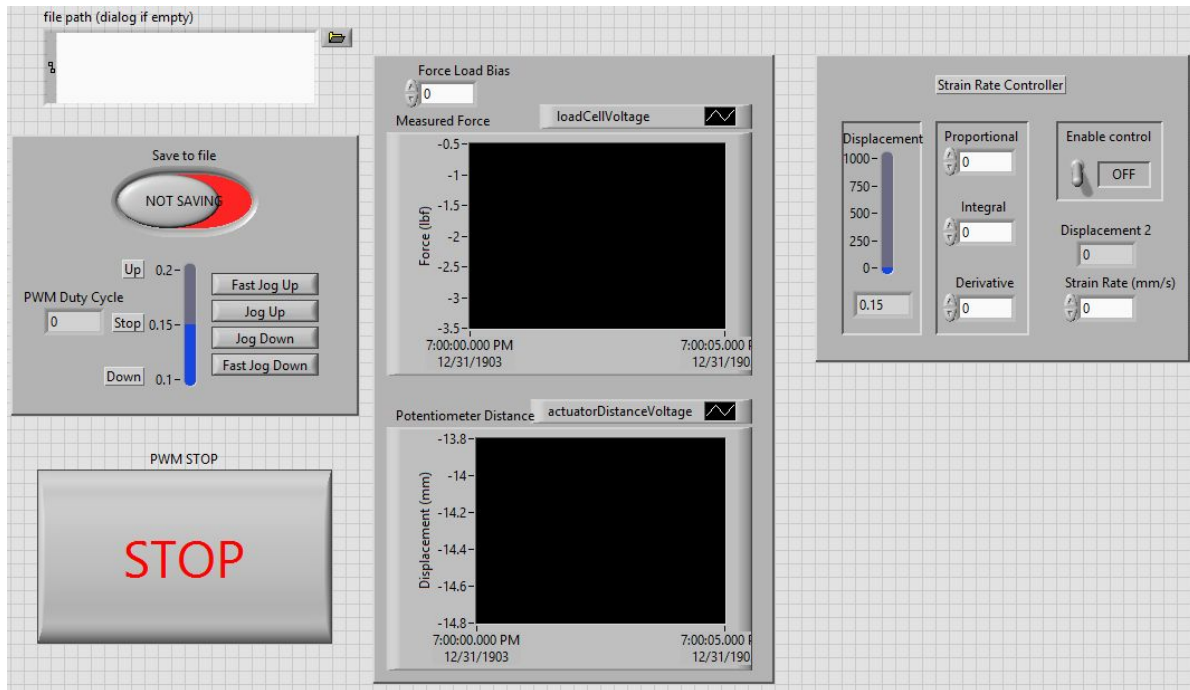


Figure (22): Strain Rate Program

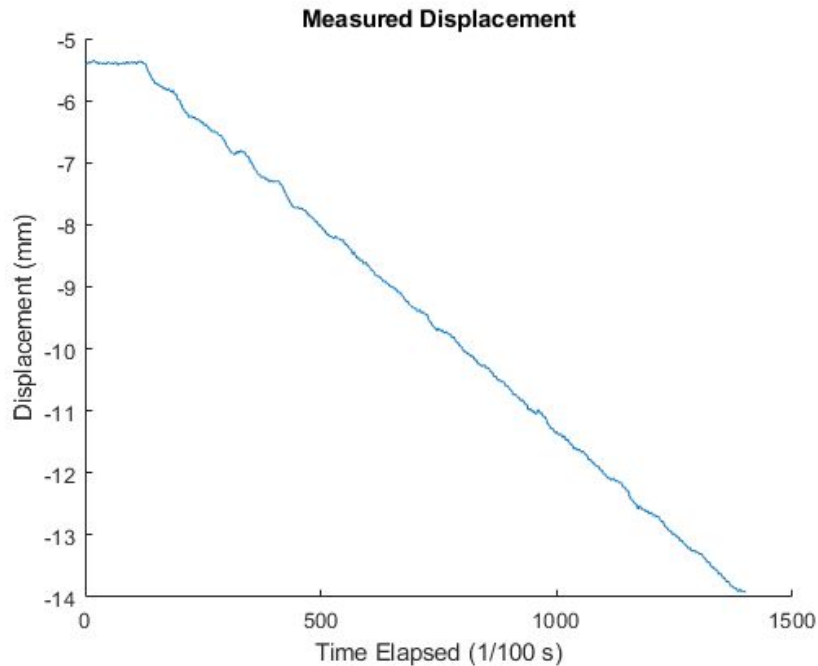


Figure (23): Enabled Strain Rate Controller

4.5 Tensile Tester Data

The first few tests performed with the tensile tester were to determine the functionality of the new programming controls. These samples were not recorded for their strain measurement due to several reasons. Primarily, the camera required to record the samples was not available then. As a secondary reason, recording was not done with the use of mobile devices since it was determined more would be done with the analysis of the data that is available through LabView signal conversion from the instruments.

During the next batch of tests, it was realized that the graduate program that owned the lens, didn't have the adapter needed to attach to the camera. A new adapter set was ordered in order to continue borrowing the lens and still be able to use the camera instead of having to get a specific lens for it. This decision was determined from short research into buying a lens and buying an adapter and finding that most lenses were much more expensive than buying a CS-C mount lens adapter and a C-F mount lens adapter. Because of the wait for the lens adapters, it

was resorted to momentarily using the data from the linear potentiometer, and the force cell to calculate the stress-strain curve.

For the final 4 tests, good data resulted from them. These tests had a much denser pattern on it made from painting the sample white in several layers. On top of it small dots were added in a random pattern using a fountain pen. The ink adhered and was dense enough for the DIC to properly analyze. The data obtained from the tests are shown below. One feature to note of the tests below, the raw strain data of test 4 shows a peak in the strain going up to about .55 (55% strain), which appeared to be an abnormality. In looking for sources of error, it was found that the peak is from a single frame, which corresponded to the single frame captured at the instance of breakage and captured the motion of the sample.

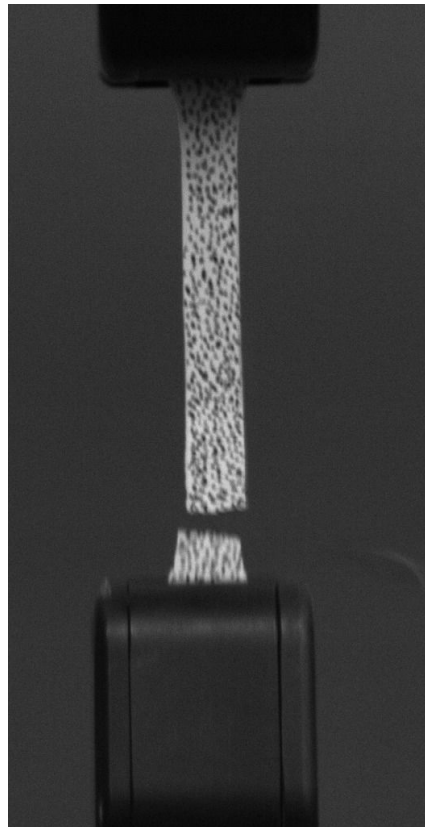


Figure (24): Acrylic Test 4 Strain Plot at $t = 18.75$ sec (Image Captured During Breakage)

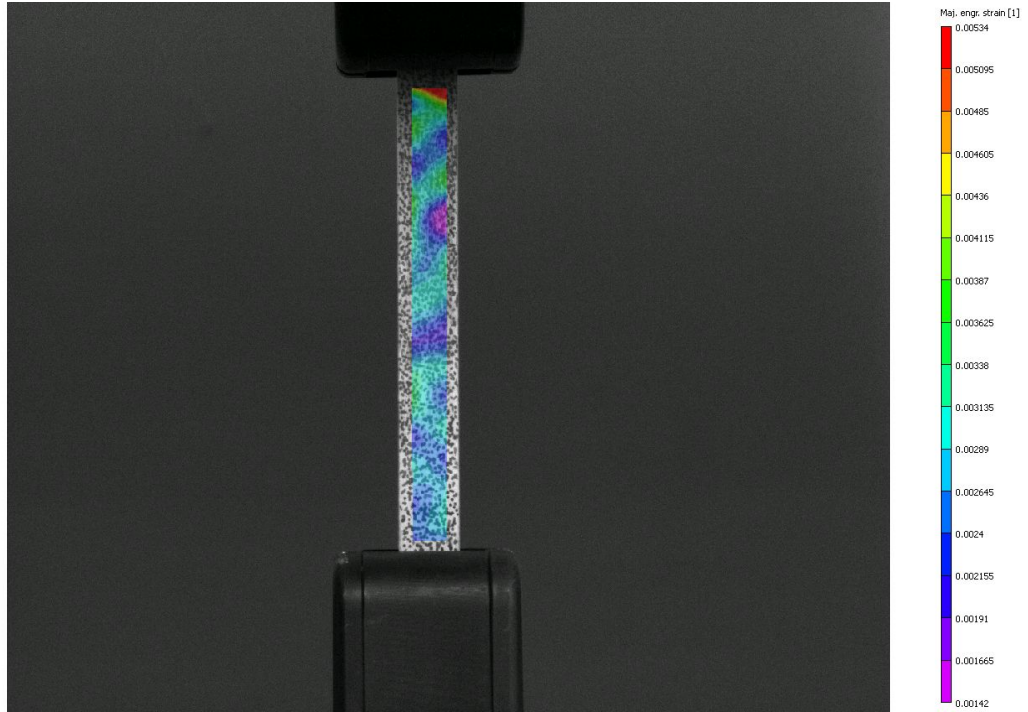


Figure (25): Acrylic Test 3 Strain Plot of Image at $t = 5.875$ sec

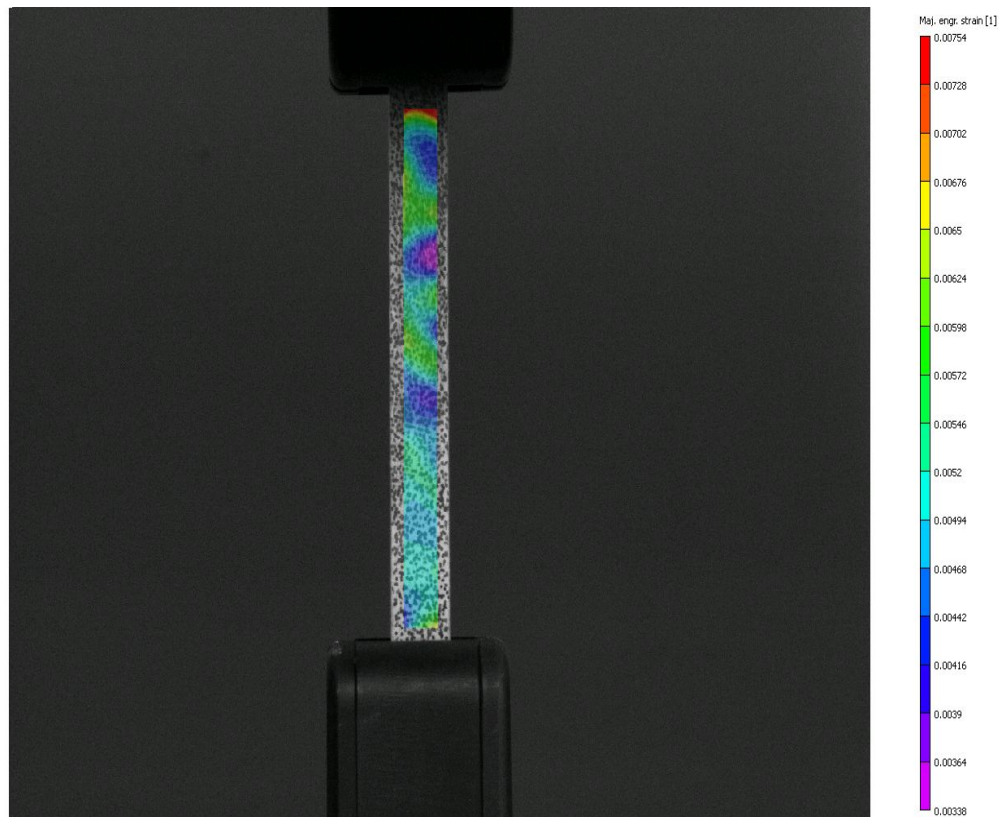


Figure (26): Acrylic Test 3 Strain Plot at $t = 8.53125$ sec

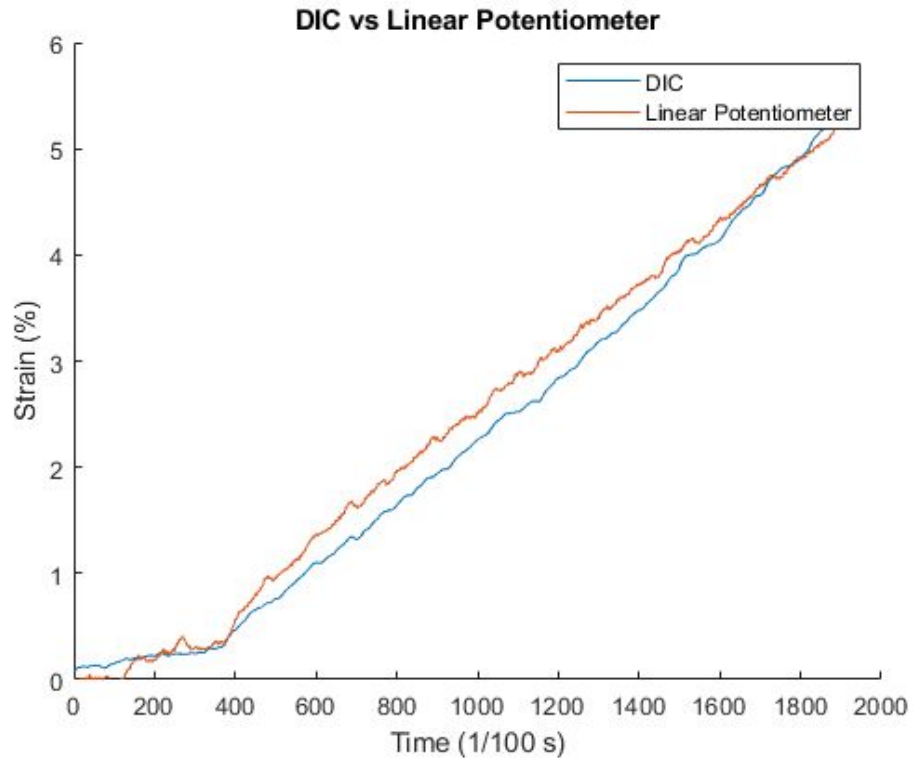


Figure (27): Acrylic Test 4 Strain Graph Comparison

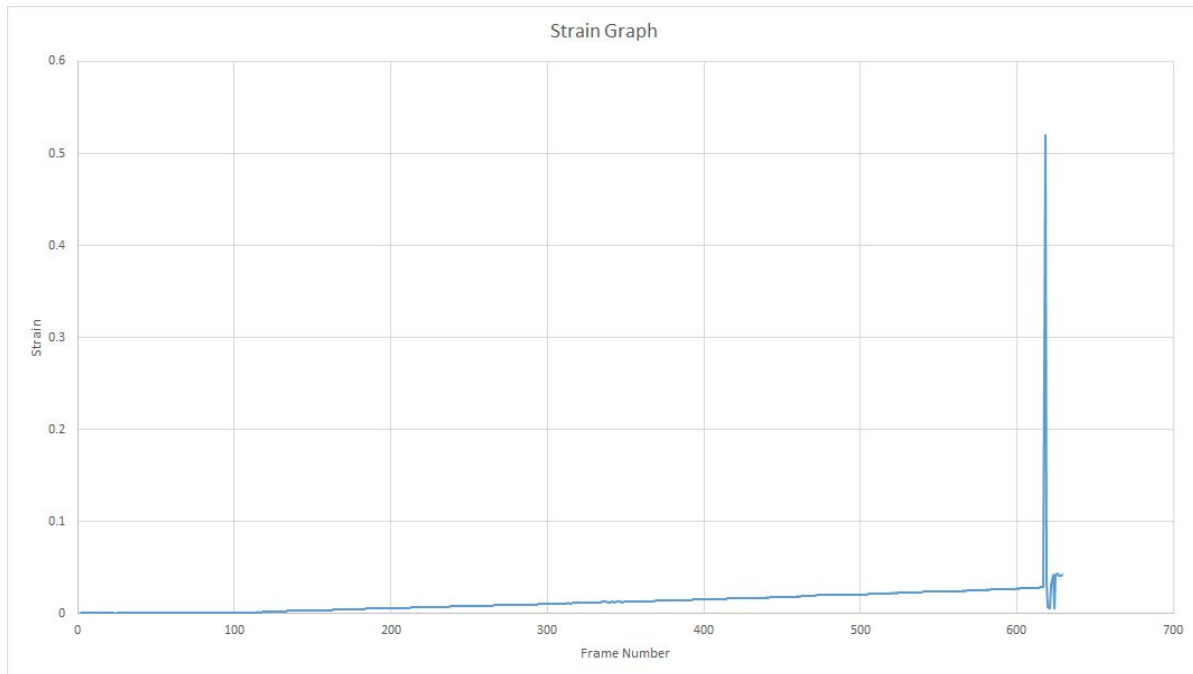


Figure (28): Acrylic Test 4 Raw Strain Graph

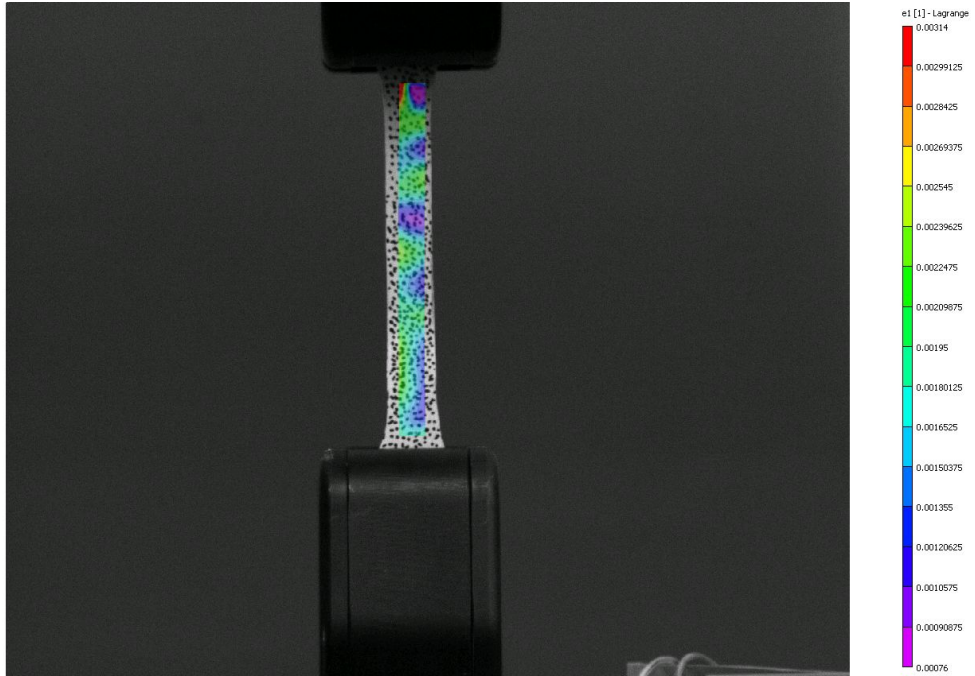


Figure (29): Acrylic Test 4 Strain Plot at $t = 3.15625$ sec

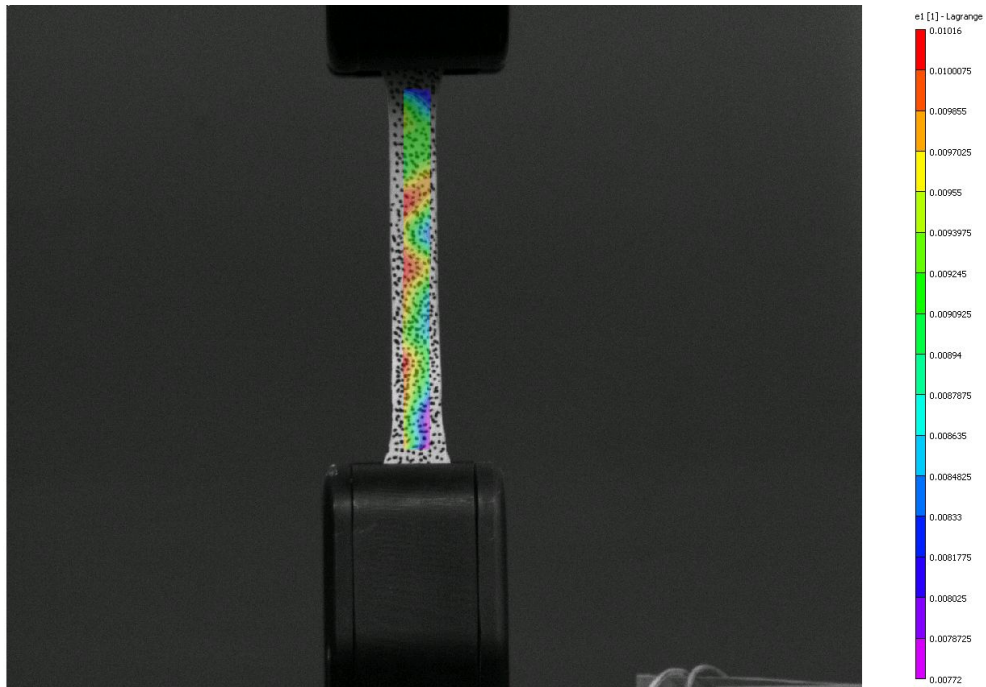


Figure (30): Acrylic Test 4 Strain Plot at $t = 7.875$ sec

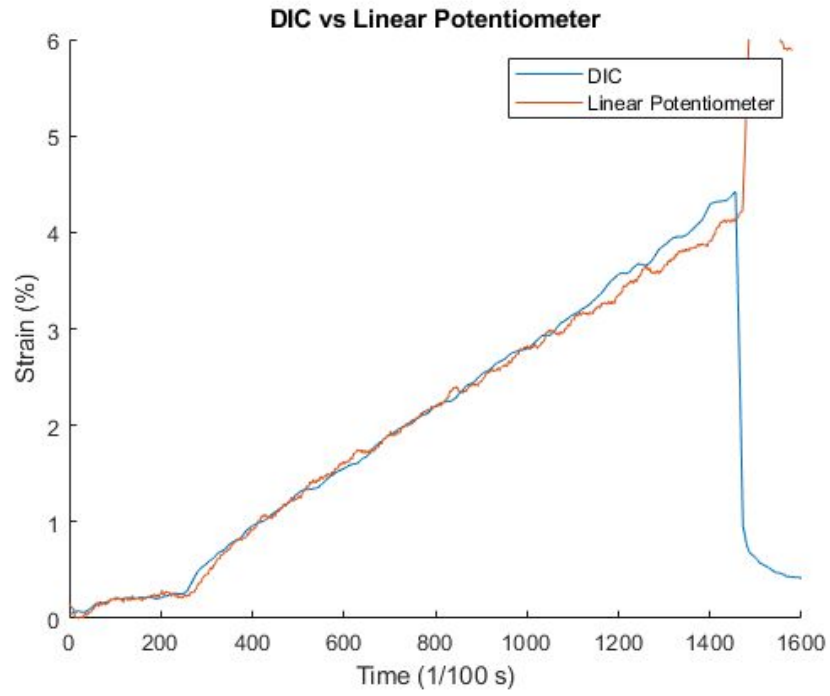


Figure (31): Acrylic Test 5 Strain Graph

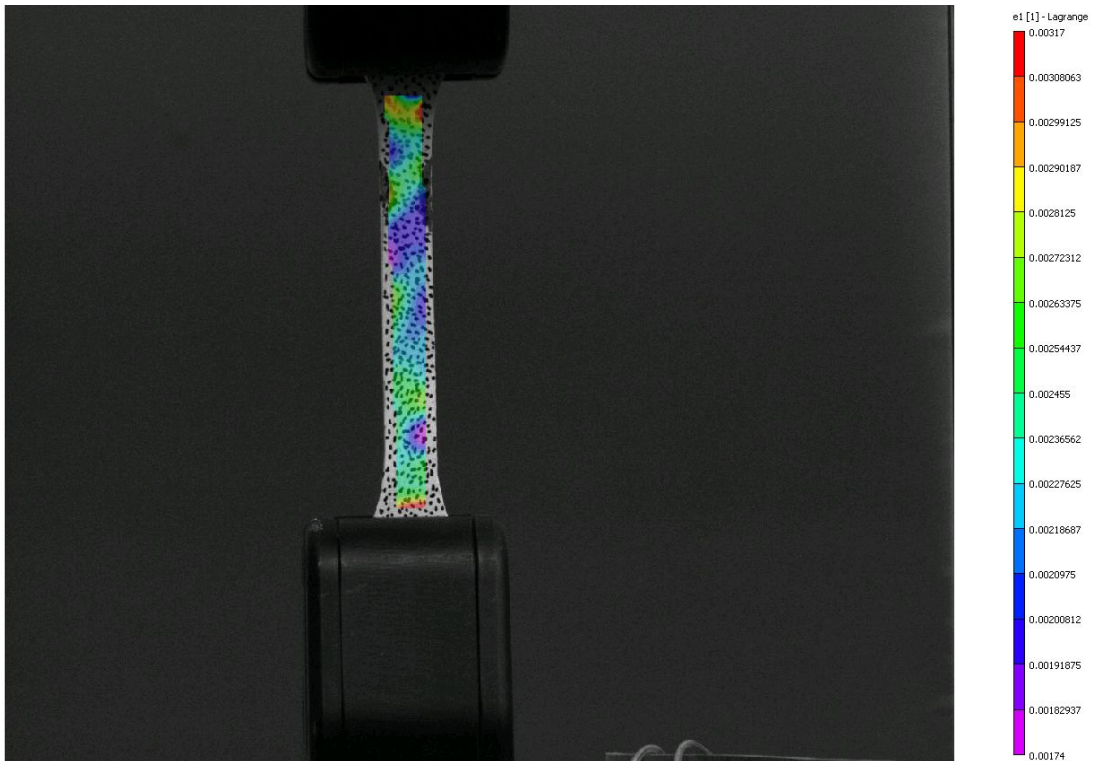


Figure (32): Acrylic Test 5 Strain Plot at $t = 2.71875$ sec

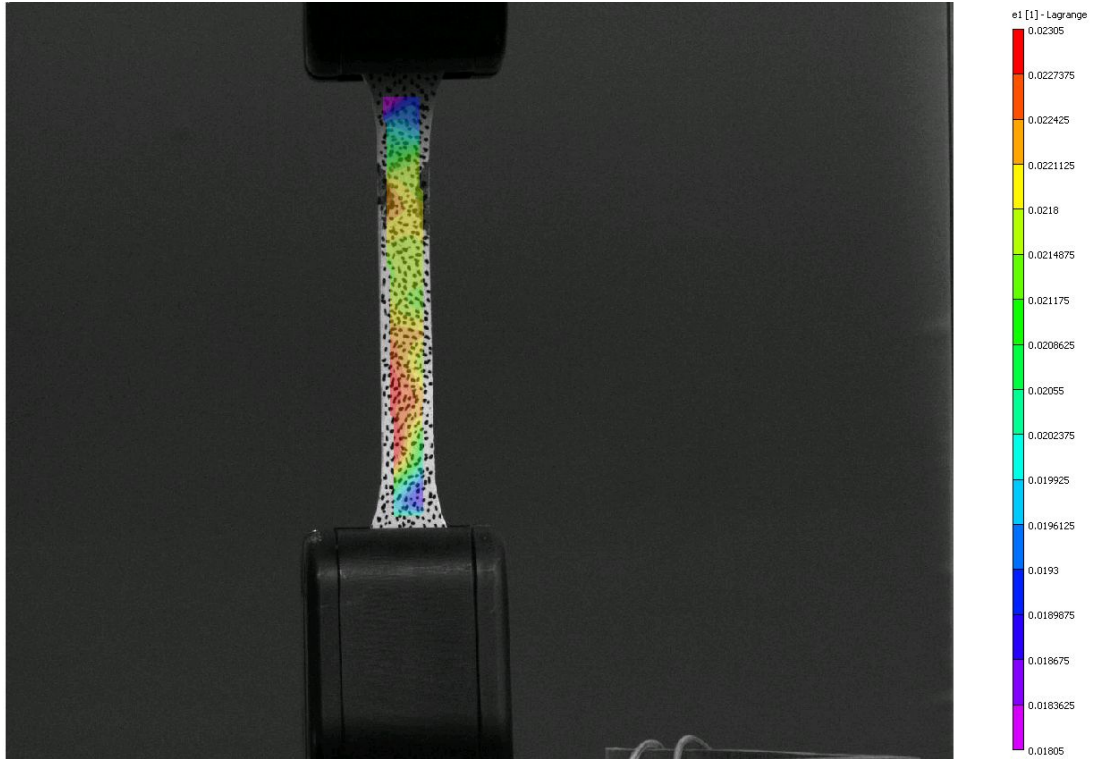


Figure (33): Acrylic Test 5 Strain Plot at $t = 13.625$ sec

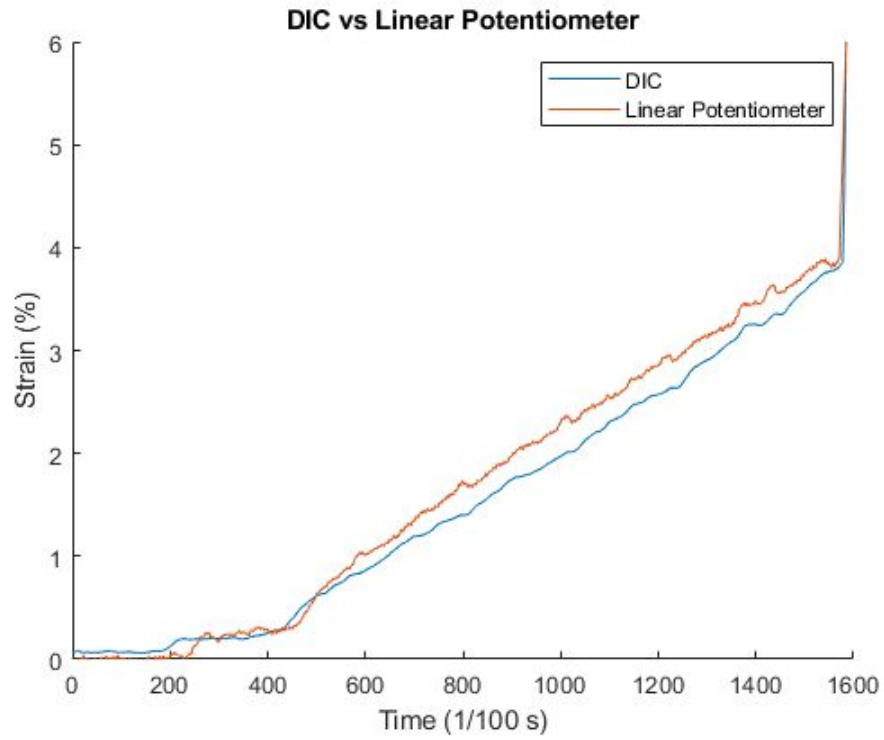


Figure (34): Acrylic Test 6 Strain Graph

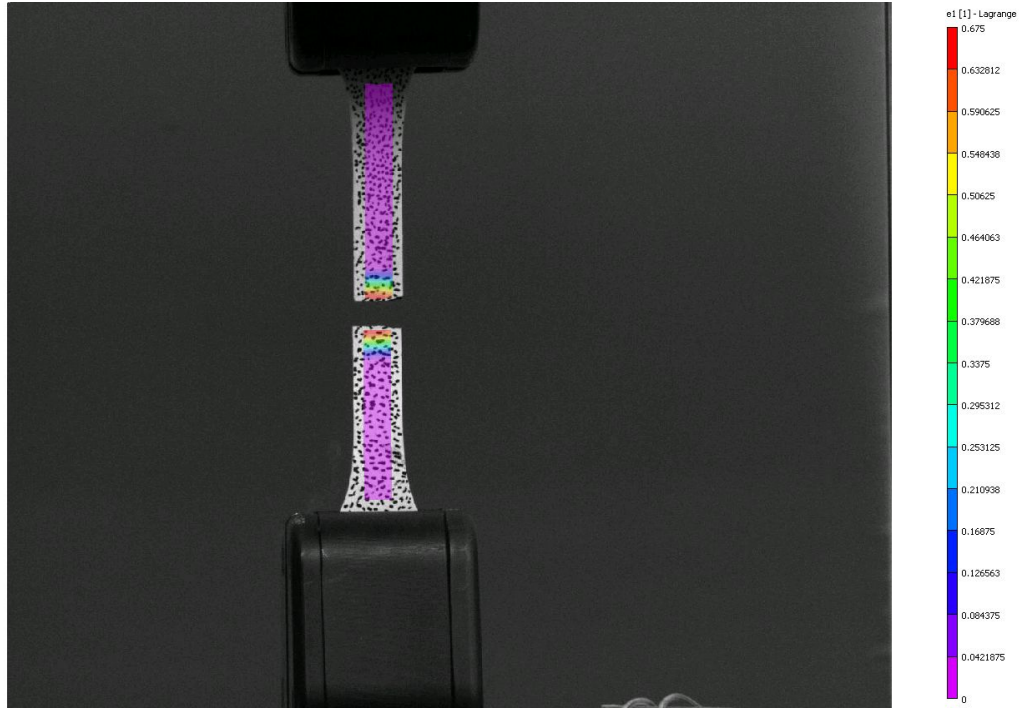


Figure (35): Acrylic Test 6 Strain Plot at $t = 15.625$ sec

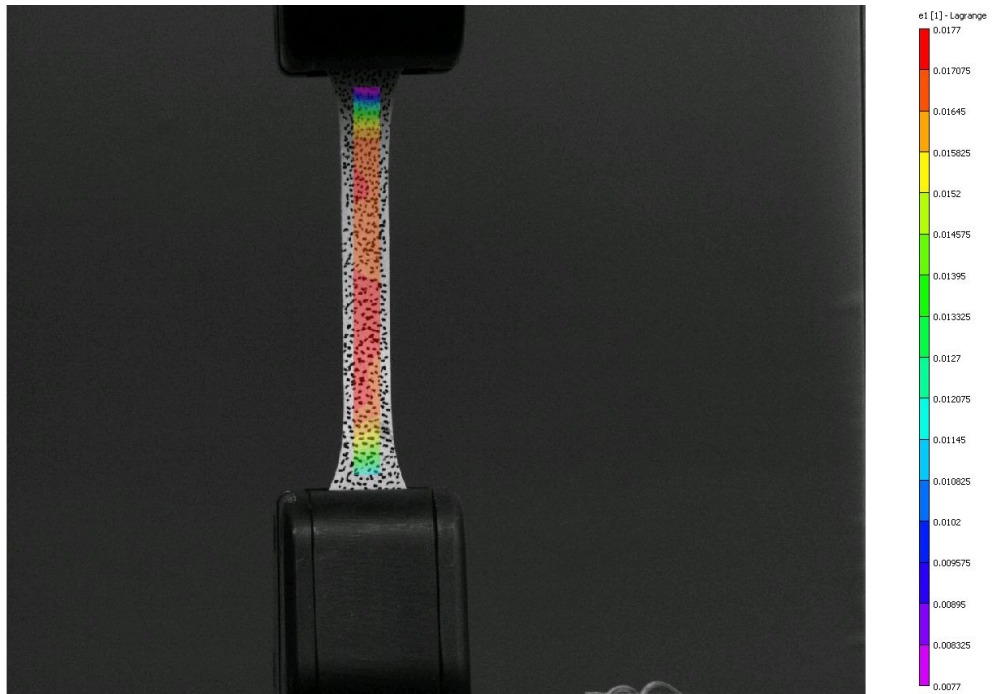


Figure (36): Acrylic Test 6 Strain Plot at $t = 14.84375$ sec

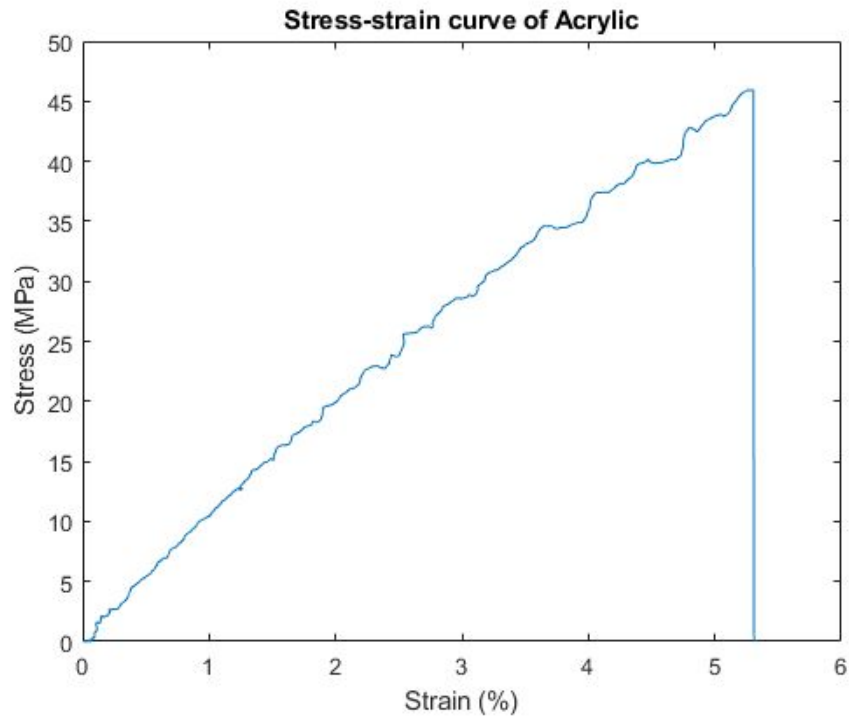


Figure (37): Acrylic Test 4 Stress-strain Curve

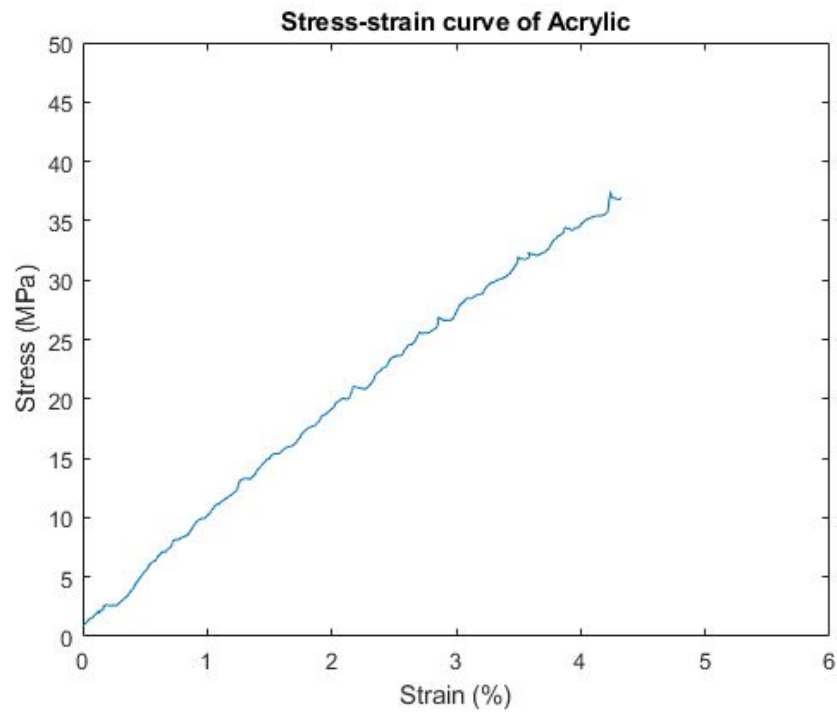


Figure (38): Acrylic Test 5 Stress-strain Curve

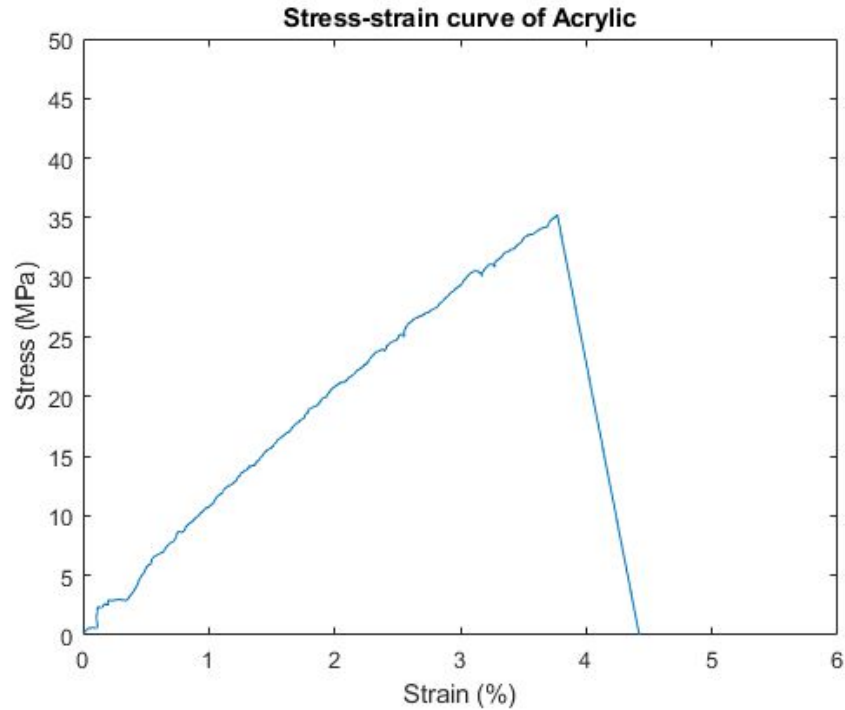


Figure (39): Acrylic Test 6 Stress-strain Curve

5. Split Hopkinson Pressure Bar Modifications

5.1 Summary of Modifications to the SHPB

Two previous WPI MQP teams had worked on the SHPB in the past. These teams built the physical setup, designed an original version of the circuit, designed a working matlab code to process gathered data, and conducted several tests. These tests showed a working SHPB that successfully gathered a stress-strain curve, however these curves did not prove that the SHPB was accurate, not matching outside results for the same material. This was likely due to the previous MQP team using a different alloy hardness than that tested by other groups. The setup itself successfully worked, but was severely flawed. The circuit would often have loose wires, shunt resistors would not work properly, and the wheatstone bridge was never well balanced. These circuit issues resulted in less accurate test results, and often failure for the system to acquire data. The trigger that the former MQP team had designed had a tendency to activate prior

to a test again resulting in a failure for data to be recorded, as well as wasting test samples. The design of the pulse shapers being used in tests created further issues in gathering reliable data. Furthermore, when the current MQP team first attempted tests with the SHPB, the circuit had degraded to a state that conducting tests back to back was nearly impossible. Finally, even when data was gathered, the matlab code over processed this data, and was far from user friendly making it even more difficult to obtain accurate results.

Building off of this work done by the previous two WPI MQP teams, numerous modifications were made to the SHPB to fix these and other issues making the setup more reliable and accurate. These modifications were carried out on the circuits themselves, the oscilloscope triggering method, the size and thickness of the pulse shapers being used, location of the strain gauges, construction of a blast box, the matlab code used to process the data, and the alignment process. Each of these modifications will now be discussed in greater detail.

5.2 Circuit Improvements:

When testing first began for this project to repair the SHPB to a reliably running condition again after months without use, the original circuits used for the bars were noted to be located on simple solderless breadboards. This made adjustments to them extremely easy, however it also resulted in wires coming loose, and losing contact with the metallic plugs of the breadboard, an issue that only increased with repeated use of the setup. Furthermore, these problems were often hard to spot and required checking each wire connection until the issue was found, far from an efficient method. It was decided that the best way to fix this was to replace the solderless breadboards with solderable breadboards creating a much more permanent setup that would no longer be prone to loose wires. The exact same layout for the general connecting wires, strain gauges, and shunt resistors was kept.

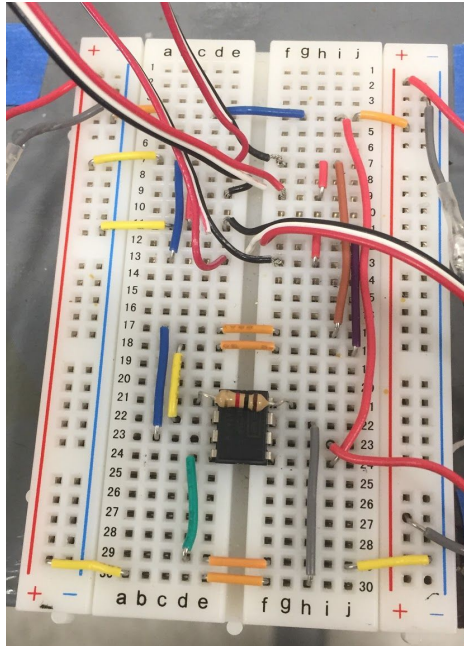


Figure 40: Previous Solderless Breadboard

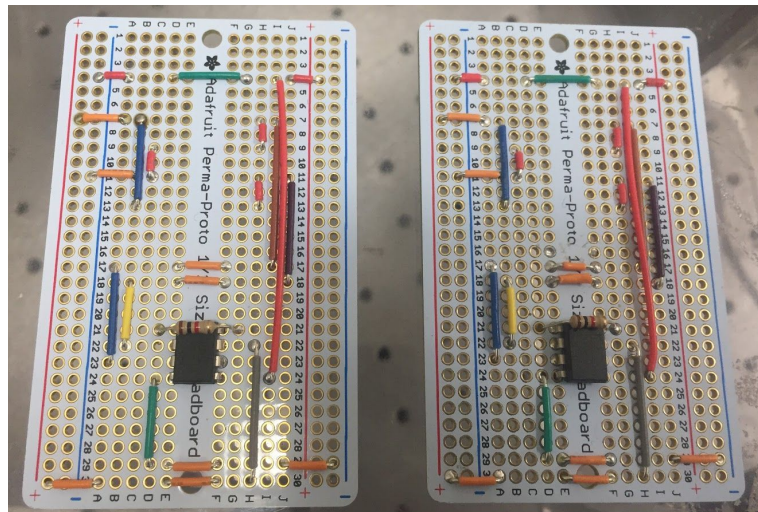


Figure 41: New Soldered Breadboards Unconnected to the SHPB

The original SHPB circuit also contained as shunt resistors, two strain gauges that were mounted to an aluminum block and covered in hot glue to keep them in place. While this originally may have been adequate, in the months since the setup had been used the condition of these shunt resistors had deteriorated, and the leads of these strain gauges would at times come

into contact with the aluminum block underneath the hot glue. This resulted in the shunt resistor completing a circuit with the block and throwing the wheatstone bridge out of balance ruining several attempted tests. After these frustrations it was decided that these shunt resistors would have to be replaced to this frequent source of issues to improve the reliability of the setup. As the strain gauges being used were of 120-ohm resistance, 120-ohm resistors were purchased and soldered in their place. These new shunt resistors never caused fluctuations in resistance as the previous shunt resistors had, or caused the circuit to overload, reducing another source of error and reliability issues.

The original SHPB wheatstone bridge was never closely balanced, as the difference in resistance of its branches was dependent on the specific resistances of the wires, resistors, strain gauges, and even the solder used on each side. This imbalance was reduced by replacing the solderless breadboards and hot glued shunt resistors, producing a more constant amount of resistance on each side, however these sides were never close to being balanced. This resulted in the wheatstone bridge producing a constant voltage difference between the two branches of upwards of 30 mV. Though sounding insignificant, when dealing with voltage differences from the strain gauges within the same order of magnitude of the low tens of millivolts, this then becomes a potentially very significant source of error. To reduce this difference in the branch resistances, one of the two shunt resistors in each circuit was replaced with a combination of a 100 ohm resistor and a 0 - 100 ohm variable resistor connected in series (totaling 120 ohms to create a balanced wheatstone bridge with the strain gauges). Finding a variable resistor easily adjustable in such a low range of voltages was difficult. Variable resistors below 1000 ohms were relatively hard to find, and it was also desired to have a variable resistor that could be easily adjustable with a screwdriver. Furthermore, the design of the circuit on a breadboard also eliminated some physically larger options. Eventually the choice was narrowed down between a 0 - 100 ohm variable resistor which would have to be mounted in series with another resistor, or one that is adjustable on a range of 0 - 1000 ohms, both of which were readily available already in the lab, and were adjustable with a knob that could take a flat blade screwdriver. After testing with both, it was decided that the 0 - 1000 ohm variable resistor was much less accurately adjustable in the range of the 120 ohms required and would only produce slightly more accurate

results at best being able to adjust to the nearest 10 ohms, while the 0 - 100 ohm variable resistor could be adjusted to achieve a wheatstone bridge that could be balanced within 1 mV of zero, a massive improvement upon the original design. This much closer balance further resulted in more accurate data.

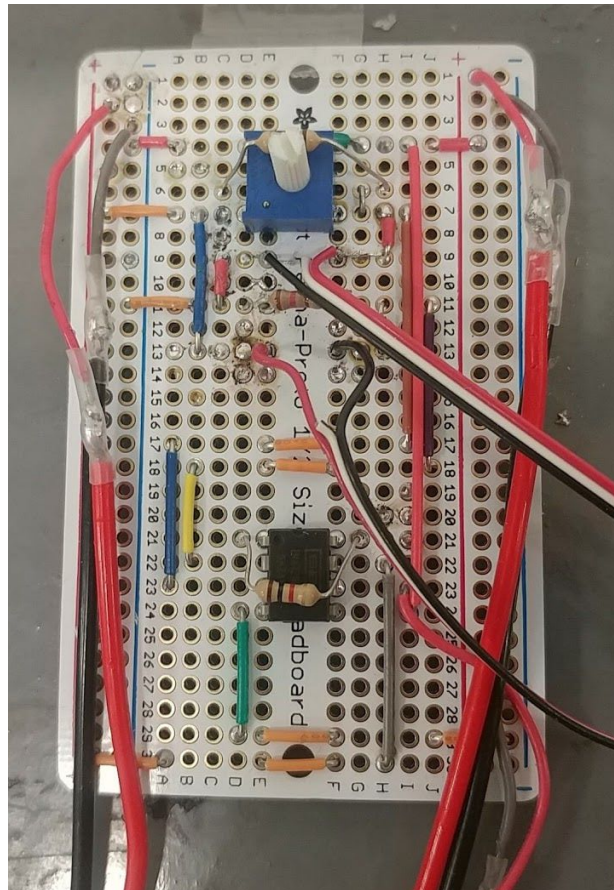


Figure 42: Soldered Circuit With 120 Ohm Shunt Resistor and Variable Resistor Setup

Together, these improvements to the circuit resulted in far fewer issues with the breadboards, the shunt resistors, wires coming loose or breaking, wires shifting and coming into contact with each other, as well as allowing for a much closer balance of the wheatstone bridges. This greatly increased the reliability of the setup, as well as its accuracy, allowing for much less difficulty in obtaining accurate results than the former setup.

5.3 Trigger Improvements:

The trigger on the oscilloscope is used to determine when the oscilloscope should begin recording data. The original trigger was set to activate whenever the oscilloscope read any disturbance in the incident bar wheatstone bridge greater than 100 mV from the steady state value of the bridge. While this would activate the trigger from the strain wave, it also led to a great deal of mistriggers. These could be caused by numerous, sometimes unavoidable, actions such as opening the valve to the gas gun, or something as simple as bumping the I-beam and causing a slight voltage difference in the wheatstone bridge. These mistriggers wasted pulse shapers, samples, and unnecessarily stressed the SHPB breaking strain gauges and wires from use. Because of these costly (both in time and equipment) mistriggers, fixing the trigger was made a priority. The trigger settings were changed to trigger on a square pulse of greater than 50 microseconds in length, of 50mV - 150mV in magnitude. The length of the pulse was determined to be optimally 50 microseconds as this is less than the length of a strain wave pulse (about 150 microseconds) while long enough that the only causes for the oscilloscope to trigger would be physically adjusting the wheatstone bridge, or reading an actual strain wave. This trigger adjustment led to a massive increase in reliability with only tests triggering the oscilloscope no longer leading to wasted tests and samples.

5.4 Pulse Shapers:

Pulse shapers are used in tests to reduce the oscillations that occur in a strain wave during a SHPB test. Pulse shapers are made of a softer material, such as copper, that plastically deforms spreading the strain wave out while reducing this noise [Split Hopkinson (Kolsky) Bar, Page 43, 2011]. The original setup used copper pulse shapers about two millimeters thick, and three quarters of an inch in diameter. These pulse shapers successfully filtered out the noise, however their size allowed for a great deal of plastic deformation greatly stretching out the strain wave and creating a triangular wave that never allowed the sample to reach stress equilibrium.

Trapezoidal waves are preferred for this reason to ensure stress equilibrium. Through a trial and error process, the size and thickness of the copper pulse shapers was then varied in an attempt to find a pulse shaper that would filter out only the noise while keeping the strain wave trapezoidal. The thinner copper gauges that were experimented with were 24 and 26 gauge. 26 gauge copper of half inch in diameter was found to be the best pulse shaper for this setup, though the deformation of the strain waves still only provided slightly trapezoidal shapes, meaning that a better pulse shaper could still likely be found, especially for lower strain rates in which these waves would be more triangular. These new thinner pulse shapers still much better fit the assumption that the sample reaches stress equilibrium, and also filters many of the oscillations that would be seen in a test without a pulse shaper.

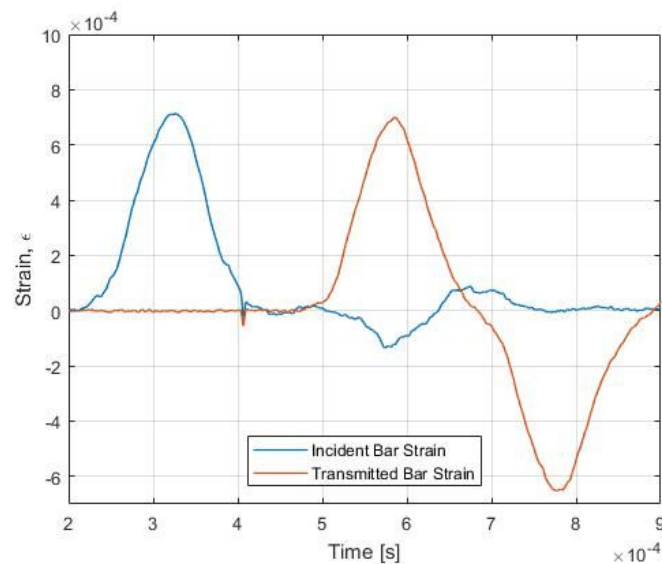


Figure 43: Test Using 2mm Pulse Shaper With Long Triangular Strain Waves

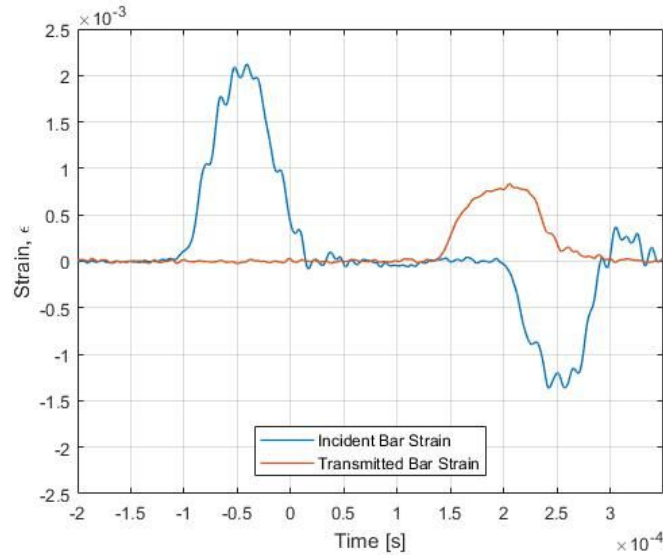


Figure 44: Test Using 26 Gauge Pulse Shaper With Trapezoidal Strain Wave

5.5 Strain Gauge Location:

The location of the strain gauges on the incident and transmission bars is influenced by the length of a strain wave. If the strain gauges are mounted too close to the end of a bar, a strain wave may reflect off the end of the bar prior to the original wave making its way through the strain gauges. This could result in the waves combining and the data thus becoming inaccurate. The original location of the strain gauges on the incident bar were far enough from the end of the bar such that this was never an issue, and there was a relatively great deal of time between the incident pulse and reflected pulse, however the shorter nature of the transmission bar nearly led to overlapping strain waves as can be observed in Figure 41. In this test using the original placement of the strain gauges on the transmission bar, and a thick pulse shaper, the transmission wave, and the wave reflected off the end of the bar very nearly combine, and never appear to truly zero out. To increase the distance between these waves, the strain gauges were moved from their original position of 18 inches from the sample end of the transmission bar, to about 13 inches from the sample end. This movement along with use of a thinner pulse shaper greatly increased the distance between the transmission wave and its reflected wave as seen in Figure 42 which shows a test after this change where the reflected wave off the transmission bar cannot be

seen in the time frame of the figure. This change greatly reduces the possibility of strain waves combining to create inaccurate data, further improving the performance of the setup.

5.6 Blast Box:

During testing it was noticed that samples had a tendency to slide out from between the incident and transmission bars and fly several feet across the room. This was caused by the necessary application of grease to the sides of the sample to help hold the sample in place between the bars, however it did pose a potential safety risk. The prior MQP team had noticed this potential as well, and had designed and cut the parts to a blast box. While the basic parts were already cut, the box had never been assembled. New holes were drilled in the already cut parts and built the protective box for use on the SHPB. The box itself is made of acrylic, screwed together at its ends, and features a latch on the top to allow the box to split in two to allow easy placement around the bars, and also features a window on the side facing the wall to allow for someone to adjust the sample within while the box is in place. This blast box will help ensure that nobody will be injured from a flying sample, and if more brittle materials are tested will prevent splinters from these materials also causing injury.

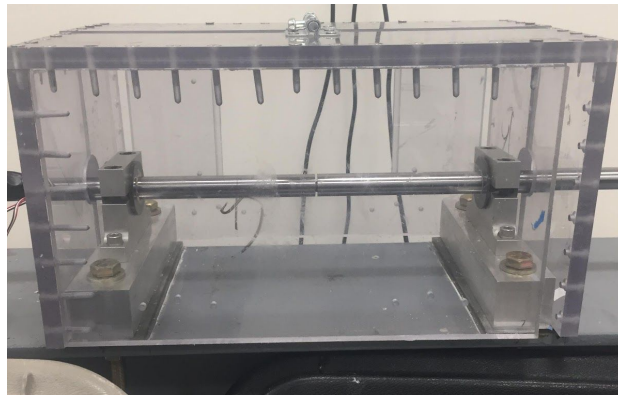


Figure 45: SHPB With Blast Box

5.7 Matlab Code Improvements:

Prior MQP teams had developed working Matlab code that could take test data recorded by the oscilloscope, and calculate stress-strain curves from this data for a tested material. Several improvements were made to this code to improve its accuracy and user friendliness.

To filter out noise from the data, the code utilizes a low pass filter, with a cutoff frequency set by the past group to be twenty thousand hertz. While this cutoff frequency successfully removed the noise from the data, it was decided that the amount of noise removed was too great, and that there was the potential for this filter to be removing potentially significant variations within the data. The cutoff frequency was thus increased to fifty thousand hertz allowing more variation into the data, while still filtering the very high frequency noise in the data. The new cutoff frequency was decided upon by examining the data at a range of cutoff frequencies and choosing one which filtered out the noise, yet still allowed the significant data to pass through.

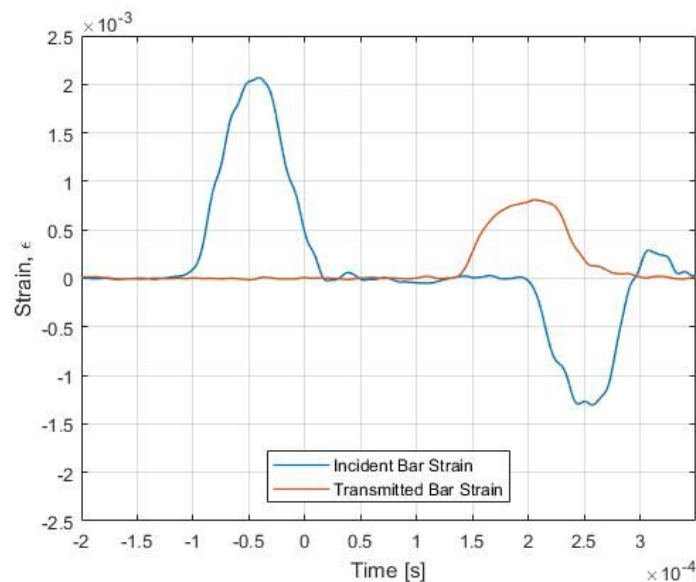


Figure 46: Test With 20000 Hz Low Pass Filter

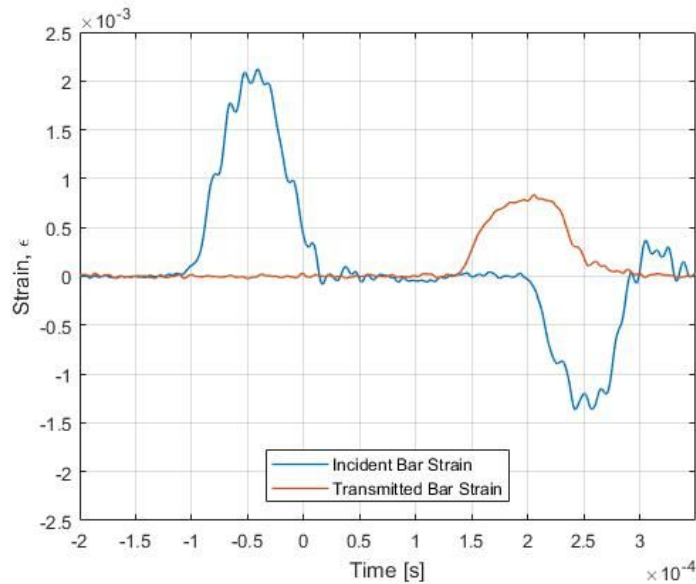


Figure 47: Test With 50000 Hz Low Pass Filter

The code requires a user to input the starting point of the incident, reflected, and transmitted waves, however it failed to provide a user friendly way in which to determine if the starting points of these waves were being correctly chosen. To aid in this, a new plot was added plotting each wave starting at its user selected starting point. This allows for the user to much more accurately determine whether the selected point and length of the wave is correct, leading to the production of more accurate stress-strain curves. Though seemingly insignificant, this new plot saves the user a great deal of time precisely determining the starting points of these waves, and greatly improves the ability of the user to accurately determine these points. Accurately determining the start of these waves, and the overall length of the data sample is vital to obtaining an accurate stress-strain curve. The stress and strain of the sample relies on the magnitude of each wave, these waves must be precisely lined up to accordingly associate the correct stress with the correct strain. Failure to do this accurately can result in stress-strain curves of an inaccurate shape, or with incorrect magnitudes.

A further improvement in the matlab code was the determination of the gains that were applied by the amplifiers on the circuit to the wheatstone bridge voltage that the oscilloscope would read. The amplifiers produced gains that had been assumed to be about 52 times based on

the use of 1000 ohm resistors across the amplifiers. These values were not exact, and depended on the original accuracy of the specific amplifier, as well as the actual exact resistance of the 1000 ohm resistors used to bring the gain from these amplifiers down to 52. These gains were experimentally determined to allow for more exact values to be added to the Matlab code to improve its accuracy. The amplifier works by measuring the voltages of both of the branches of the wheatstone bridge, and then outputting the difference between the voltages multiplied by the specific gain. It was thus necessary to control and measure the inputs to the amplifier as well as the output when the amplifier was isolated from the wheatstone bridge for this calculation. Originally this was attempted using a model 9514 pulse generator, and applying slightly different voltages to the inputs of the amplifier, however this instrument proved unable to accurately achieve this. This pulse generator was not capable of creating pulses below two volts, making it necessary to rely on two separate pulses of only slightly different magnitudes which would be read by the oscilloscope as well as the output. The issue with this was that the pulse generator itself was unable to accurately provide voltages to the tenth of a volt which was the required accuracy to produce a similar voltage difference that the strain gauges would produce in a test. Furthermore, the minimum voltage of two volts meant that the pulse generator was also unable to produce a very small voltage to one input while keeping the other input zero. A different method was then used by applying a very small voltage through the use of a NI DAQ controller instead of the pulse generator and LabVIEW. This voltage was applied to one of the two inputs of the amplifier, and was also measured by the oscilloscope through a connection to the same input row. The amplified voltage was also measured by the oscilloscope in the same manner of its measurement during a regular experiment. To obtain the gain, the voltages were measured of a span of time in which they were relatively steady, and then were averaged over this time span to produce the average gain. This process was repeated multiple times over input voltages of ten and twenty millivolts. The results of these tests showed an average gain of 52.75 for the amplifier on the incident bar, and an average gain of 51.97 on the transmission bar. These values were inputted into the Matlab code to further improve the accuracy of tests.

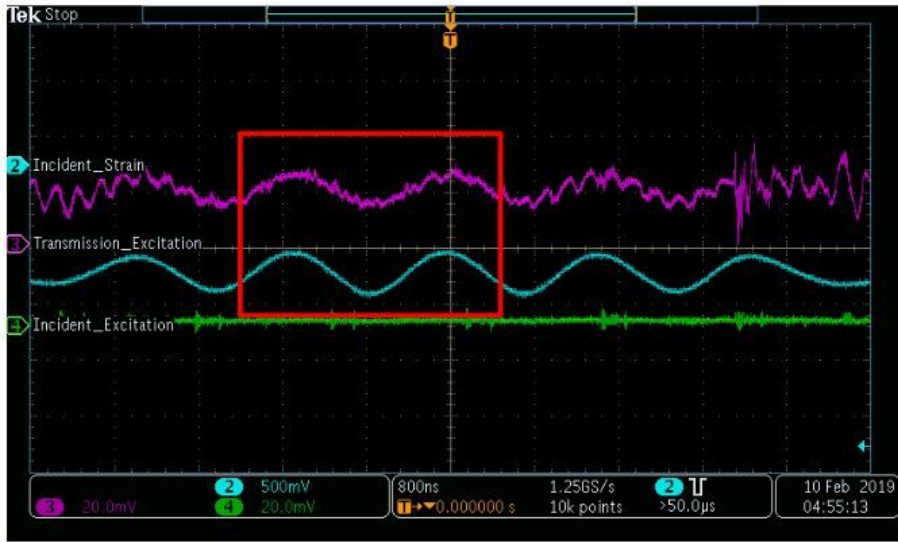


Figure 48: Snapshot Showing Area Where Gain Was Averaged (Pink is the input, Blue is the output, Green is the second input of zero mV)

5.8 Alignment

The SHPB assumes one dimensional wave propagation, that the strain wave only travels lengthwise through the bar. This can only be assumed, however, if the SHPB is well aligned without losses in the strain wave. There are several steps to properly aligning the SHPB, unfortunately prior groups failed to properly document their methods of alignment, so a new system was established.

The first step is using a laser alignment system to ensure that each delrin bar mount is level with the gas gun barrel, and the other bar mounts. To do this a laser is placed in the barrel of the gas gun, and adjusted such that the laser hits the center of the target marked on the momentum trap.



Figure 49: Laser Mounted Inside Gas Gun Barrel

To align the mounts, a specific altered delrin mount was made to serve the purpose as a standard mount that could be used to level each mount such that the laser would show alignment between all of the delrin mounts. This specific delrin mount is of the exact same dimensions as the actual delrin mounts used to hold the steel incident and transmission bars, however its center hole has been covered and marked to show the center of the mount. Using a caliper on several sides of the mount, the exact center was marked.

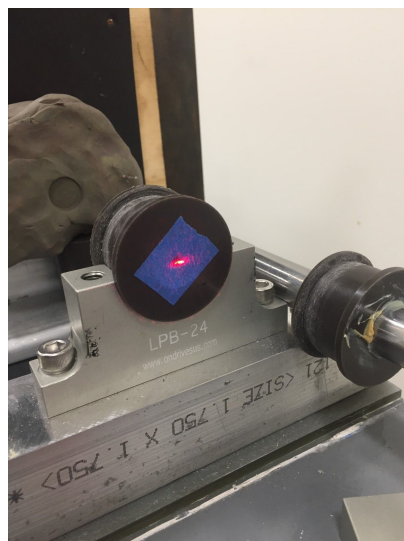


Figure 50: Delrin Mount Designed for Alignment With Laser Showing Alignment

For aligning the bar mounts, the first mount to be aligned is the transmission bar mount located furthest from the gas gun itself. To align the mount, the standard delrin mount for alignment is placed in the metal bolted mount, and adjusted until the laser from the gas gun is located in the center of the delrin mount. Unfortunately the metal mounts themselves are bolted to the steel I-beams, and cannot be adjusted. To adjust the mount, paper shims are instead placed underneath or slightly to the side of the delrin mount until the laser is well aligned.

This process is then repeated moving the standard to each consecutive metal mount moving towards the gas gun and aligning each until the standard can be placed in any metal mount with the laser located directly in the center of the mount.

Following the laser alignment the incident and transmission bars are then placed back into their proper metal mounts and secured, note however, that when tightening the top of the metal mounts, these should only be tightened until they resist any further threading, tightening past this point may result in the delrin mounts being compressed and deformed, thus undoing the alignment process that was just completed.

The next step to align the SHPB is through more physical interaction with the bars themselves. If properly aligned when the incident bar is placed against the transmission bar, the seam between the two should be difficult to identify both visually and through feel. In order to properly align the two bars it may be necessary to make further slight adjustments to the position of the delrin mounts even after the laser alignment. To do this adjust the transmission bar to the level of the incident bar moving the entire bar either up or down until the seam between the two is no longer noticeable. Paper shims can again be used to achieve this placing equal amounts (or removing equal amounts) from each of the two mounts for the transmission bar (the transmission bar is the more adjustable of the two having only two mounts compared to four for the incident bar).

Furthermore, when well aligned, the movement of the bars within the mounts should be as frictionless as possible when the bars are properly greased using motor grease. If moving one of the bars is even slightly difficult, then better alignment can be achieved by finding the mount that is producing excess friction and further adjusting this mount until the bar slides almost effortlessly through.

The final product of this alignment process is no noticeable seam between the incident and transmission bars, the projectile centered within the gas gun barrel impacting the center of the incident bar, and both the incident and transmission bars being able to easily move within their mounts. If these conditions are met, the SHPB is then ready for calibration.

5.9 Calibration

As the SHPB relies on one dimensional wave propagation theory, this assumption must be checked prior to performing an actual experiment. The system must be tested to ensure that the SHPB is properly aligned, of which one common method is to perform a bars together test. A bars together test consists of firing a projectile as if a normal test, but instead of a sample placed in between the incident and transmission bars, the two bars are in contact with each other [Split Hopkinson (Kolsky) Bar, Page 28, 2011]. With no sample between the bars, and the bars made of the same material, then there is theoretically no impedance mismatch between the materials, meaning that no stress will be reflected or lost when moving from the incident into the transmission bar. Thus if properly aligned, the strain measurement should be the same in the incident and transmission bars, with no reflected pulse from the seam between the bars [Split Hopkinson (Kolsky) Bar, Page 28, 2011]. If a test showing this result is conducted, then the SHPB is well aligned.

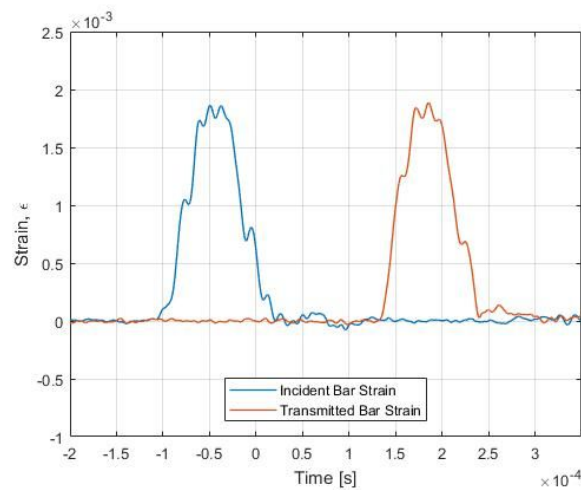


Figure 51: Well Aligned Bars Together Test

If the results do not show that the incident and transmission pulses are of the same size and magnitude, and that there are no reflected pulses, then the SHPB's alignment should be checked again and the bars together test repeated until a test shows these results.

5.10 Accurate and Consistent Data Acquisition

One of the ultimate goals of this MQP was to make modifications to the SHPB such that it would consistently gather correct, repeatable, data without mistriggers or the other problems that plagued the original setup. The modifications that were made to the circuit, oscilloscope, and bars themselves allowed for this to become a reality. Consistent tests were conducted on steel, copper, and aluminum samples, all of which showed accurate stress-strain curves for their respective materials. These tests verified the accuracy and reliability of the setup for a range of materials and strain rates, proving that the modifications greatly improved the setup.

4340 Steel Tests:

The first samples that were tested were made of 4340 steel. These samples were cut using a CNC Lathe cutting them to a diameter of one quarter inch, and a thickness of about an eighth of an inch. The diameters of these samples were very consistent having been cut by machine, however the ends of the samples had to be manually sanded to a flat surface. This manual sanding resulted in larger variations in thickness. Though there are greater variations, this is still a variation of within a millimeter, and as long as the dimensions of each sample were accurately measured before and after testing, this slightly different thicknesses will produce no noticeable differences.

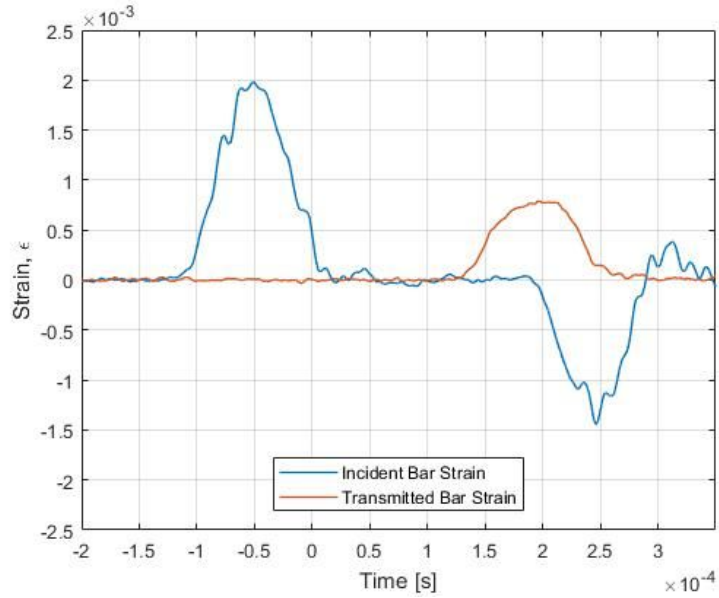


Figure 52: Steel Sample Strain Waves

The steel samples, as the bars were also steel, resulted in a low impedance mismatch, thus the transmitted wave was relatively large. This was the typical result characteristic of a steel test. The following shows the stress-strain curves for three steel tests across several different strain rates showing the consistency of the SHPB.

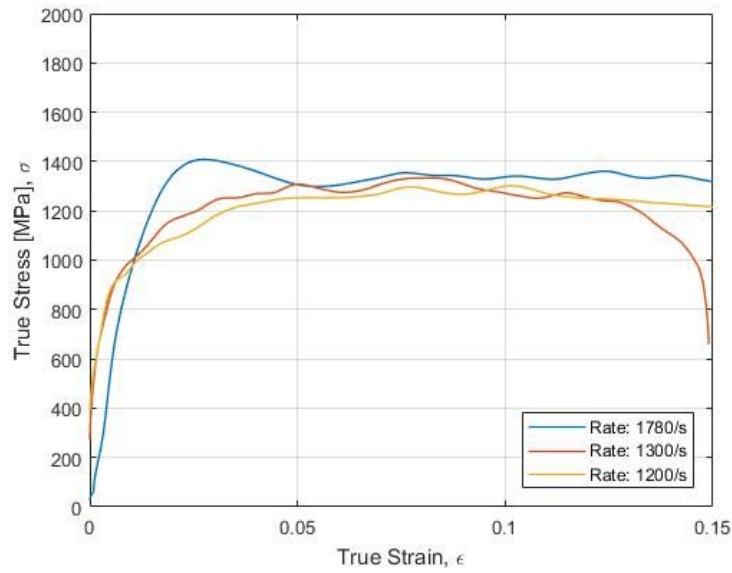


Figure 53: 4340 Steel Sample Engineering Stress-strain Curves

This steel was originally chosen as it was the sample material by the previous team that had worked on the SHPB, which would thus give a baseline to compare performances to. These results were also compared to stress-strain curves of the same 4340 steel alloy obtained by other sources.

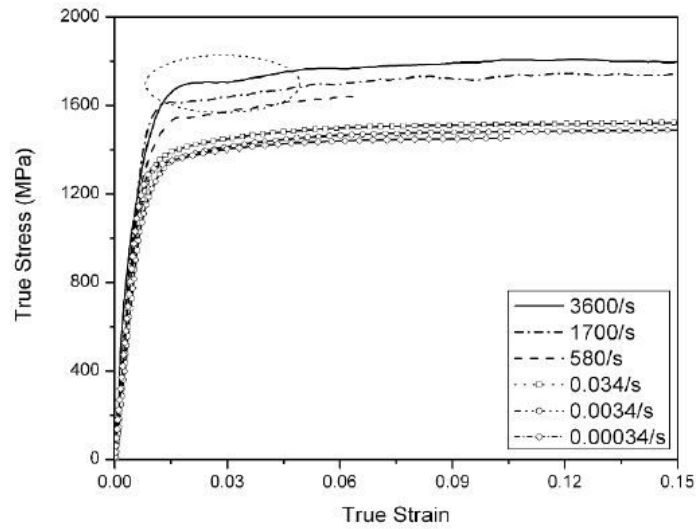


Figure 54: 4340 Steel Stress-strain Curve [Split Hopkinson (Kolsky) Bar, 2011]

The true stress-strain curve that was obtained from experiments had the same problem than the prior MQP team when comparing to the true stress-strain curve from other sources. Unfortunately the true stress-strain curve obtained by Weinong Chen and Bo Song appearing in Figure 54 [Split Hopkinson (Kolsky) Bar, 2011], represents a different hardness than the alloy tested on the setup at WPI. The softer alloy tested in the experiments and the prior team led to a lower stress required for the various strains. These tests on steel then do not show the exact accuracy of the improved SHPB setup, however it does show this setup's consistency. Three different samples tested at three different strain rates (Figure 53) show that results in the same shape and magnitude were obtained multiple times, and that as the strain rate was increased, the required stress to produce the same amount of strain also increased, proving the increased stress required from dynamic loading.

It should be noted as well, that the steel tests also show the effect that a pulse shaper may have on the resulting stress-strain curve by distributing the loading in a more gradual fashion. The highest strain rate of 1780/s shown in blue in Figure 53, was conducted with no pulse shaper, and resulted in a much sharper stress-strain curve with a more clear abrupt increase prior to the plateau. The thickest pulse shaper made of 24 gauge copper and one half inch in diameter was used in the test with a strain rate of 1300/s shown in Figure 53 by the orange true stress-strain curve. This curve compared to without a pulse shaper has a much more bulbous appearance without either a sharp increase at the start of loading, or decrease afterwards. This was most likely caused by the thick pulse shaper. The third true stress-strain curve at a strain rate of 1200/s shown in yellow in Figure 53, was conducted with a 26 gauge copper pulse shaper of one half inch in diameter. This too showed a more bulbous shape though not to the extent of the 1300/s curve. This implies that perhaps an even thinner pulse shaper would be able to create even less of a rounded true stress-strain curve while still dampening high frequency noise during loading.

Copper Tests:

Tests were also done on copper discs to determine the stress-strain curve for copper. For a softer material such as copper, the stress required to produce a specific strain is much less than that of steel. Furthermore, because copper is a softer material, there is a greater impedance mismatch between the sample and SHPB bars, resulting in a larger reflected wave and decreasing the transmitted wave. During the tests, there were still large enough transmitted waves to accurately measure the stress-strain curves for this material. The copper samples used in these tests were a half inch in diameter and made from a 12 gauge copper sheet.

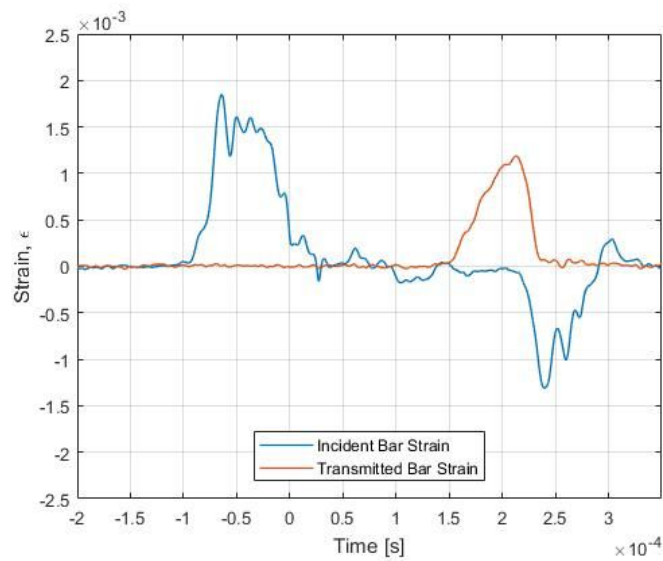


Figure 55: Copper Sample Test

The stress-strain curves produced were again consistent and showed that in dynamic testing, a higher strain rate again generally corresponds to a higher required stress, though this is not as obvious as in the tests with steel. Experimental stress-strain curves were chosen over true stress-strain curves for copper due to the lack of available results to compare to from other sources. The most reliable source that could be found plotted the experimental instead of true stress- stress-strain so thus this was chosen to enable a more accurate comparison.

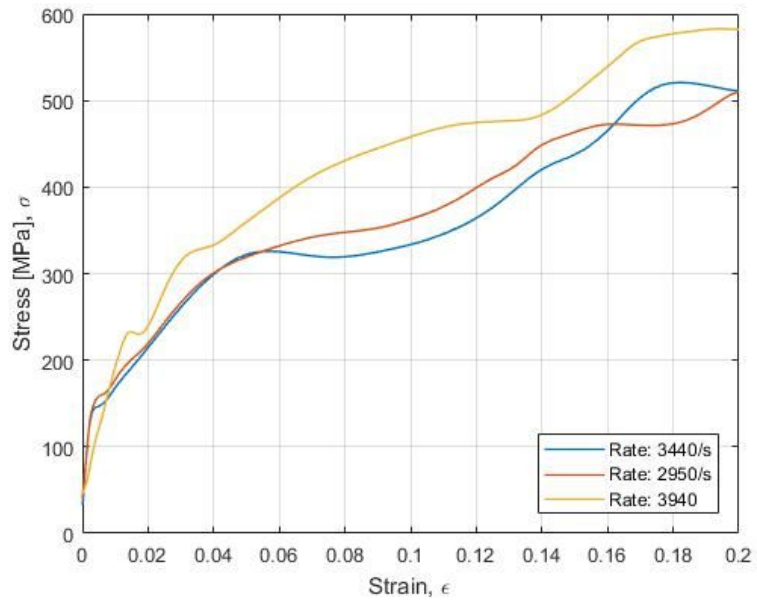


Figure 56: Copper Stress-strain Curves

These stress-strain curves were again compared to another source to determine the accuracy of the setup. The most reliable source was obtained at the Oklahoma State University.

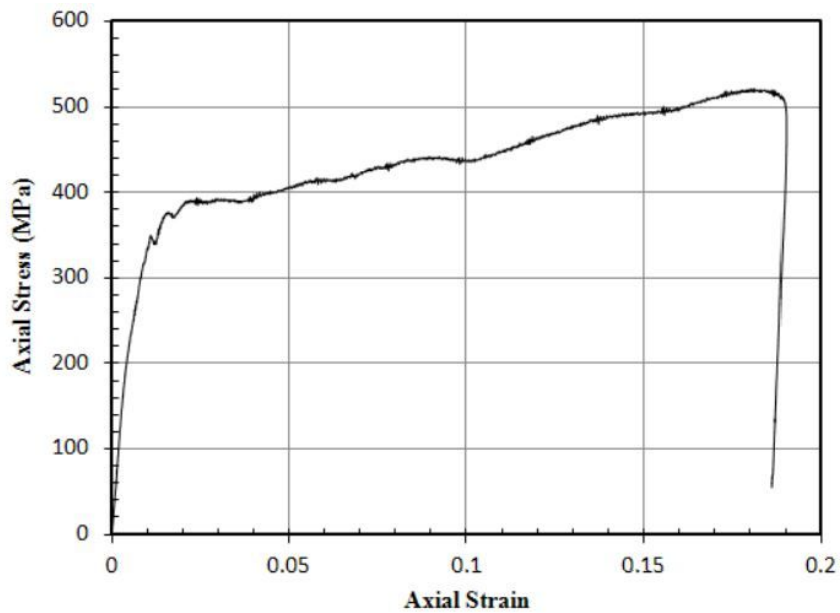


Figure 57: Copper Stress-strain Curve From Outside Source [Dynamic Testing at Oklahoma State University, 2011]

The results show stress-strain curves of the same magnitude as the outside source over the same strain levels. The only major difference was again the lack of an abrupt increase in stress at the start of the stress-strain curve. Instead the curves have again a generally more rounded increase until reaching the plateau and the eventual highest strain value shown in the outside source. Though not an exact match, these stress-strain curves for copper do show that the modified setup is able to record and calculate consistent and generally accurate results for a material softer than steel.

Aluminum Sample:

Tests were also conducted on half inch samples made of 6061-T6 aluminum. Aluminum is a softer material, thus like copper, the reflected wave is relatively large. These tests were done without a pulse shaper as they were conducted at a max psi of 60 psi which was determined to be below the accurate operating pressure for the 26 gauge copper pulse shapers without significantly altering the shape of the resulting stress-strain curve. The magnitude of the waves measured again proved the capability of the SHPB to measure strain waves through softer material samples than steel.

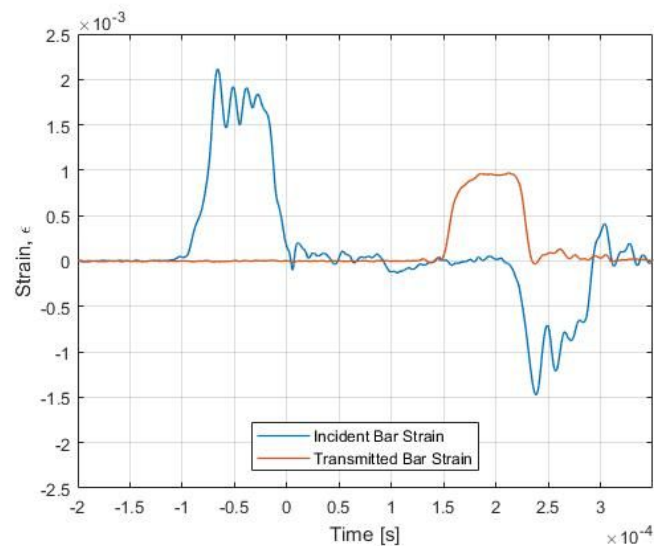


Figure 58: Aluminum Sample Test

These samples were tested over a range of strain rates in an effort to compare to an outside stress-strain curve obtained with a strain rate of 830/s. Stress-strain curves were experimentally obtained for this aluminum alloy at strain rates of 1600/s, 930/s, and 690/s, strain rates around the target rate of 830/s.

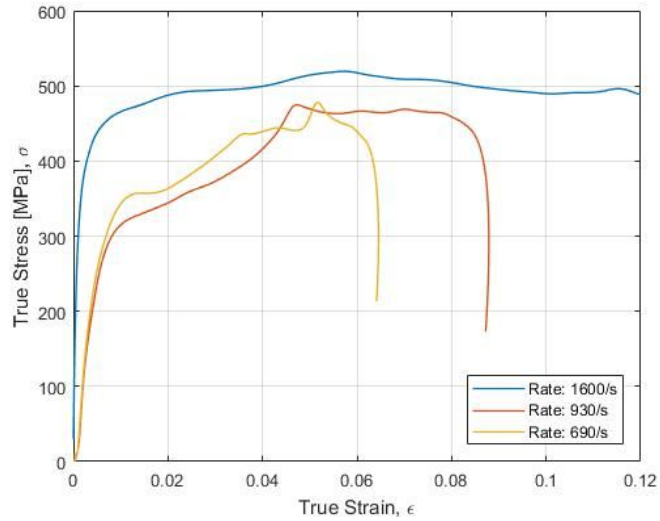


Figure 59: Aluminum True Stress-strain Curves

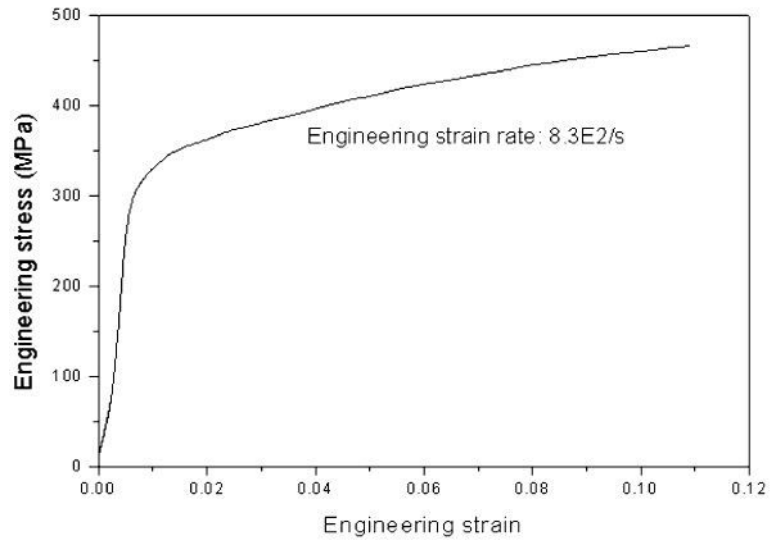


Figure 60: Outside 6061-T6 Aluminum Stress-strain Curve [Split Hopkinson (Kolsky) Bar, 2011]

The magnitude of the true stress-strain curves were nearly identical to the outside source with an identical rise time to the same value of just over 320 MPa for the lower strain curves at 930/s and 690/s. These results prove the accuracy of the SHPB when compared to a standard sample from another source. Furthermore the multiple tests again prove the consistency of this setup when performing tests.

Acrylic Sample:

One test was also done on a sample made of acrylic that was about a half inch in diameter and a quarter inch thick. Acrylic is many times softer than steel or copper, so this test was conducted to see whether with such a soft material, steel bars could still be used to obtain a transmitted strain wave with a large enough magnitude to still produce accurate results.

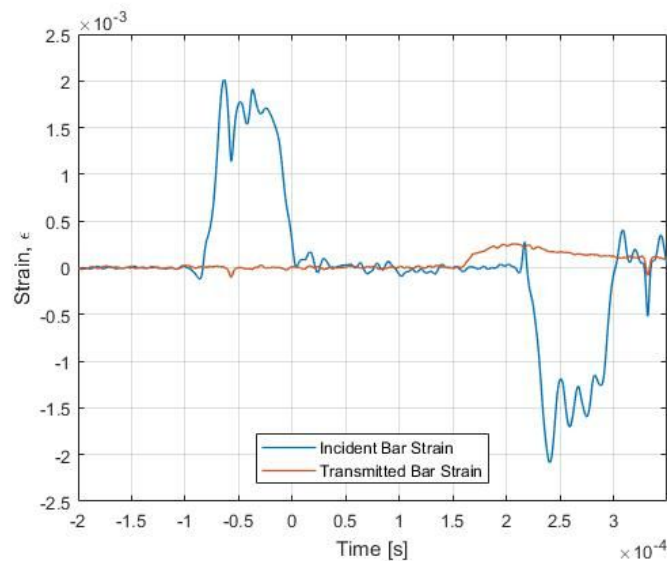


Figure 61: Acrylic Sample Test

This acrylic test resulted in a true stress-strain curve that could accurately compared to another experimentally found stress-strain curve.

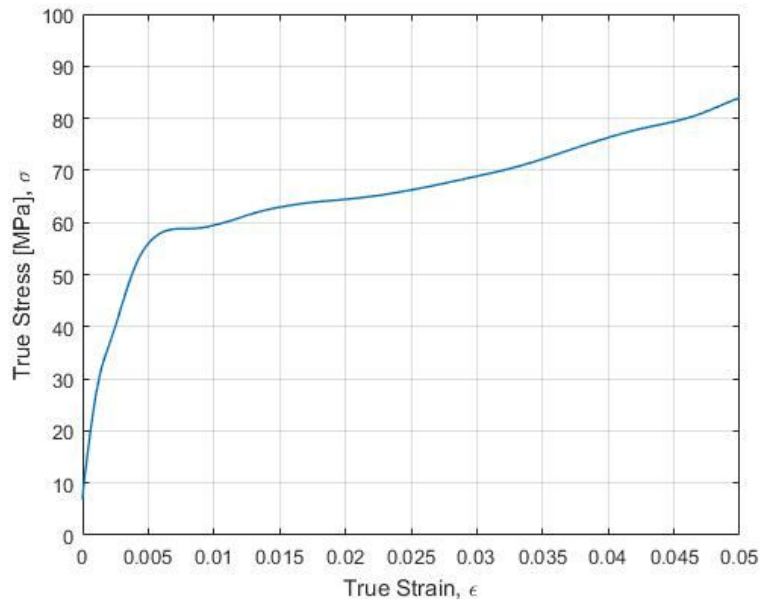


Figure 62: Acrylic True Stress-strain Curve 1830/s Strain Rate

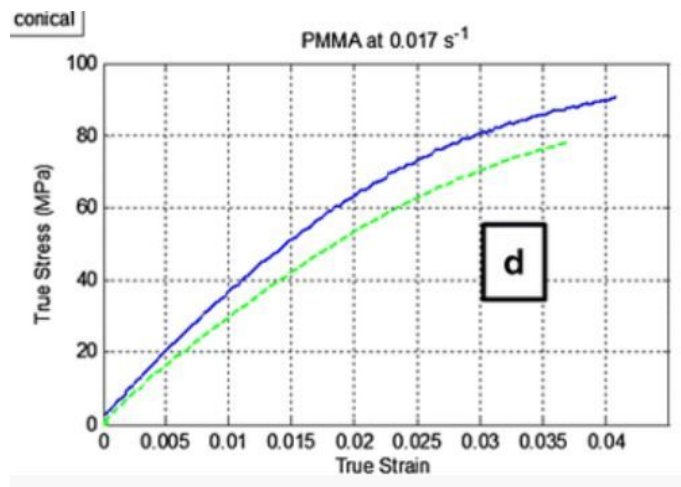


Figure 63: Acrylic Outside Source True Stress-strain Curve 560/s Strain Rate [Dynamic Behavior Mater, 2015]

Comparing the two true stress-strain curves, the magnitude of the values again are very close, and the shapes also match well. The difference between the difference in stress can be explained by examining the strain rates that these tests were conducted at. The test was

conducted at a strain rate of 1830/s, over three times the strain rate of the outside source at 560/s. This higher strain rate requires a greater amount of stress to result in the same strain. Thus by examining this greater strain rate, these curves are seen as being close to each other proving the SHPB's accuracy even when testing much softer materials than steel or copper.

6 Summary

During this project, two material testing machines were developed for the use of the WPI student body. In the splitting up of the work, two groups were made within this project that each worked on a testing setup that was to be updated and improved. For the tensile tester, it required a redesign of the LabView code that runs the tensile tester, in order to make the software be able to run consistent tests that can be controlled easier, with less variation in the applied loads. With the need for digital image correlation software (DIC), the components had to be found and purchased with the budget given the required camera and associated equipment needed to capture the images that would need to be analyzed by the DIC.

For the SHPB, the overall goal was to improve the reliability and accuracy of the setup to allow for use by other students. This required making numerous modifications to the setup including to the circuit, the oscilloscope settings, the matlab code, and the bars themselves. Much of the modifications were based on experience using the SHPB and discovering the issues during use, and then finding appropriate solutions to try to fix these issues. An ANSYS simulation of a bars together test was also created to compare with experimentally gathered data. This simulation could also potentially be used to find the exact position on each bar that the strain gauges should be placed. Tests were conducted with the SHPB on steel, copper, aluminum, and acrylic samples, and the results of these samples compared to results from other organizations.

7 Conclusion

At the beginning of this MQP, the Tensile Tester could apply a force to a sample and measure that force. The force was difficult to adjust because the PA-17 linear actuator had to be manually controlled with a slider in LabView. Displacement measurement was possible, but the noise from the sensor was larger than the expected signal. After several improvements, the Tensile Tester can now directly measure displacement, and can automatically control the linear actuator using a closed-loop PID algorithm. Both constant-force creep tests and constant strain-rate tests are now possible to complete. Additionally, a more accurate form of strain measurement using DIC has been implemented, allowing post-processed strain data to be more accurate than otherwise possible.

When tests were first attempted using the SHPB, the setup was no longer in a reliably working condition. The modifications restored the SHPB to a working condition, improved its reliability and accuracy greatly hardly ever triggering before a test and ruining data, and with the addition of the blast box improved its safety. With these modifications in place tests were conducted on several materials of varying hardness. Steel, copper, and aluminum tests proved that the SHPB is capable of producing both accurate and repeatable results calculating accurate stress-strain curves for multiple strain rates, sample sizes, and different pulse shaper thicknesses. An acrylic test was also completed which presented the capability for the SHPB to measure stress-strain curves for much softer materials. Furthermore, various guides to aid in using the SHPB, including in troubleshooting the server, were made which will save future groups and individuals a great deal of time when conducting tests.

8. Recommendations for Future Work

It was suggested as an alternate way of removing any issues with preloading, that a slack adapter should be developed. With the slack adapter, it would allow for the tester to start its movement and allow for it to start to move at its constant rate, and not have issues with its signal processing, making it have a variable rate as it updates as it starts up.

To further reduce wires connected to the strain gauges from breaking it is suggested that thinner gauge wires may reduce the moments of inertia of the wires and thus reduce the likeliness of breaks. Strain gauges do liberate themselves at times with leads breaking, more research into further reducing the likeliness of these leads breaking could reduce the time and monetary cost of operating the SHPB. While softer materials were investigated with the acrylic test, more tests of softer materials could show the true potential for the SHPB to measure these materials. If necessary it could also be beneficial to replace the incident and transmission bars to a softer material such as aluminum to increase the strain wave that will be transmitted through the sample for more accurate measurements of other softer materials.

9. Project Broader Impacts

Since the development of these testers are for the WPI Aerospace Department, for the use of students, the testers will aid the professors in the teaching of material science and/or structural analysis. The development of these testing systems and protocols allows for students to be able to understand how material properties are tested and represented by the material's response. It will help students learn how to use equipment similar to the testers for future projects they may be a part of while at WPI or even when involved in the engineering industry.

The tensile tester will be used to conduct tests with the students of WPI conducting the tests. This tester will be most useful in the material classes provided by WPI, in the teaching of material properties and structural applications. It will help demonstrate how varying materials have varying uses due to their inherent properties and the requirements of certain parts in the industry. The DIC software and hardware could be utilized in other applications now that WPI has it setup. This setup could be used in different applications for strain measurement. Some such applications could be for testing of prototypes such as a plane wing and determining the deflection and strain on the end of a wing. The DIC could even be implemented like shown in Swapnil's paper, for the use on the samples from the split Hopkinson pressure bar. The DIC could realistically be used in any application like these for strain or displacement measurement. Provided the future purchase of a second camera, the VIC software can also be used for three-dimensional strain measurement as well.

As for the Split Hopkinson apparatus it will have a lasting impact on the student population utilizing this system in order to conduct dynamic load experiments and testings. Specifically for the students in the Aerospace Department it will be especially crucial due to the fact that the SHPB is frequently used in fundamental Aerospace Engineering applications to test how materials used in aircraft will be affected by loaded stress and impact. This can be seen during engine tests such as the bird impact test and aircraft collision with external objects, both relatively common and plausible situations to occur in Aerospace Engineering. Exposing the students to industry testings and machinery as well as give the undergraduate students a greater idea on how to conduct dynamic tests on material.

These two systems will prove to be important for the undergraduate and graduate students in WPI as a whole and not just the Aerospace Department. The Tensile Tester as well as the Split Hopkinson Pressure bar can be used to test material to be applied to a variety of different majors. Long term benefits can be foreseen for students in the Mechanical, Civil, Robotics, and even the Physics departments. This would add a material analysis component to projects such as the MQP as well as multiple courses in different disciplines. This could also open up the opportunity of conducting material design research alongside sponsoring companies or other academic institutions. Which would lead to potential collaborations with companies in the aerospace industry in an area interested in dynamic testing of materials. These systems will not just be geared towards the engineering industry or university level students, but also these systems can be used during community outreach programs such as Touch Tomorrow. Touch Tomorrow is an annual event known for being a festival of science, technology, and robots, takes place every summer which allows guests, specifically the children, to spend the day exploring the campus, meeting animals, touring the labs, and even conducting experiments, in the upcoming future one of those experiments would be the Tensile Tester and the Split Hopkinson Pressure Bar apparatus. The importance of these two systems is that they would allow both undergraduate and graduate students the opportunity to research and apply their theoretical studies from their courses onto a tangible experiment, further aiding the learning process. The systems would also serve as foundation to create relationships with external companies and other academic institutions. Lastly, the Tensile Tester and the Split Hopkinson Pressure Bar would serve as an component in an academic outreach program geared toward the youth of Worcester and New England, leaving a lasting impact on the community as a whole.

References

Anon, CM3-U3-13Y3M 1/2. Edmund Optics Worldwide. Available at:

<https://www.edmundoptics.com/p/cm3-u3-13y3m-12-chameleon3-monochrome-camera/2861/#> [Accessed March 14, 2019].

Anon, Country Household Voltages and Plug Styles. Wall Plug and Voltage Standards Worldwide Countries, plug styles, voltages, frequency 50Hz or 60Hz. Available at:

<https://www.powerstream.com/cv.htm> [Accessed March 14, 2019].

Anon, Digital image correlation (DIC). Digital Image Correlation | Veryst Engineering.

Available at:

<https://www.veryst.com/what-we-offer/mechanical-testing-modeling-validation/Testing-Library/digital-image-correlation> [Accessed March 14, 2019].

Anon, Long Term Performance of Polymers. Available from:

<http://www.me.umn.edu/labs/composites/Projects/Polymer%20Heat%20Exchanger/Creep%20description.pdf>

Anon, Preloading, and How It Affects Your Mechanical Test. Instron. Available at:

<https://www.instron.us/en-us/our-company/press-room/blog/2014/august/preloading-and-how-it-affects-your-mechanical-test> [Accessed March 14, 2019].

Anon, Tensile Test Experiment. Michigan Technological University. Available at:

<https://www.mtu.edu/materials/k12/experiments/tensile/> [Accessed March 14, 2019].

Anon, Tensile Testing. Instron. Available at:

<https://www.instron.us/en-us/our-company/library/test-types/tensile-test> [Accessed March 14, 2019].

Anon, Tensile Testing Composite ASTM D3039. *Intertek*. Available at:

<http://www.intertek.com/polymers/tensile-testing/matrix-composite/> [Accessed March 19, 2019].

Anon, Vic-2D Reference Manual. Available at:

<http://www.correlatedsolutions.com/installs/Vic-2D-2009-Manual.pdf>

- Anon, What is a Strain Gauge? *Omega Engineering*. Available at:
<https://www.omega.com/prodinfo/strain-gauges.html> [Accessed March 19, 2019].
- Anon, 2013. Potentiometers and Trimmers. Available at:
<https://www.vishay.com/docs/51001/potentiom.pdf>
- Anon, 2014. Technical Spotlight: Using Digital Image Correlation to Measure Full Field Strain. *ADVANCED MATERIALS & PROCESSES* , pp.23–24. Available From:
<https://www.asminternational.org/documents/10192/22116322/amp17210p23.pdf/69654c95-2a2f-4f5d-b150-b3c65def5e6e>
- Anon, 2016. What is a LVDT? <https://www.omega.co.uk/>. Available at:
<https://www.omega.co.uk/technical-learning/linear-variable-displacement-transducers.html> [Accessed March 19, 2019].
- Anon, 2018. Hooke's Law and Stress-strain Curve: Analysis, Videos and Examples. Toppr. Available at:
<https://www.toppr.com/guides/physics/mechanical-properties-of-solids/hookes-law-and-stress-strain-curve/> [Accessed March 14, 2019].
- Chen, W. & Song, B., 2011. Split Hopkinson (Kolsky) Bar: Design, Testing, and Applications , Springer Science Business Media.
- Davis, J.R. ed., 2004. Tensile Testing Chapter 1. In Tensile Testing. ASM International, pp. 1–12. Available from:
https://www.asminternational.org/documents/10192/3465262/05105G_Chapter_1.pdf/e13396e8-a327-490a-a414-9bd1d2bc2bb8
- Foster, M., Love, B., Kaste, R. et al. J. dynamic behavior mater. (2015) 1: 162.
<https://doi.org/10.1007/s40870-015-0020-8>
- Frew, D.J., Forrestal, M.J. & Chen, W., 2005. Pulse shaping techniques for testing elastic-plastic materials with a split Hopkinson pressure bar. *Experimental Mechanics*, 45(2), pp.186–195.
- Kambiz Arab Tehrani and Augustin Mpanda (2012). PID Control Theory, Introduction to PID Controllers - Theory, Tuning and Application to Frontier Areas, Prof. Rames C. Panda (Ed.), ISBN: 978-953-307-927-1, InTech, Available from:

<http://www.intechopen.com/books/introduction-to-pid-controllers-theory-tuning-and-application-to-frontier-areas/theory-of-pid-and-fractional-order-pid-fopid-controllers>

Keshavanarayana, S., Stroke rates and Strain rates: A parametric Study. Available from:

https://www.niar.wichita.edu/niarworkshops/Portals/0/workshops/Stroke_rates_and_strain_rates_a_parametric_study-Raju.pdf

Khlystov, N. et al., 2013. Uniaxial Tension and Compression Testing of Materials. Available at:

<http://web.mit.edu/dlizardo/www/UniaxialTestingLabReportV6.pdf>.

Kwon, J.B., Huh, H. & Ahn, C.N., AN Improved Technique for Reducing the Load Ringing Phenomenon in Tensile Tests at High Strain Rates. In Dynamic Behavior of Materials, Volume 1: Proceedings of the 2015 Annual Conference on Experimental and Applied Mechanics. pp. 253–258.

Song, B. & Chen, W., 2005. Split Hopkinson pressure bar techniques for characterizing soft materials. Latin American Journal of Solids and Structures, pp.113–152. Available at:

https://www.researchgate.net/publication/228995770_Split_Hopkinson_Bar_Techniques_for_Characterizing_Soft_Materials.

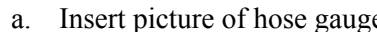
Swapnil S, 2011. Dynamic Testing to Determine Some Mechanical Properties of Aluminum, Copper, and Dry Eglin Sand Using Split Hopkinson Pressure Bar (SHPB), High Speed Photography and Digital Image Correlation (DIC). thesis. Oklahoma State University. Available from:

https://shareok.org/bitstream/handle/11244/10054/Sankaye_okstate_0664M_11522.pdf?sequence=1

Veitch, J.A. & McColl, S.L., 1995. Modulation of fluorescent light: flicker rate and light source effects on visual performance and visual comfort.

Appendix A

How to Use the Split Hopkinson Pressure Bar

1. Check the pressure gauges directly mounted on the gas gun, ensuring that they read zero, and that the two valves on the gas gun are in the closed position.
2. Check strain gauges and terminals to ensure that the gauges are properly connected to the terminals, and all pieces are firmly glued to the transmission and incident bars.
3. Adjust the variable resistors in the circuits to balance the wheatstone bridges
 - a. Using a handheld multimeter measure the difference in the voltage of the two branches of the wheatstone bridge with one probe measuring the voltage in row 22 columns A-E, and the second probe measuring the voltage in row 23 columns A-E.
 - b. Using a small screwdriver turn the knob on the resistor clockwise or counterclockwise until the difference between the branches is within one millivolt of zero.
4. Ensure that the oscilloscope is set to the desired scale, sample rate, and that the trigger is positioned correctly (see oscilloscope guide).
5. Turn the air compressor on, and pressurize the volume until the pressure within the hose reads ten psi higher than the desired test pressure.
 - a. 
6. Remove the clay section of the momentum trap and ensure that one side is flattened.
7. Push the incident and transmission bars towards the momentum trap, increasing the amount of space to push the projectile back.
8. With the bars still pushed back place a pulse shaper on the gas gun end of the incident bar using motor grease to allow it to stick to the bar. Place as close to the center as possible.
9. If conducting a bars together test to check alignment place a small dab of motor grease in between the incident and transmission bars and push the bars tightly together.
10. If conducting an actual test prepare the sample:
 - a. Measure the diameter and thickness of the sample. Accuracy is vital, as even a small variation in this measurement has a great effect on the stress-strain curve obtained from the test.

- b. Place small amounts of motor grease on both sides of the sample.
 - c. Place the sample in between the incident and transmission bars as centered as possible.
 - d. Push the bars together such that the sample is held securely in place.
11. With the bars still pushed back against the momentum trap, pressurise the gas gun to twenty psi.
12. Load the projectile to the desired depth, further depths will produce larger strain rates.
13. While applying force to maintain the tight fit between the incident and transmission bars, move the bars forward towards the gas gun until there is enough room to place the clay block in between the transmission bar and the momentum trap.
14. Place the clay block against the rest of the momentum trap and once more move the bars away from the gas gun until the end of the transmission bar is in contact with the clay block.
15. Fully pressurize the gas gun to the desired test pressure.
16. Press the Run/Stop button on the oscilloscope (the Single button should be lit green).
17. Before firing warn others in the lab, and ensure that nobody is in the firing line of the SHPB.
18. Fire the projectile by rapidly opening the valve at the back of the gas gun.
19. After firing, save the data on the oscilloscope by pressing the save button.
20. If conducting a sample test measure the dimensions of the sample again.
21. Run the data with these dimensions in the provided Matlab code adjusting as necessary (see Matlab code guide) until a stress-strain curve is obtained.

Appendix B

How to Use the Oscilloscope for the SHPB

- The oscilloscope should be reading four voltages, ensure that the following channels are connected in the following fashion:
 - Channel 1: Reading the output of the amplifier on the transmission bar, connected in row 23 column g,h,i, or j of the transmission bar circuit.
 - Channel 2: Reading the output of the amplifier on the incident bar, connected in row 23 column g,h,i, or j of the incident bar circuit.
 - Channel 3: Reading the transmission bar excitation, connected directly to the output voltage from the power supply for the transmission bar.
 - Channel 4: Reading the incident bar excitation, connected directly to the output voltage from the power supply for the incident bar.
- To adjust the scale for each channel adjust the appropriately labeled scale knob for each numbered and labeled channel. The suggested scales are follows: 500mV for channels 1 and 2, 5 V for channels 3 and 4.
- The overall time scale can be adjusted with the appropriately labeled scale knob under the Horizontal section. The suggested scale is 200 microseconds per division, enough time to show multiple reflections of the strain wave. This will also automatically adjust the sample rate to 5.00 MS/s.
- The trigger, when set correctly, ensures that the SHPB does not activate prior to a test from vibrations in the setup, or from other factors reducing the risk of a false trigger and a test returning no useable data. To properly set up the trigger follow these instructions:
 - The trigger is currently set to trigger after detection of a pulse of a particular width. To set this press the Menu button under Trigger, and for Type choose “Pulse Width”.
 - The trigger is set to trigger on a pulse from the incident strain gauges. To set this press the Menu button under Trigger, select source, and select channel 2.
 - Polarity tells the trigger to activate on either a negative or positive pulse. To set this press the Menu button under Trigger, select Polarity and choose “Negative”.

- To set the pulse length to trigger on select Trigger When under the trigger menu, and choose “Pulse Width > Limit”, and set the limit underneath to 50 microseconds.
- As the circuits on each bar are currently set, a strain wave results in a negative reading from the wheatstone bridge. The trigger should thus be set to below the steady value of the incident bar by about 50mV-150mV. The trigger value is shown by a blue arrow on the right side of the display, and can be adjusted vertically with the trigger knob.
- When conducting a test, to prepare the oscilloscope to read data and trigger upon a test press the Run/Stop button on the top right such that the Single button should be lit green. If this button is not green then the oscilloscope will not trigger.
- When conducting a test, prior to firing the gas gun press the Force Trig button (under the Trigger area) to ensure that the levels of the various voltages appear to be correct. Occasionally after pressing the run button again following a force trigger the display will not erase the previous data, resulting in two sets of data being displayed at once, if this happens press the force trigger and then run buttons again until the display is blank.
- Upon completion of a test pressing the save button should save an image of the display, the results in .csv format, and a file containing the settings for the run. To ensure this navigate the menus through the following:
 - Press the menu button at the bottom of the oscilloscope.
 - Select “Assign Save to:”.
 - Choose on the right side of the display “Image, Waveform, and Setup”.

Appendix C

Trouble shooting the SHPB

While using the SHPB numerous quirks and issues were uncovered, the following is a list of potential issues and various potential causes as well as potential solutions.

1. Voltage reading from one of the two wheatstone bridges (channels one or two) is greater than four volts.
 - a. Most likely this is the result of a broken strain gauge.
 - i. Check each strain gauge to ensure that both leads are securely soldered to the terminal. Check by lightly putting pressure on each lead, if the lead does not move DO NOT put increasing pressure, the pressure should be just enough to move the lead if it is disconnected. If a lead is loose either resolder if possible, or replace the strain gauge.
 - b. Could be an issue with the wires leading to the terminal.
 - i. Check the wires leading to the terminal. Occasionally these will fray after repeated tests and may break. If a wire is broken, restrip and solder the wire to the terminal.
 - c. Could possibly be a broken wire on the circuit itself.
 - i. Most likely this again would be a frayed wire from the strain gauges, but this time on the circuit end, but other wires in the wheatstone bridge may have liberated themselves, or could be loose. Check the connections for every wire. Replace the problem wire if found.
2. Almost instantaneous spike in the voltage reading during a test.
 - a. Likely caused by a loose terminal.

- i. Check each terminal ensuring that the terminal is completely glued onto its respective bar. Even if a corner is loose, the movement from this during a test can result in a spike. Fix by gluing the loose part of the terminal.
- ii. One of the terminals itself could be loose. This is the part of the terminal that wires are soldered to, and at times has come loose from the base of the terminal. If this is the case, replace the problem terminal completely, glue on this specific part is unlikely to hold.



Figure 64: Example of spikes caused by a loose terminal

3. Trigger fails to go off during a test.
 - a. Most likely cause is that the trigger was incorrectly set.
 - i. Ensure that the trigger is set below the zero value for the incident strain, not above the zero value.
 - ii. Ensure that the trigger is set close enough to the zero value. The trigger should be set 50mV - 150mV below the zero value, this is far enough to avoid noise triggering the oscilloscope, yet small enough that even low pressure tests will set off the trigger.
4. A strain wave is recorded and the wave oscillates without zeroing out between waves.
 - a. One cause is that the strain gauges are too close to the end of its respective bar.
 - i. To fix this move the strain gauges away from the ends of the bar to ensure that the reflected waves do not overlap with the target wave.

- b. Another possibility is that the pulse shaper being used is too thick. This would result in the pulse shaper absorbing too much energy and stretching the length of the strain wave such that the waves will overlap.
 - i. To fix this simply use a thinner pulse shaper.



Figure 65: Example of overlapping waves on transmission bar.

5. Power Supply Overloading

- a. One cause is that two rows on the circuit may be accidentally soldered together.
 - i. To fix, check the soldering of each row and wire, especially on the back side of the board, ensuring that the solder is in contact with only one row.
- b. Another cause is that the board may be in contact with the beam in such a way that the beam is allowing electricity to flow between two rows.
 - i. To check this lift the board off of the beam, if the overload goes away, this was the cause and just ensure that the board is slightly elevated so that this does not happen again.

Appendix D

How to Use the Tensile Tester

1. Turn on the computer in the Multipurpose lab
2. Load up the LabView VI code
3. Load up the Point Grey FlyCap2 software
4. Setup the Camera and insert the test sample into the tester (with a speckle pattern on it)
5. Link the correct pathway of the excel file the data is to be written to
6. Open up saving system for FlyCap 2
7. Choose .jpg output and desired frame capture system (all frames recommended)
8. Run both software at the same time
9. End after sample failure
10. Wait for data to write and save

How to Use the LabView Programs

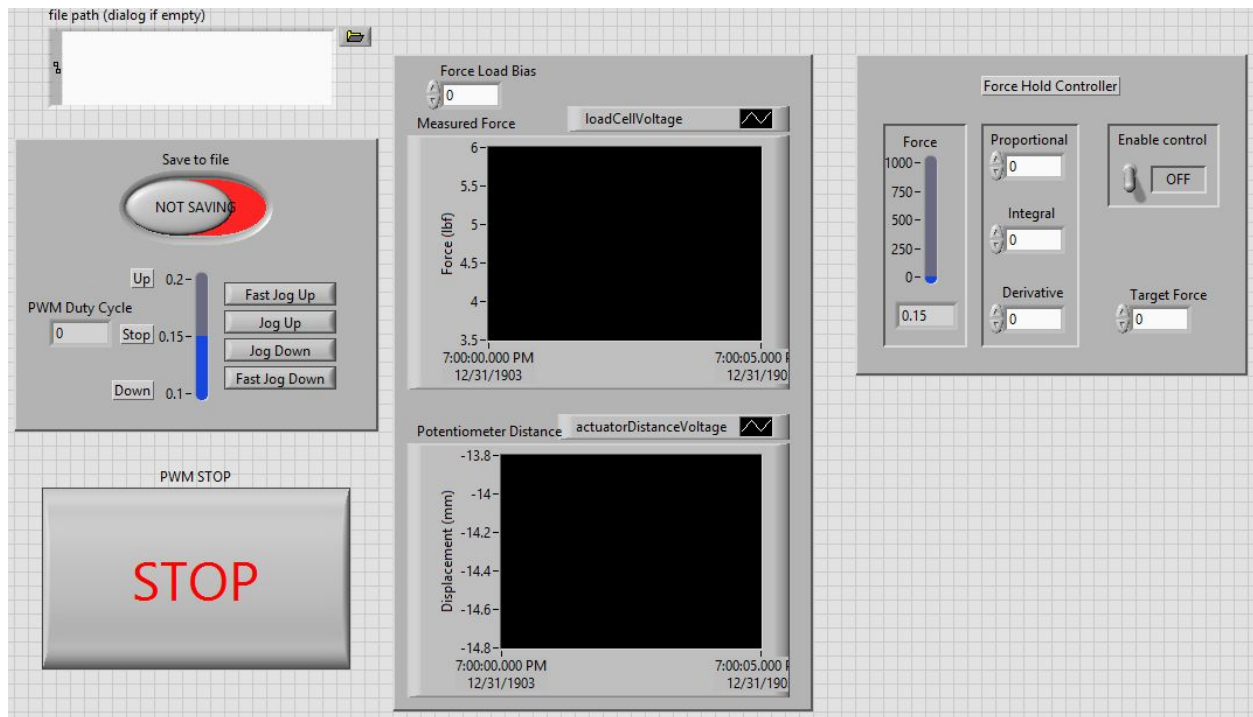


Figure 66: Example LabView Panel

Panel Description:

- File Path (Top Left): This path is where the program will save your test data. Usual file format is a .xls file.
- Save To File (Left Block): Either SAVING or NOT SAVING. Controls writing test data to the file. Will need to be enabled to save test data.
- Manual Control (Left Block):
 - Fast Jog Up: Moves the base up quickly
 - Jog Up: Moves the base up slowly
 - Jog Down: Moves the base down slowly
 - Fast Jog Down: Moves the base down quickly
- PWM STOP (Bottom Left): Stops the linear actuator immediately
- Plots (Center): Top plot graphs the force on the load cell in pounds. Bottom plot graphs the actuation distance of the linear potentiometer in millimeters

- Force Load Bias (Top Center): adjusts the zero setpoint of the load cell, as it tends to drift during warmup
- Force Hold/Strain Rate Controller (Right Block):
 - Force/Displacement (Left Column): Displays the current force or displacement that is being fed into the PID controller
 - Proportional/Integral/Derivative (Center Column): Advanced tuning values for PID Loop. A version of the LabView programs exist with pre-tuned values that should work for most materials.
 - Enable Control (Right Top): Enables PID feedback loop control. Manual Control is no longer functional.
 - Target Force/Strain Rate (Right Bottom): Sets a target force or strain rate for the PID loop to obtain.

Operation:

1. Set a file to save to using the File Path dialog box
2. Adjust the base so that the sample can be grabbed by both grips using the Jog buttons
3. Tighten the sample
4. Adjust the zero of the load cell
5. Set the target force or strain rate in the controller
6. Enable data logging by clicking the Save To File button
7. Begin the test by flipping the Enable Control switch to the ON position
8. End the test by flipping the Enable Control switch to the OFF position
9. Disable data logging by clicking the Save To File button

Appendix E

How to Use the VIC 2D 2009 Software

(Access to software provided by Grad Dept. and Professors)

1. Separate out Video file into frames
2. Upload frames to software
3. Hit the black square and select the calibration image (first frame works fine)
4. Hit the red question mark on the top left
5. Place a marker in each section of the sample used (both the Reference and the Deformed AOI) that corresponds close to the same points on the speckle pattern and hit add point
6. Set 3 reference points total on the section brought up
7. Move to the next image and if it automatically turns to a check mark continue to the next one
8. Repeat for each image as needed
9. Close it out
10. Change the subset and step to a reasonable size (25+ and 5+ respectively)
11. Hit the green arrow
12. Select all the images to be used
13. Select your output directory and hit run
14. Wait - it takes time to run
15. Go to Data tab, post processing options, calculate strain
16. Go to calibrate, calibrate scale and create a line from the top to bottom of the sample on the image and set it to the correct size scale
17. Go to Data tab, post processing options, apply function, under select equation, select major eng. Strain
18. Go to Data tab, export statistics, select all, and export it
19. The exported file will be in a .csv file format which you can use Excel to open and read - just save as a new style excel file
20. You can graph the strain as ϵ_1 , and major eng. Strain
21. The data can then be used in Matlab to be graphed as a Stress-strain graph

Appendix F

SHPB Matlab Code:

When using this Matlab code and processing test datas make sure to adjust the following: The target folder for the code to read .csv data from, the dimensions of the sample both before and after the test, and the start points of the incident, transmission, and reflected waves.

```
clear all; close all; clc;
```

```
%% Select Trial
```

```
%The following command, when run, will prompt the user to select a .csv  
%file of his or her choosing. This makes it user friendly and easier to  
%select various trial runs rather than have MATLAB try and find the  
%desirable file.
```

```
filename = uigetfile('./*.csv'); %This prompts you to select a file
```

```
filepath = strcat('C:\Users\Jake\Desktop\2-24-2019\',filename); %This will open the  
experimental data and pull the array we want without the things we dont
```

```
%% Initialize variables.
```

```
%The .csv produced by the Oscilloscope is formatted so that the data  
%collected begins at row 21, column 1. This sets the boundaries of the  
%data table we want imported
```

```
delimiter = ',';
```

```
startRow = 21;
```

```
%% Format for each line of text:
```

```
% column1: double (%f)
```

```
% column2: double (%f)
```

```
% column3: double (%f)
```

```
% column4: double (%f)
```

```
% column5: double (%f)
```

```
% For more information, see the TEXTSCAN documentation.
```

```
formatSpec = '%f%f%f%f%f%*s%*s%*s%[\n\r]';
```

```
%% Open the text file.
```

```

fileID = fopen(filepath,'r');

%% Read columns of data according to the format.
% This call is based on the structure of the file used to generate this
% code.
textscan(fileID, '%[^\n\r]', startRow-1, 'WhiteSpace', '', 'ReturnOnError', false, 'EndOfLine',
'\r\n');
dataArray = textscan(fileID, formatSpec, 'Delimiter', delimiter, 'TextType', 'string',
'EmptyValue', NaN, 'ReturnOnError', false);

%% Close the text file.
fclose(fileID);

%% Create output variable
%This is the selected data from each of the resepective channels.

MOAD = table(dataArray{1:end-1}, 'VariableNames', {'TIME','CH1','CH2','CH3','CH4'});

%% Clear temporary variables and rename data
%We clear all unnecessary variables here to enable the program to process
%the data at a faster rate. We also rename each of the channels with their
%proper names to make things easier when we calculate. We also transform
%the data table into an array to make the math functions simpler.

clearvars filepath delimiter startRow formatSpec fileID dataArray ans;

time = double(table2array(MOAD(:,1))); %Time in seconds
SS_I = 1*double(table2array(MOAD(:,3))); %Stress-strain of Incident Bar
Vex_I = double(table2array(MOAD(:,5))); %Excitation voltage of Incident
SS_T = 1*double(table2array(MOAD(:,2))); %Stress-strain of Transmitter Bar
Vex_T = double(table2array(MOAD(:,4))); %Excitation voltage of Transmitter

clear MOAD

%% Clear infinities in original data CHECK TO MAKE SURE THESE ARE NOT IN ACTUAL
WAVES
SS_I_Infinities = find(isinf(SS_I))
SS_T_Infinities = find(isinf(SS_T))
for i = 1:length(SS_I_Infinities)

```

```

    SS_I(SS_I_Infinites(i))=0;
end

for i = 1:length(SS_T_Infinites)
    SS_T(SS_T_Infinites(i))=0;
end
%Again check to make sure these numbers do not fall within the actual waves

%% Input Constant Parameters
% Here we will need to input our known parameters as well as perform a
% fourier calculation to reduce the noise of the system.
L_S = 0.00616; %m, specimen length
L_S_F = 0.00564; %m, specimen length, final
D_S = 0.0135; %m, specimen diameter, original
D_S_F = 0.01415; %m, specimen diameter, final
R_l = 0; %Ohms, Resistance of lead wire, assume zero unless measured
R_g = 120; %Ohms Nominal gage resistance
GF = 2.14; %Gage Factor of the strain gauge in use
AmpI = 52.75; %Op amp gain, depends on input resistor
AmpT = 51.97;
Fs = 5e6; %S/s, Oscilloscope sample rate, changes with sample length of time
cutoff_freq = 50e4;%20e4 default %Hz, Low pass filter cutoff frequency 20e4
D_B = 0.018796; %m, diameter of bars
K = 160e9; %Pa, bulk modulus of bars
rho = 8.08e3; %kg/m^3, density of bars
E_B = 200e9; %Pa, elastic modulus of bars
C_B = sqrt(K./rho) %m/s, speed of sound in bars
C_B_1 = (2.*(28.125*0.0254))./(0.0003204 - 7.6e-06);
C_B_2 = (2.*(28.125*0.0254))./(0.000324 - 8.4e-06);
C_B = (C_B_1+C_B_2)/2 %m/s, speed of sound in bars, measured (=C_B if not measured)
wave_lwr_I = 4600; %sample point number, start of incident wave
wave_lwr_R = 6100; %sample point number, start of reflected wave
wave_lwr_T = 5800; %sample point number, start of transmitted wave
wave_length = 400; %sample points, length of shortest of three waves
wave_upr_I = wave_lwr_I + wave_length; %5700
wave_upr_R = wave_lwr_R + wave_length; %6955
wave_upr_T = wave_lwr_T + wave_length; %6934

%% Strain Calculation

```

```

%In order to calculate strain from the voltage outputs of the strain gages
%we must know the unstrained relationship between input and output
%voltages.
%This section takes an average over the first 1000 samples, a period when
%the bars should be in an unstrained state as triggering occurs at the
%midpoint of the dataset (5000).
V_out_unstrained_I = mean(SS_I(1:1001));
V_out_unstrained_T = mean(SS_T(1:1001));
V_in_unstrained_I = mean(Vex_I(1:1001));
V_in_unstrained_T = mean(Vex_T(1:1001)); % assumes trigger occurs at ~5000

```

```

%The following equations are sourced from Omega literature on using half
%bridge strain gage configurations. The literature assumes gages are
%located on the same branch and in opposite strains, however, this should
%be equivalent to equal strains on opposing corners of the bridge.
%Vr_I = ( (SS_I./Vex_I) - (V_out_unstrained_I./V_in_unstrained_I) );
%Vr_T = ( (SS_T./Vex_T) - (V_out_unstrained_T./V_in_unstrained_T) );
Vr_I = SS_I - V_out_unstrained_I;
Vr_T = SS_T - V_out_unstrained_T;
Strain_I = -((2.*Vr_I)./GF).*(1+R_l/R_g).*(1./AmpI)./V_in_unstrained_I;
Strain_T = -((2.*Vr_T)./GF).*(1+R_l/R_g).*(1./AmpT)./V_in_unstrained_T;
%% Plot Code

```

```

%Plot code to compare the strain of the incident bar and
%the strain of the transmitter bar vs. time.
figure('name','Incident and Transmitted Bars Strain Plot')
plot(time, Strain_I)
hold on
plot(time, Strain_T)
legend('Incident Bar Strain','Transmission Bar Strain','location','south')
xlabel('Time [s]')
ylabel('Strain, \epsilon')
xlim([-0.0002 0.0003])
grid on

```

```

%% plot waves but against point number, not time
figure('name','Incident and Transmitted Bars Strain Plot, point based')
plot(Strain_I)
hold on

```

```
plot(Strain_T)
legend('Incident Bar Strain','Transmission Bar Strain','location','southwest')
xlabel('Point #')
ylabel('\epsilon')
xlim([4000 6500])
ylim([-0.001 0.0020])
grid on
```

```
%% Filtering
```

```
figure('name','FFT')
```

```
%FFT
```

```
%remember to adjust sample frequency
```

```
T = 1/Fs;
```

```
L = length(time); %length of time
```

```
t = (0:L-1)*T;
```

```
y = Strain_I; %signal to be examined
```

```
Y = fft(y);
```

```
P2 = abs(Y/L);
```

```
P1 = P2(1:L/2+1);
```

```
P1(2:end-1) = 2*P1(2:end-1);
```

```
f = Fs*(0:(L/2))/L;
```

```
plot(f,P1)
```

```
title('Single-Sided Amplitude Spectrum of X(t)')
```

```
xlabel('f (Hz)')
```

```
ylabel('|P1(f)|')
```

```
%Design Filter
```

```
%remember to adjust sample frequency above
```

```
low = (cutoff_freq)/((Fs)*2);
```

```
[b,a] = butter(2,[low], 'low');
```

```
%Apply Filter
```

```
filt_Strain_I = filtfilt(b, a, Strain_I);
```

```
filt_Strain_T = filtfilt(b, a, Strain_T);
```

```

%remove filter
%filt_Strain_I = Strain_I;
%filt_Strain_T = Strain_T;

figure('name','Filtered Incident and Transmitted Bars Strain Plot')

plot(time, filt_Strain_I, 'linewidth', 1)
hold on
plot(time, filt_Strain_T, 'linewidth', 1)

legend('Incident Bar Strain','Transmitted Bar Strain','location','south')
xlabel('Time [s]')
ylabel('Strain, \epsilon')
xlim([-0.0002 0.00035])
ylim([-0.0025 0.0025])
grid on

%% Calculate stress-strain curves of materials, first using unsimplified equations

%We need to determine the starting and ending of each wave
Inc_Strain = filt_Strain_I(wave_lwr_I:wave_upr_I);
Ref_Strain = filt_Strain_I(wave_lwr_R:wave_upr_R);
Tra_Strain = filt_Strain_T(wave_lwr_T:wave_upr_T);

%If calculations are desired without the filter:
%Inc_Strain = Strain_I(wave_lwr_I:wave_upr_I);
%Ref_Strain = Strain_I(wave_lwr_R:wave_upr_R);
%Tra_Strain = Strain_T(wave_lwr_T:wave_upr_T);

figure('name','Wave Point View')
plot(Inc_Strain)
hold on
plot(Ref_Strain)
plot(Tra_Strain)

figure('name','Wave Addition')
plot(Inc_Strain+Ref_Strain)
hold on
plot(Tra_Strain)

```

```

%Particle velocities at ends of each bar
v1 = C_B.*(Inc_Strain - Ref_Strain);
v2 = C_B.*(Tra_Strain);

%Average engineering strain and strain rate
Strain_rate_ave = (v1 - v2)./L_S;
t_int = 1/Fs;
Strain_ave = (C_B./L_S).*t_int.*cumtrapz(Inc_Strain - Ref_Strain - Tra_Strain);

%Convert bar and sample diameters into areas
A_B = (((D_B)/2).^2).*pi; %m^2
A_S = (((D_S)/2).^2).*pi;

%Stresses at both ends of specimen
Stress_1 = (A_B./A_S).*(E_B).*(Inc_Strain + Ref_Strain);
Stress_2 = (A_B./A_S).*(E_B).*(Tra_Strain);

%Plot stress at both ends of specimen, should be equal if in equilibrium
figure('name','Stress-strain Curve, unsimplified')
plot(-Strain_ave, Stress_1./1e6)
hold on
plot(-Strain_ave, Stress_2./1e6)
ylabel('Stress [MPa], \sigma')
xlabel('Strain, \epsilon')
xlim([-0.005 .40])
legend('Interface 1','Interface 2','location','south')
grid on

%% Calculate stress and strain in the sample using simplifying assumptions to reduce equations
%simplify expressions
Strain_rate_ave = -2.*(C_B./L_S).*Ref_Strain;

t_int = 1/Fs; %s, amount of time between sample data points

Strain_ave = -2.*(C_B./L_S).*t_int.*cumtrapz(Ref_Strain);

Stress_ave = (A_B./A_S).*E_B.*Tra_Strain;

```

```

figure('name','Stress-Strain Curve, simplified')
plot(Strain_ave, Stress_ave./1e6, 'linewidth', 1)
ylabel('Stress [MPa], \sigma')
xlabel('Strain, \epsilon')
xlim([0 .05])
ylim([0 100])
grid on

% attempt 2 to change from engineering stress/strain to true stress/strain
true_stress = Stress_ave.*(1-Strain_ave);
true_strain = -log(1-Strain_ave);
figure('name','True stress vs. True strain')
plot(true_strain, true_stress./1e6, 'linewidth', 1)
ylabel('True Stress [MPa], \sigma')
xlabel('True Strain, \epsilon')
xlim([0 .05])
ylim([0 100])
grid on

figure('name','Strain Rate, simplified, vs time')
%create time vector
for i = 1:length(Strain_rate_ave)
    wave_time(i) = i.*t_int;
end

plot(wave_time, Strain_rate_ave)
mean(Strain_rate_ave)
xlabel('Time, [s]')
ylabel('Strain rate, [s^-1]');
grid on

eng_strain_stress(:,1) = Strain_ave;
eng_strain_stress(:,2) = Stress_ave;
true_strain_stress(:,1) = true_strain;
true_strain_stress(:,2) = true_stress;

%Save to .dat file, be sure to rename with each trial
dlmwrite('eng_strain_stress_4340_short_100psi_2.dat',eng_strain_stress)
dlmwrite('true_strain_stress_4340_short_100psi_2.dat',true_strain_stress)

```

Appendix G

Tensile Tester MATLAB Code:

Use this script after testing a sample and using DIC to generate the principal strain in the material. The .xlsx files used contain the data required for the test.

```
clear variables; close all; clc;
```

```
%%sample and test properties
```

```
sample_length = 100; %length of sample in mm  
sample_width = 10; %width of sample in mm  
sample_depth = 5.66; %depth of sample in mm  
zero_offset = 2.260425; %initial position of base  
relative_rate = 3.2; %data logging rate/DIC framerate
```

```
%%data input
```

```
dic_strain = xlsread("Test 4.xlsx","BL2:BL600")*2*100;  
lin_strain = (xlsread("2-28_2_Acrylic.xlsx","D400:D2300")+zero_offset)*-100/sample_length;  
%4.448 N per lbf  
sens_load =  
xlsread("2-28_2_Acrylic.xlsx","C400:C2400")*4.448/(sample_width*sample_depth);
```

```
%%smoothing
```

```
lin_strain = movmean(lin_strain,20);  
dic_strain = movmean(dic_strain,5);  
sens_load = movmean(sens_load,5);
```

```
%%time array generation
```

```
lin_time = [0:1:length(lin_strain)-1].';  
dic_time = [0:1:length(dic_strain)-1].'*relative_rate;
```

```
%%potentiometer vs DIC strain plot
```

```
figure(1);  
hold on;  
plot(dic_time,dic_strain);  
plot(lin_time,lin_strain);
```

```

title("DIC vs Linear Potentiometer");
legend("DIC","Linear Potentiometer");
xlabel("Time (1/100 s)");
ylabel("Strain (%)");
axis([0 2000 0 6]);

%%Load cell to DIC mapping
dic_load = [];
for i = 1:length(dic_time)
    if i < length(sens_load)
        dic_load(i) = sens_load(floor(i*3.2));
    else
        dic_load(i) = 0;
    end
end

%%Stress-strain Curve
figure(2);
plot(dic_strain-.082,dic_load);
title("Stress-strain curve of Acrylic");
xlabel("Strain (%)");
ylabel("Stress (MPa)");
axis([0 6 0 50]);

```